The copyright of this thesis rests with the University of Cape Town. No quotation from it or information derived from it is to be published without full acknowledgement of the source. The thesis is to be used for private study or non-commercial research purposes only.

University of Cape Town

Gold catalysts prepared by ion exchange for use in ethylene glycol oxidation: An exploratory study

University of Cape Town

Jennifer Margaret Case

Submitted to the University of Cape Town in fulfilment of the requirements for the degree of

Master of Science in Chemical Engineering

November 2009

Abstract

Heterogeneous catalysis using supported gold nanocrystallites has attracted increasing attention over the last two decades for its applicability to a wide range of reactions, offering activity under ambient conditions, as well as high selectivities towards particular products. This study focuses on a relatively uncommon method of gold catalyst preparation, ion exchange, which involves the suspension of the support in a solution containing cationic or anionic gold complex precursors at a fixed pH, followed by separation of the solid catalyst from this solution, drying and calcination. Theoretically, ion exchange preparation offers the possibility of highly dispersed gold crystallites, which are desirable in gold catalysis.

A series of catalysts was prepared using both anionic and cationic exchange, with $[AuCl_4]^-$ and $[Au(NH_3)_4]^{3+}$ respectively as gold precursors, with such solution concentrations that maximum loadings in the region of 3 to 4 wt-% Au could be obtained. Activated carbon and γ-alumina were used as supports. Catalysts were prepared at different pHs theorised to influence electrostatic adsorption differentially. Calcination was conducted at 300ºC in hydrogen.

Gold loading was established using Atomic Absorption Spectroscopy (AAS) and Thermogravimetric Analysis (TGA). Loading to full capacity was noted in a number of instances with the carbon supported catalysts. Most of the gold uptake took place in the first two hours of aging. In many but not in all cases higher loadings were noted at pHs further away from the iso-electric point (IEP), in the region where the support is oppositely charged to the complexed gold ion, thus confirming the electrostatic adsorption theory for ion exchange.

The size of gold crystallites was determined using Transmission Electron Microscopy (TEM), X-Ray Diffraction (XRD) and oxygen chemisorption. TEM results were used to calculate average crystallite sizes as well as to give an indication of size distributions. Measurable XRD gold peaks were only visible for supported carbon catalysts, and the crystallite sizes estimated using this technique were notably lower than average crystallite sizes from TEM for these catalysts. The carbon supports showed a large uptake of oxygen in the chemisorption process, and thus this technique was only used as a method for crystallite size determination for alumina supported catalysts. These crystallite sizes showed general

University of Cape Town

agreement with the average sizes derived from TEM. In summary, the carbon supported catalysts had average crystallite sizes greater than 10 nm with wide size distributions, while the alumina catalysts had average crystallite sizes nearly all under 10 nm and narrow size distributions.

Ethylene glycol oxidation under atmospheric pressure was employed as a test reaction, using 0.05 M ethylene glycol at a temperature of 60 ºC and at a pH of 11. Only the alumina supported catalysts displayed activity under these conditions, with initial reaction rates in the range of 2 to 15 mmol EG / g Au . min which are comparable to those reported in the literature. Across the range of crystallite sizes represented in these catalysts there was no evidence of dependency of activity on crystallite size.

University of Cape Town

Acknowledgements

Prof Eric van Steen played a key role as primary supervisor for this project and I am deeply appreciative of his gentle encouragement from the outset, his wise counsel throughout, and his superb knowledge and experience in the field of catalysis. A/Prof David Gammon was a warm and enthusiastic co-supervisor who added important knowledge from his field of expertise in organic chemistry and also who accommodated me in his laboratory for these studies.

I am grateful for excellent assistance with key parts of the analytical work. The team in the Department of Chemical Engineering comprising Mrs Helen Divey, Mrs Suzana Vasic and Mr Lonwabo Mtebeni performed the catalyst characterisations with AAS and chemisorption. Mr Mohamed Jaffer from the Electron Microscopy Unit produced the TEM images. Two final year chemical engineering students, Puleng Khumalo and Eugene Mbolekwa, prepared an additional series of alumina catalysts to investigate the influence of preparation pH.

I have called on many of my fellow postgraduate students for help during this project. Thanks are especially due to Brendan Beeming for general advice on ion exchange and liquid alcohol oxidation, to Caryn Vengadajellum and Kerry Horne for help with HPLC, to Patrick Mogorosi for instruction on the XRD and to all the students in the Gammon group for help in the laboratory. Sophie Rees-Jones assisted with finding and ordering chemicals.

My friends and colleagues, too many to acknowledge, are an ongoing source of encouragement in my learning endeavours. My mother, Glynne Case, has done her usual superb job of proofreading. My deepest appreciation is reserved however for the love and support of my husband, Roger. Our life together and with James and Julia keeps me (relatively) sane.

University of Cape Town

Table of Contents

University of Cape Town

University of Cape Town

List of Figures

University of Cape Town

University of Cape Town

List of Tables

University of Cape Town

Chapter 1. Introduction

Following the fairly recent discovery of the catalytic activity of highly dispersed gold, there has been a dramatic growth of activity in the area of gold catalysis over the last two decades (Hutchings and Haruta, 2005). Gold catalysts have been shown to demonstrate activity in a range of oxidation, hydrogenation and reduction reactions, with the most intensively studied reaction being that of CO oxidation. Particular interest relates to the observation that these catalysts tend to be both active at low temperatures and also show high selectivities towards particular products. They therefore are worth investigating for practical industrial applications on the basis of both cost and environmental implications. This is also a favourable research area for the pursuance of key scientific questions around the behaviour of nanocrystallites (Haruta, 2004).

1.1 Determinants of gold catalyst activity

Studies in gold catalysis traditionally focused on the influence of preparation methods, but more recent scholarly work has as a point of departure the fundamental issues of the size of the gold crystallites, and the nature of the support. In fact, gold catalysts prepared by different colloidal preparation regimes have been found to exhibit similar activity in the oxidation of ethylene glycol if they have similarly sized crystallites and are on the same supports (Porta et al., 2000).

1.1.1 Gold crystallite size

For gold catalysed CO oxidation, a clear relationship between the turn-over frequency (TOF) and the size of the supported gold crystallites has been demonstrated (Haruta, 1997, Valden et al., 1998, Choudary and Goodman, 2002). As the size of the crystallites decreases from 20 nm there is a marked increase in activity starting at about 7 nm, reaching a maximum at about 3 nm, below which there seems to be a dramatic decrease in activity.

There have been some investigations of crystallite size dependency for other gold catalysed reactions, where it can be seen that this effect depends not only on the particular reaction but also on the nature of the support. For ethylene glycol oxidation, Porta et al. (2000) show a

University of Cape Town

peak in activity at about 7.5 nm for gold on an activated carbon support, while Berndt et al. (2003) report no indication of a crystallite size effect for Au/Al_2O_3 catalysts.

1.1.2 Nature of the support

Gold catalysts have been synthesized on a range of supports, mainly metal oxides, but including other solids such as carbon. 'Reducible' oxides, namely titania, zirconia and ceria, have been found to form the most highly active catalysts for CO oxidation (Ivanova et al., 2006a), with ceria surmised to be the most suitable support for the water-gas shift reaction owing to its high oxygen storage capacity (Andreeva, 2002).

The primary purpose of the support is to keep the metal crystallites apart, but it is clear that interaction with the support may cause some change in properties and behaviour of the metal crystallites (Bond and Thompson, 1999). For example, it has been shown that for two samples with similar gold crystallite sizes, Au/TiO_2 catalysts are more active than Au/Al_2O_3 catalysts (Wolf and Schüth, 2002). Furthermore, the degree of crystallinity of the support is significant. Gold deposited on well-crystallized zirconia and titania showed higher water gas shift activity than that on the equivalent amorphous support (Andreeva, 2002).

The support also plays an important role during catalyst preparation, influencing crystallite size and size distribution. Gold catalysts on TiO_2, TiO_xN_y and TiN were prepared using deposition-precipitation and it was found that only TiO_2 produced a homogeneous distribution of gold crystallites less than 4 nm, while TiN has gold crystallites ranging from 3 nm to 1 μm (Centeno et al., 2003). On TiO_xN_y it was found that gold only deposits on the oxide. Only the Au/TiO_2 catalyst was active for CO oxidation. In another study on Au/TiO_2 catalysts it was found that gold deposited on the rutile phase but not on the anatase phase (Akita et al., 2001).

1.1.3 Other factors influencing activity

Catalyst loading has been considered as a factor influencing activity. For example, 3 wt-% catalysts have been found to be more active for the water-gas shift reaction than 1 wt-% or 5 wt-% catalysts (Andreeva, 2002), and this has been ascribed to an optimum ratio between the number of gold active centres and proportion of free support surface. In another study, a decrease in activity was noted with an increase in loading, but only for catalysts calcined at

University of Cape Town

300 °C and not for those calcined at 200 °C (Wolf and Schüth, 2002), suggesting that agglomeration of gold crystallites at higher loadings is the underlying factor for this observation.

Calcination temperature has also been investigated as a potential determinant of catalyst activity. Temperatures ranging from 250 °C to 400 °C have been used for the preparation of gold catalysts (Haruta et al., 1993, Berndt et al., 2003, Ivanova et al., 2006a), yet a systematic study has demonstrated that for metal oxide catalysts prepared by deposition-precipitation there is an increase in CO oxidation activity with a decrease in calcination temperature down to 200 °C (Wolf and Schüth, 2002).

1.1.4 Explanations for gold catalyst activity

A possible explanation for the size effect described above lies in a proposed CO oxidation mechanism which has as gold active sites the edges and corners of metallic gold crystallites (Haruta and Daté, 2001). This involves adsorption of one reactant (for example, CO) on these active sites and the counter reactant (for example, O_2) on the interface with the support. With smaller crystallite sizes, there is an increasing proportion of edge and corner sites, and thus the greater activity observed. This mechanism also explains the significance of the nature of the support described above, since different supports will give rise to different contact structures with the gold crystallites. When turnover frequencies per edge or corner atom have been calculated, it has been shown that for at least two different supports this value is identical (Janssens et al., 2006), lending further support to this theory.

A possible explanation as to why the perimeter is able to activate O_2 molecules is that these contain oxidic gold species, most probably $Au(OH)_3$ or Au(OH) (Haruta, 2004). This mechanism therefore involves both metallic gold on the surface of the crystallite, as well as oxidic gold on the periphery. A similar but slightly different model involves a combination of layers of metallic and oxidic gold with the latter ions forming a ‘chemical glue’ which binds the crystallite to the support (Bond and Thompson, 2000).

An alternative explanation for the crystallite size effect depends on the observation that as gold crystallite sizes decrease towards 3 nm, there is a change from metallic to non-metallic gold, as seen in the increased cluster band gap (Valden et al., 1998). A ‘quantum size effect’ has therefore been proposed, based on crystallites which are two layers thick of gold atoms.

University of Cape Town

Below 3 nm the Au-Au bond length also decreases with a concomitant increase in the d-electron density (Miller et al., 2006). This theory therefore considers non-metallic gold to form the active sites in gold catalysis.

In order to determine the nature of the active gold species, cyanide was used to leach crystalline gold from the surface of gold catalysts (Fu et al., 2005). The activity of the catalysts remained unchanged after this treatment, suggesting that the activity was due to cationic gold species embedded in the support which would not have been removed by leaching. However, in a subsequent similar experiment it was found that the unleached catalysts had significantly higher activity (Kim and Thompson, 2006), lending support to the original explanation that the active species is nanocrystalline (metallic) gold.

Alternative explanations have been advanced on the basis of theoretical calculations. Density Functional Theory (DFT) studies show that gold atoms with high coordination number will have a repulsive interaction with CO or O_2 while those with low coordination have a feasible interaction (Janssens et al., 2006). The energy differences that have been calculated support the experimental observations which show an order of magnitude change in activity. Using advanced structural analysis turnover frequency (TOF) per corner atom has been calculated, and it has been shown that for some systems that this is equivalent despite different geometries and different supports. This therefore provides further support for the 'edge mechanism' outlined above.

Calculations of the relative energy of the d-band show a relative upshift at about 3 nm size which provides a further explanation for the crystallite size effect (Phala and van Steen, 2007).

University of Cape Town

1.2 Methods of catalyst preparation

Three major categories of methods for the preparation of gold catalysts are reported in the literature (Bond and Thompson, 1999)[1].

1. Precipitation: either co-precipitation of gold and support or deposition precipitation of gold onto support

2. Impregnation: adding precursor solution to the support and then removing the solvent by evaporation

3. Ion exchange: between ions in solution and ions on the support, followed by removal of excess solution through filtration

Common to all these methods is that they involve a slurry. Many researchers seem to focus on deposition precipitation to synthesize supported gold catalysts since this has been considered to offer easy handling (Haruta, 2004), and indeed is already working on a commercial scale. The influence of various preparation parameters in the deposition precipitation process has been extensively studied. A useful study in this regard presents an optimisation of the preparation process for CO oxidation catalysts through analysis of more than 300 samples with various conditions (Wolf and Schüth, 2002). For the purposes of the present study it is worth noting that the loading efficiencies obtained with this method are relatively poor, ranging between 20 and 60 %.

However, deposition precipitation has not been considered suitable for metal oxide supports with iso-electric point (IEP) below 4 ('acidic' supports) or for carbon supports (Porta et al., 2000). In the latter regard, deposition precipitation on carbon has been shown to produce aggregates of widely varying crystallite size (5 - 50 nm) (Prati and Martra, 1999), while a 'reductive precipitation' with formaldehyde has been successfully used to produce active catalysts for organic oxidation reactions (Hutchings et al., 2006).

Impregnation and ion exchange are widely used in the preparation of other metal catalysts (cf. Guerreiro et al., 1997), but are less commonly used in gold catalyst preparation. They are

[1] Other methods using gas phase deposition or colloidal systems are also reported but not widely used or likely to have easy commercial application. The focus for the present study is on 'working real catalysts' as opposed to model studies.

University of Cape Town

similar methods in that both involve suspending the support in a precursor solution, with no precipitation of the gold. The only difference in these methods is that in impregnation there is no filtration of the slurry but rather an evaporation of the solvent (water) so that any gold in solution will remain on the solid catalyst. Impregnation therefore implicitly yields 100 % uptake of available gold, but it is possible that this unattached gold might cause aggregate deposits during drying or calcination and thus impact negatively on the final crystallite size (Brunelle, 1978). Gold impregnation on carbon supports has been shown to yield large crystallites (>200 nm) (Prati and Martra, 1999). However, Hutchings et al. (2006) successfully used impregnation to produce active Au/C catalysts for organic oxidation reactions, in addition to their use of reductive precipitation mentioned above.

With ion exchange the slurry is filtered, and any gold not attached to the solid will be discarded in the filtrate. There is at least theoretically the possibility of achieving highly dispersed catalysts, given the avoidance of precipitation or deposition of unattached gold. This has been demonstrated in the case of platinum on silica (Brunelle, 1978). Ion exchange as a method of gold catalyst preparation was thus judged a useful focus for the present study.

University of Cape Town

1.2.1 Ion exchange

Impregnation and ion exchange were traditionally judged to be unsuitable for the preparation of highly dispersed catalysts because of the relatively low affinity of Au for metal oxides, compared to other noble metals where they are widely applied as preparation methods. Another problem is that using the $HAuCl_4$ precursor results in the presence of chloride ions during calcination which are known to promote sintering. Ion exchange as a method is therefore usually described in terms of using cationic gold complexes in the precursor solution (for example, Bond and Thompson, 1999), and here the problem is the availability of cationic gold complexes. Those reported in the literature are the ethylene diamine complex $[Au(en)_2]^{3+}$ (Riahi et al., 2002, Bulushev et al., 2004, Zanella et al., 2005) and a gold phosphine complex $[Au(PPh_3)]^{+}$ (Guerreiro et al., 1997). A 'direct anionic exchange' method has also been proposed which involves an $HAuCl_4$ precursor solution (Ivanova et al., 2004). The problem of chloride-promoted sintering can be avoided by washing with an ammonia solution prior to calcination.

The term 'ion exchange' implies that a gold ion complex in solution exchanges place with an ion on the surface of the support. A mechanism whereby this takes place builds on the

observation that in low pH solutions, supports such as metal oxides or carbon become protonated and hence positively charged, and in high pH solutions they become deprotonated and negatively charged (Brunelle, 1978). The pH at which the surface is neutral is termed the isoelectric point (IEP). It has been proposed that the adsorption of metal complexes onto such supports is electrostatic, and that positive complexes will be most favourably attracted to supports in solution below the IEP, while negatively charged complexes will favour adsorption above the IEP (Brunelle, 1978). What is not clear is the nature of the adsorption. The term 'ion exchange' implies a stoichiometric exchange of ions, but it is possible that there is rather an electrostatic attraction taking place between the ions and the support surface. Investigating the adsorption of a positive Pt cationic complex onto a silica support, it has been noted that the maximum extent of adsorption seems to have a steric rather than a stoichiometric limit and it has been suggested that in this instance at least the term 'strong electrostatic adsorption' would be more appropriate than ion exchange (Schreier and Regalbuto, 2004). The term 'liquid phase grafting' has been used when a liquid solution of a cationic gold complex is involved, but implied here is a mechanism involving an exchange of ligands in the gold complex (Okumura and Haruta, 2000, Haruta, 2004).

The number of adsorption sites as represented by the surface area of the support is an important parameter when considering metal loading via ion exchange (Brunelle, 1978). For a support such as α-alumina with a surface area of 10 m^2/g it will not be possible to load more than 0.2 wt-% Pt while for γ-alumina with a surface area of 200 m^2/g a maximum of 3 wt-% is possible. Further parameters that need to be borne in mind are the stability of the metal complex and the solubility of the oxide at the pH which will be favourable for ion exchange.

University of Cape Town

1.2.1.1 Anionic exchange using $AuCl_4^-$

Depending on the pH of an $HAuCl_4$ precursor solution different anionic gold species are present (Ivanova et al., 2004). The $[AuCl_4]^-$ ion is a square planar complex, and as the pH increases Cl^- ions are progressively exchanged with OH^- ions to form the following gold chloro-hydroxy species:

$$\underset{pH\leq 2}{[AuCl_4]^-} \rightleftharpoons \underset{pH\approx 3}{[AuCl_3(OH)]^-} \rightleftharpoons \underset{pH\approx 4}{[AuCl_2(OH)_2]^-} \rightleftharpoons \underset{pH\approx 5\text{-}6}{[AuCl(OH)_3]^-} \rightleftharpoons \underset{pH\geq 7}{[Au(OH)_4]^-}$$

It is important to note that different species co-exist and that these pH ranges are only approximate. At pH=7 the precipitate $Au(OH)_3$ forms which is utilised in the deposition-precipitation method. For anionic exchange on γ-Al_2O_3, precursor solutions below this pH are used.

When the support is added to the $HAuCl_4$ solution a slight increase in pH is noted, and this is attributed to the loss of protons in solution when the surface hydroxyl groups of the metal oxide are protonated. These OH_2 groups depart as water and it is posited that the gold chloro-hydroxy species then rapidly take up these vacant Lewis acid sites, implying an overall process of ion exchange. The $[AuCl_2(OH)_2]^-$ species is considered to be optimal, given the possibility of a bidentate adsorption on the support surface (Ivanova et al., 2004). This concurs with experimental results which yielded more active catalysts when prepared at pH≈4 compared to lower pH. It is suggested that $[AuCl_4]^-$ may not be able to chemically bond to the surface since it possesses no OH groups; it can be physically adsorbed but it may be lost during washing. Any lost gold might therefore be attributed to unhydrolysed $[AuCl_4]^-$. This argument suggests that supports with IEP close to 6-7 are needed if using this method of catalyst preparation. A low IEP would result in a negative support surface at the optimum preparation pH which would not facilitate the adsorption of these anionic gold species. The minimum possible IEP would be 2 since this is the pH for the exchange of at least one Cl^- ligand. This would therefore suggest that activated carbon (IEP≈1) is not amenable to anionic exchange. Supports with very high IEP, for example MgO (IEP = 12) would cause the pH to rise above 7 when added to the $HAuCl_4$ solution and would thus cause the precipitation of $Au(OH)_3$.

As noted above, the chloride ions need to be removed after the initial step of catalyst preparation. Firstly, they are known to promote sintering during calcination, and secondly they cause deactivation of the catalyst during reaction, both effects due to the formation of Au-Cl bridges (Ivanova et al., 2004, Ivanova et al., 2006b). This was supported by a comparison of the activity of catalysts prepared by washing with water and those that were washed with ammonia, with the latter showing smaller crystallite size and corresponding superior activity. The ammonia allows for the substitution of chloride ions with hydroxyl groups. An important safety note here is that it needs to be established that all complexed gold is attached to the surface prior to addition of ammonia, in order to avoid the formation of explosive gold ammonia complexes at high pH.

University of Cape Town

In later studies on gold catalysts prepared by anionic exchange it was confirmed that ammonia is indeed a good washing agent compared to other bases such as urea or NaOH and that the optimal washing time is between 20 and 60 minutes (Ivanova et al., 2006c). A loss of approximately 30 % of the gold is noted in all cases, attributed to the removal of non-attached gold complexes. For washing times greater than 24 hours an increase in gold loading was noted, attributed to the deposition of $Au(OH)_3$ which also explains the presence of larger crystallites in these samples.

An important finding in this work is that with an anticipated loading of 5 wt-% gold, only 3.7 % was obtained, confirming earlier theoretical work suggesting a limit on the capacity for adsorption on γ-alumina somewhere in this region (Brunelle, 1978).

1.2.1.2 Cationic exchange using $[Au(NH_3)_4]^{3+}$

There appears to be only one report so far in the literature on using the tetraammine gold complex cation in the preparation of supported gold catalysts. Tuzovskaya et al. (2003) used this method to introduce gold nanocrystallites into HY zeolite, obtaining crystallite sizes of 10-40 nm.

Tetraammine gold(III) nitrate can be produced from $HAuCl_4$ solution using ammonium nitrate (Skibsted and Bjerrum, 1974); further experimental details are given in the following chapter. In acid medium, $[Au(NH_3)_4]^{3+}$ hydrolyzes slowly and irreversibly, firstly to $[Au(NH_3)_3OH]^{2+}$ in the pH range 2-5, and then at pH lower than 1 to $[Au(NH_3)_3H_2O]^{3+}$. In basic solution the $[Au(NH_3)_4]^{3+}$ ion acts as a weak acid and forms $[Au(NH_3)_3NH_2]^{2+}$ which decomposes easily to the amorphous precipitate without a definite chemical characterisation known as 'fulminating gold' (Steinhauser et al., 2008). All of these gold complexes can be assumed to be in a square planar form, similar to the anionic complexes described above.

1.3 Gold catalysed oxidation of liquid alcohols

The selective oxidation of liquid alcohols is a growing focus of interest in gold catalysis. Traditional methods utilize stoichiometric inorganic oxidising agents but there is increased interest in developing environmentally benign alternatives (Mallat and Baiker, 2004). Heterogeneous catalysts to facilitate oxidation with molecular oxygen are of particular interest in developing methods with industrial application due to their ease of separation from

University of Cape Town

reaction products. Much focus to date has been on supported platinum-group metals but gold (and silver) are starting to be explored due to comparable activity and potentially superior selectivity and stability. The one possible drawback of gold catalysts is that an alkaline medium has been shown to be necessary for alcohol oxidation, thus yielding a carboxylate product (Hashmi, 2007). The various categories of alcohol oxidation reactions for which gold catalysts have been shown to be active can be summarised as follows:

1. Primary alcohols to aldehydes (under solvent-free conditions)
    a. benzyl alcohol, octan-1-ol, geraniol to corresponding aldehydes (Enache et al., 2005)
2. Primary alcohols to carboxylic acids
    a. ethanol to acetic acid (Jørgensen et al., 2007)
3. Diols and triols to monocarboxylic acids
    a. glycerol to glyceric acid (Carrettin et al., 2002, Carrettin et al., 2003, Carrettin et al., 2004, Porta and Prati, 2004, Demirel-Gülen et al., 2005, Demirel et al., 2007a, Demirel et al., 2007b, Demirel et al., 2007c, Ketchie et al., 2007)
    b. ethylene glycol to glycolic acid (Berndt et al., 2003, Prati and Porta, 2005)
    c. propane-1,2-diol to lactic acid (Demirel et al., 2007a)
    d. propane-1,3-diol (Biella et al., 2002a)
    e. diethylene glycol (Biella et al., 2002a)
    f. phenylethane-1,2-diol (Biella et al., 2002a)
4. Sugars to sugar (aldonic) acids
    a. Pentoses (Mirescu and Prüße, 2007)
    b. Hexoses (Mirescu and Prüße, 2007)
       including glucose to gluconic acid (Biella et al., 2002b, Önal et al., 2004, Beltrame et al., 2006, Comotti et al., 2006b, Mirescu et al., 2007)
    c. Disaccharides including maltose & lactose (Mirescu and Prüße, 2007)
5. Aminoalcohols to aminoacids (Biella et al., 2002a) – amines usually deactivate noble metal catalysts but not Au catalysts
6. Primary alcohols to methyl esters (with methanol in rxn mixture)
    a. 1-hexanol, cinnamyl alcohol, 2-hydroxymethylpyridine (Nielsen et al., 2007)
    b. Ethylene glycol to methyl glycolate (Hayashi et al., 2006)

University of Cape Town

The focus for the present study is on the selective oxidation of polyols to primary monocarboxylic acids under atmospheric pressure. There is an ultimate interest in developing a route for the oxidation of glycerol, given the current surplus of glycerol as a by-product of biodiesel production. However, owing to low reactivity at atmospheric pressure as seen in exploratory work, it was decided for the purposes of this study to focus on the oxidation of ethylene glycol, a simpler polyol, using a similar methodology to that of Demirel et al. (2007a).

1.3.1 Mechanism of gold catalysed alcohol oxidation

In general, oxidation of a primary alcohol to form an aldehyde can proceed via 1. removal of a proton from the hydroxyl group and 2. 'abstraction' of a hydride ion from the primary C-atom, forming the carbonyl double bond, as shown in Figure 1.1 below.

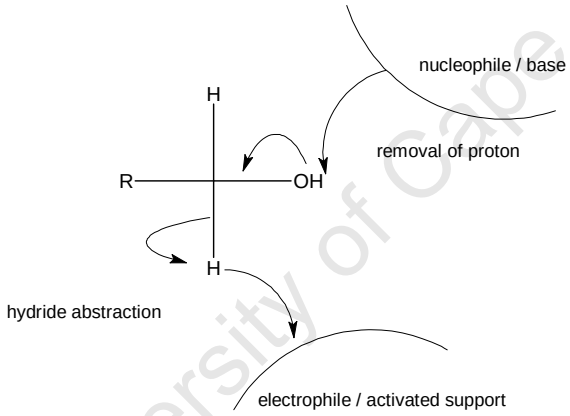

Figure 1.1. Possible route for formation of aldehyde (shown as a concerted mechanism)

The further oxidation of the aldehyde to form a carboxylic acid, shown in Figure 1.2, can proceed firstly through a nucleophilic attack by a hydroxide ion on the C centre ('oxygen insertion') with the transferral of one electron pair from the double bond to the carbonyl oxygen. This is followed by a further alpha-hydride abstraction leading to the reformation of the carbonyl bond.

University of Cape Town

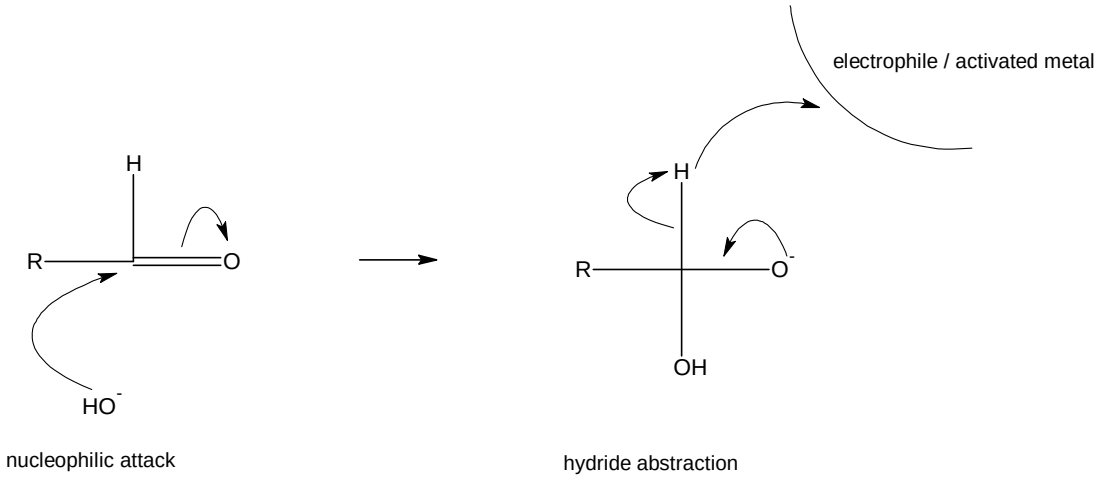

Figure 1.2. Formation of carboxylic acid

Particular mechanisms for the metal catalysed oxidation of alcohols have focused on the formation of the aldehyde. A number of mechanisms have been identified, which differ in the particular agents that they propose as nucleophiles and electrophiles and also in whether they see these as sequential or synchronous steps (Mallat and Baiker, 2004).

The first mechanism, the 'classical' dehydrogenation mechanism, depicted in Figure 1.3, suggests two separate steps in the initial formation of the aldehyde. Here a cleavage of the O-H bond takes place upon adsorption on the catalyst surface, resulting in an adsorbed alkoxide and an adsorbed hydrogen atom. In the adsorbed alkoxide, the primary C-H bond is weakened due to the electron-withdrawing effect of the oxygen atom, resulting in the breakage of this bond, and the adsorption of a further hydrogen atom onto the surface. This is considered to be the rate-determining step. It has been noted that this formation of the aldehyde by hydrogen abstraction will be favoured in basic conditions (Biella et al., 2002b). These adsorbed hydrogen atoms are oxidised by reaction with surface adsorbed oxygen which causes a shifting of the equilibrium towards the formation of products, as well as liberating active sites. It has in fact been shown that molecular oxygen is not necessary for this reaction; any oxidising agent can perform the same role (oxidation of the adsorbed hydrogen atoms) and facilitate the reaction. Support for this model also comes from studies which show the metal catalyst in a reduced state. A variation of this mechanism has been proposed which holds that the key role for oxygen is to suppress catalyst deactivation by adsorption of *all* byproducts and adsorbed poisons, rather than specifically the oxidation of hydrogen (Mallat and Baiker, 2004).

University of Cape Town

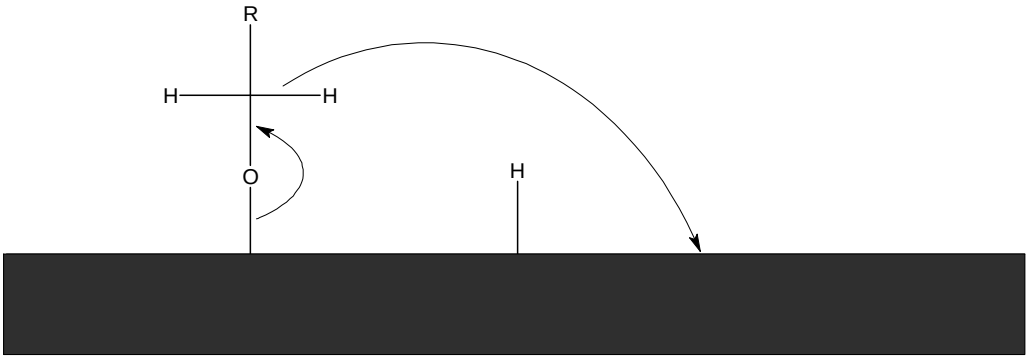

Figure 1.3. Classical metal catalysed dehydrogenation mechanism

The other major class of mechanism, shown in Figure 1.4, follows a Langmuir-Hinshelwood pattern with the rate determining step involving the adsorption of two different species on the catalyst surface. What has been proposed here is the direct interaction between the adsorbed alkoxide and adsorbed oxidising species (for example, oxygen). Support for this model comes from kinetic studies and also from evidence of partial oxygen coverage of the surface.

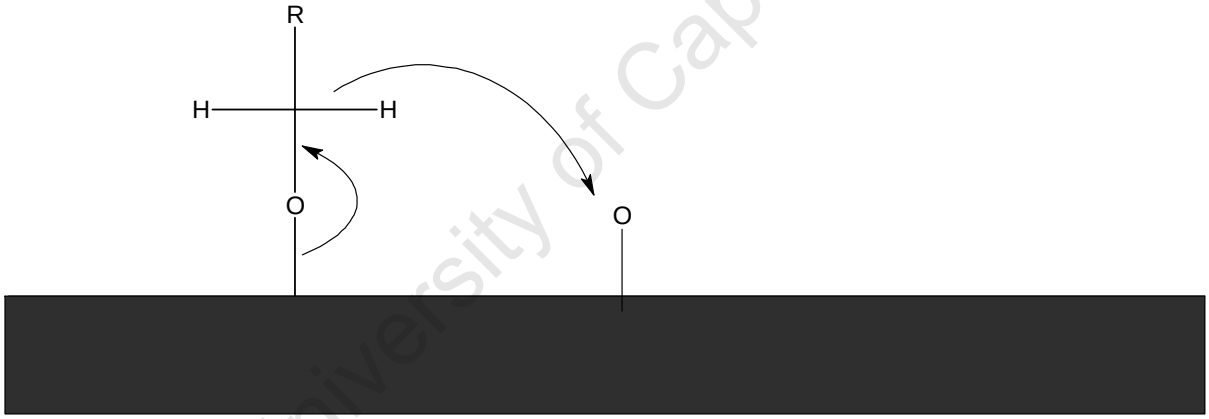

Figure 1.4. Langmuir-Hinshelwood mechanism

A further mechanism for the metal catalysed oxidation of alcohols not reviewed by Mallat and Baiker had been proposed by Kluytmans et al.(2000). They propose a simultaneous hydride transfer from the alcohol to the surface and a reduction of a surface hydroxyl group resulting in the proton removal from the O-H group, shown in Figure 1.5.

University of Cape Town

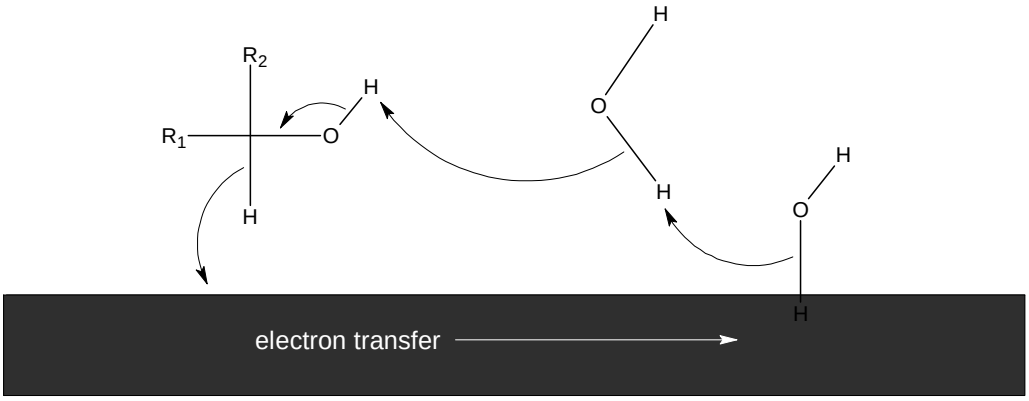

Figure 1.5. Simultaneous proton abstraction and hydride transfer (Kluytmans et al., 2000)

Mallat and Baiker note that a detailed mechanism for the gold catalysed oxidation of alcohols had not yet been proposed (in 2004), but suggest the cleavage of the primary C-H bond as the rate determining step. Because of the requirement for an alkaline medium, others have proposed that the initial proton abstraction from the hydroxyl group is the rate determining step (Carrettin et al., 2002, Carrettin et al., 2003, Carrettin et al., 2004, Hashmi, 2007).

Recent kinetic studies of gold-catalysed oxidation have focused on the glucose oxidation reaction (Önal et al., 2004, Beltrame et al., 2006, Comotti et al., 2006a). Because glucose has an acyclic aldehyde form which exists in equilibrium with the cyclic form, the oxidation of glucose is in fact the oxidation of an aldehyde to a carboxylic acid. The focus of the mechanism is therefore precisely on the oxidation step that appears to have been considered less prominent in the Mallat and Baiker review.

A Langmuir-Hinshelwood model has been proposed for the oxidation of glucose with three key reactions: the adsorption of glucose, the surface reaction of glucose to form gluconic acid, and the desorption of glucose (Önal et al., 2004). From kinetic results it was concluded that the surface reaction is the rate-determining step. In concordance with Mallat and Baiker's general mechanism described above, it has been suggested that the surface reaction produces hydrides bound to the catalyst surface, which then subsequently react with dissociatively adsorbed oxygen.

A further kinetic analysis of gold-catalysed glucose oxidation concluded that the experimental results (first order with respect to oxygen) are best fitted by an Eley-Rideal mechanism in which a fast adsorption of a glucose molecule on the catalyst surface is followed by a rate-determining step where this adsorbed molecule interacts with an oxygen

University of Cape Town

molecule from the liquid phase (Beltrame et al., 2006). Hydrogen peroxide is formed as a byproduct, and there is experimental evidence of detectable quantities of this substance in the reaction mixture (it decomposes quickly under the given reaction conditions). In a further investigation, it has been proposed that the actual mechanism takes place through a two electron-transfer from glucose to dioxygen via gold which acts as a kind of bridge as shown in Figure 1.6 below (Comotti et al., 2006a). Hydrogen peroxide is formed when the released protons bond to the electron rich dioxygen ion, O_2^{2-}. (These experiments were conducted with colloidal gold and this is represented in the figure as contrasted to the above figures.)

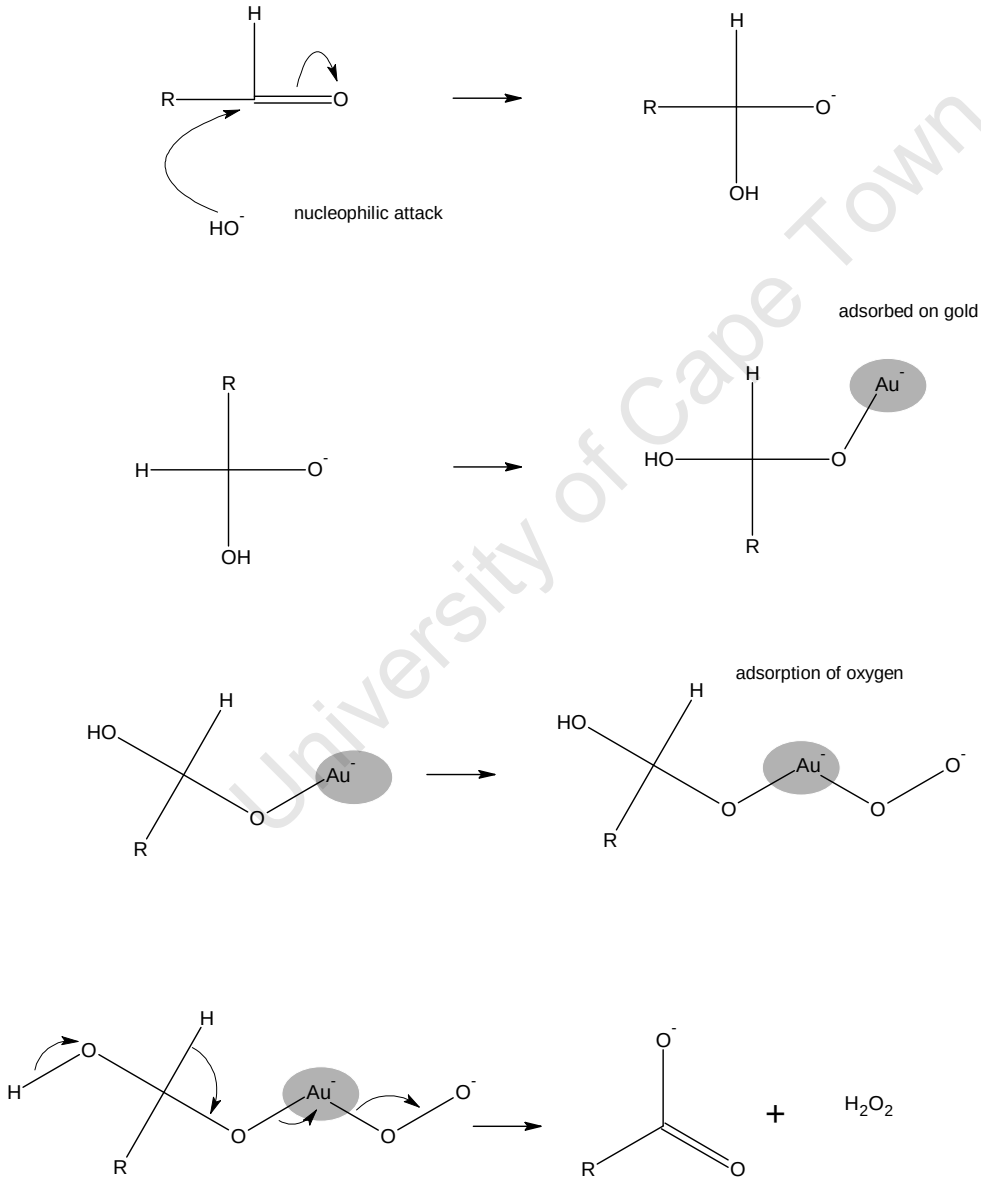

University of Cape Town

Figure 1.6. Proposed mechanism for glucose oxidation (Comotti et al., 2006a)

1.3.2 Ethylene glycol oxidation by gold catalysis

There are very few reports in the literature of the gold catalysed oxidation of ethylene glycol, even though this has been considered as one of three key industrially important alcohol oxidation reactions[2], with an estimated world production of 2000 tpa (Biella et al., 2002a). The current industrial process for production of glycolic acid by Du Pont operates via chloroacetic acid or via formaldehyde-carbon monoxide, using pressures up to 200 atm (Prati and Rossi, 1998). There is also an enzymatic route with relatively low efficiencies. Glycolic acid is used in the cosmetic and food industries, as well as an intermediate in polymer production (Bianchi et al., 2000). The full range of possible oxidation products from ethylene glycol are represented below in Figure 1.7. It is clear that selectivity is a key consideration in the proposal of new production routes for ethylene glycol.

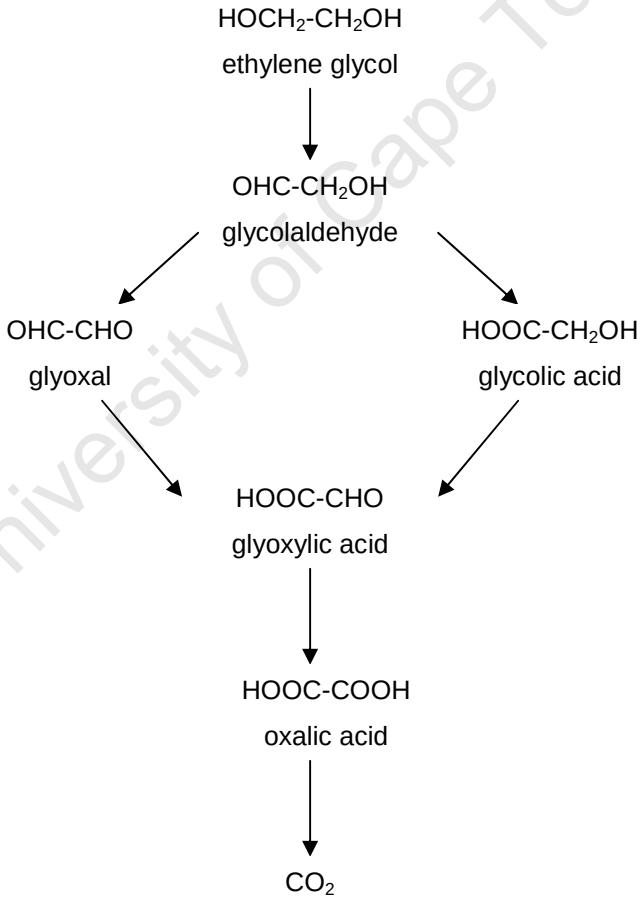

Figure 1.7. Oxidation products from ethylene glycol (Wieland et al., 1996)

[2] The other two are glucose oxidation and the synthesis of racemic lactic acid from 1,2-propanediol.

University of Cape Town

Gold sols immobilised on carbon have been used as catalysts for liquid phase alcohol oxidations (Bianchi et al., 2000, Biella et al., 2002a). Earlier work concluded that gold on carbon was a much better catalyst for these reactions than gold on alumina or other oxide materials, based both on activity and selectivity (Prati and Rossi, 1998). Subsequent work thus focused mainly on the carbon supported catalysts, generally prepared by immobilization of gold sols. Results have been reported for Au/C catalysed ethylene glycol oxidation, performed under 2 atm pressure, with 0.5 M ethylene glycol and ethylene glycol / Au = 1000 mol/mol (Bianchi et al., 2000). Favourable turnover frequencies and selectivities have been achieved, comparing the Au/C catalyst with standard Pt/C and Pd/C catalysts. The gold catalysts also showed better lifetime upon recycling. Further data under these conditions has been reported with carbon, alumina and silica supported catalysts (Porta et al., 2000). Here it was noted that the activity of gold on alumina increases with decreasing crystallite size, while gold on carbon increases with crystallite size, up to a maximum in the region of 7-8 nm. Overall in this study equally good conversions are noted for some of the carbon and alumina catalysts, thus apparently contradicting the earlier conclusion regarding the low activity of alumina catalysts for this reaction.

The ethylene glycol oxidation reaction has also been performed under 3 atm pressure, with 0.4 M ethylene glycol, again with ethylene glycol / Au = 1000 mol/mol, and similar results have been reported (Biella et al., 2002b). Nearly 100% selectivity to glycolic acid is noted, with gold less likely to promote oxidative C-C bond breaking. When comparing four Au/C catalysts with different crystallite sizes, a 'qualitative' peak in conversion in the range 7-8 nm has been observed. For oxide supported catalysts a similar relation to that reported for CO oxidation has been reported where the conversion increases as the crystallite size decreases.

Ethylene glycol oxidation has been used as a test reaction for a range of Au/Al_2O_3 catalysts which were characterised using oxygen chemisorption (Berndt et al., 2003, Berndt et al., 2004). These would appear to be the only reports in the literature of gold catalysed ethylene glycol oxidation conducted under atmospheric pressure. The practical arrangements described in these studies were used as a starting point for the catalyst test set-up in the present study, as discussed in detail in the following chapter. Using 0.5 M ethylene glycol, reaction temperatures between 50 ºC and 70 ºC, and an ethylene glycol / Au ratio of 10 000 mol/mol good activities were obtained. Selectivity to glycolic acid higher than 95 % has also been reported on all these catalyst samples, with small amounts of oxalic acid

University of Cape Town

formed at high conversions. Finding activity roughly proportional to oxygen chemisorption it has been concluded that there is no size effect for this reaction, in contrast to the results from the Rossi group (Biella et al., 2002b).

1.4 Objectives for this study

This study concerns the preparation of gold catalysts by ion exchange, for use in ethylene glycol oxidation. It is focused on two key research questions:

1. For gold catalysts prepared by ion exchange, what loading efficiencies and gold crystallite sizes can be achieved?

2. Does gold crystallite size and loading influence the reaction rate and selectivity for ethylene glycol oxidation conducted at atmospheric pressure?

In order to address these research questions, there are three main methodological concerns which underpin the study:

1. Establishing methods for determining Au loading

2. Establishing methods for determining Au crystallite size

3. Establishing a test reaction protocol for ethylene glycol oxidation to determine reaction rate and selectivity

Thus although the study is directed towards the two research questions described above, a considerable portion of the work has been directed towards resolving the three methodological issues also outlined here.

University of Cape Town

Chapter 2. Experimental methods

2.1 Catalyst preparation

For preparation of gold catalysts by the method of ion exchange, the support is suspended in a solution containing gold ions. In this study tetraammine gold(III) nitrate ($Au(NH_3)_4(NO_3)_3$) was prepared to produce a solution with gold cations ($Au(NH_3)_4^{3+}$) while aurochloric acid ($HAuCl_4$) was used as a source of gold anions ($AuCl_4^-$).

2.1.1 Gold precursor solutions

2.1.1.1 Anionic precursor

For preparing the anionic precursor solution, 5 ml of aurochloric acid ($HAuCl_4$) solution with a concentration of approximately 50 gAu/l was made up to 500 ml with deionised water. The concentration of the initial precursor solution was accurately established by performing AAS on a sample.

2.1.1.2 Cationic precursor

Tetraammine gold nitrate was prepared using the method described by Skibsted and Bjerrum (1974). A supersaturated solution of ammonium nitrate was prepared by dissolving 95 g of NH_4NO_3 in 70 ml of deionised water. 10 ml of aurochloric acid solution (corresponding to approximately 0.5 g of gold) was then added to the solution and mixed. The reaction flask was immersed into an ice bath and the pH was adjusted to 7 by the addition of ammonia solution. A white precipitate was seen to form at around pH 5 and the dark yellow solution turned a milky light yellow. The following equation represents the reaction which took place:

$$HAuCl_4 + 3\ NH_4NO_3 + 4\ NH_3 \rightarrow Au(NH_3)_4(NO_3)_3 + HCl + 3\ NH_4Cl$$

Care had to be exercised not to exceed a neutral pH since fulminating gold can form in an alkaline solution. This is an orange-brown, amorphous substance which when dried is shock sensitive and highly explosive.

University of Cape Town

The tetraammine gold nitrate suspension was left overnight in the ice bath, and the filtered precipitate was washed with chilled ethanol. This was then dried at 100 ºC for 2 hours and then at room temperature overnight. The tetraammine gold nitrate was then made up into a 1 litre standard solution with deionised water. It was noted that a small amount of material remained undissolved at this stage; it was unclear whether this was tetraammine gold nitrate (which has a low solubility) or some other impurity. The solution was therefore filtered to remove any such insoluble material and then divided into two 500 ml amounts for catalyst preparation. The gold concentration of this precursor solution was also determined by performing AAS on a sample.

2.1.2 Preparation of gold catalysts

Metal oxides are the most commonly used supports in gold catalysis (Haruta, 2004) while activated carbon is a popular support for liquid phase oxidations (Prati and Porta, 2005, Hutchings et al., 2006). It was therefore decided for the present study to use two different supports: activated carbon (Norit C Granular A-4412; S_{BET} = 1230 m^2/g) and γ-alumina (Puralox SCCa 5-150; Sasol Germany; S_{BET} = 162 m^2/g). Zeta potential measurements for each of these supports are given below in Figure 2.1 and Figure 2.2. It can be seen that for activated carbon the iso-electric point (IEP) is at about pH = 1.5, while for alumina it is at about pH = 8.

University of Cape Town

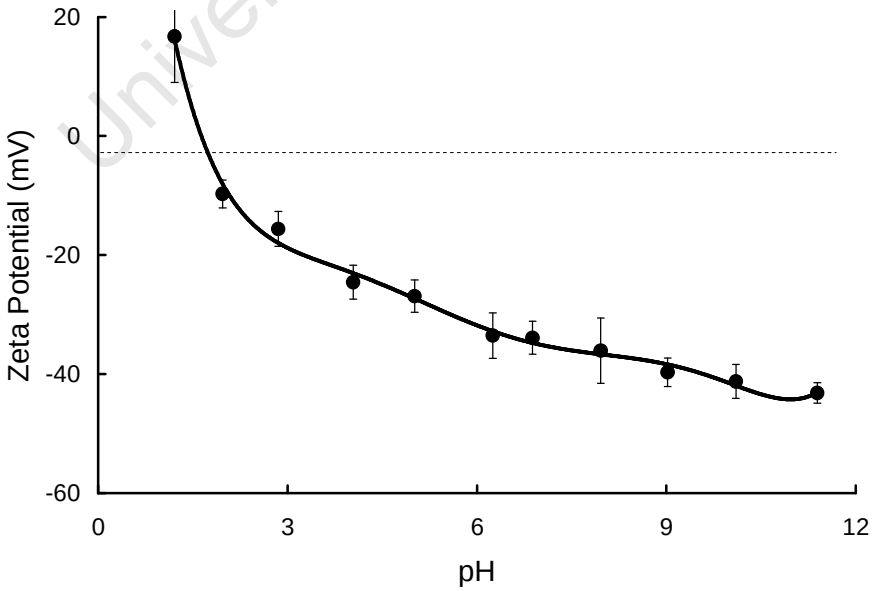

Figure 2.1. Zeta potential measurement for activated carbon (Beeming, 2009)

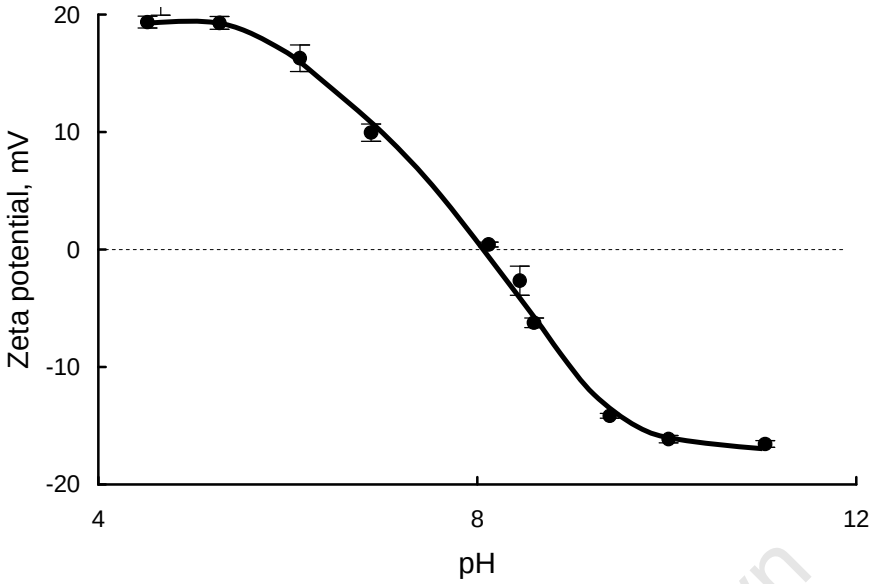

Figure 2.2. Zeta potential measurement for alumina (Zwane, 2004)

The solid support was crushed and sieved to give particle sizes less than 500 μm. Catalysts were prepared in batches using 5 g of support. This was added to a 500 ml solution of gold ions (either positive or negative) with a gold content of between 0.15 and 0.20 g (corresponding to 3-4 wt-% of the support if fully loaded). The pH was then adjusted with concentrated HNO_3 or NaOH depending on the desired pH. The suspension was aged, with stirring, for 22 hours (A shorter aging time was explored for some of the catalyst batches following early analysis but the longer aging time was later reinstated). 5 ml samples of the precursor solution were taken at time intervals for AAS to allow for analysis of the gold uptake over time. On completion the gold catalyst was filtered and washed with deionised water. This solution was made up to 500 ml for AAS analysis and was termed the initial filtrate. For catalysts prepared with the anionic precursor, an additional ammonia washing stage was incorporated which involved suspending the water washed catalyst in approximately 250 ml of a 25 wt-% ammonia solution for 20 minutes with stirring. Following this step the catalyst was filtered. This solution was also made up to 500 ml and was termed the ammonia wash filtrate. The solid catalyst was dried in the oven at 200 °C for 2 hours. Thereafter it was calcined in a fluidized bed for 2 hours at 300 °C in hydrogen with a flow rate of 50 ml(NTP)/min (heating up to 300 °C over 2 hours and cooling down again after calcination for the same period). (One batch of catalyst was divided into four portions in order to explore the effects of calcining at 200 °C or 300 °C and in air or hydrogen).

University of Cape Town

Three key preparation variables were explored in the present study, i.e. nature of support, ionic charge on gold precursor and pH of precursor solution. Both activated carbon and alumina supports were used. Precursor solutions, as noted above, were either anionic (aurochloric acid) or cationic (tetraammine gold nitrate). For each combination of these, two batches of catalyst were prepared using different pHs in relation to the IEP of the support. This initial series of catalysts is represented below in Table 2.1.

Table 2.1. Catalysts prepared to investigate the effect of support, ionic precursor, and pH of solution

Catalyst code	Support	Precursor	Initial pH
C-AN-0.6	Activated Carbon	$HAuCl_4$	0.6
C-AN-2.3	Activated Carbon	$HAuCl_4$	2.3
C-CAT-2.4	Activated Carbon	$Au(NH_3)_4(NO_3)_3$	2.4
C-CAT-5.0	Activated Carbon	$Au(NH_3)_4(NO_3)_3$	5.0
AL-AN-3.2	Alumina	$HAuCl_4$	3.2
AL-AN-6.1	Alumina	$HAuCl_4$	6.1
AL-CAT-6.4	Alumina	$Au(NH_3)_4(NO_3)_3$	6.4
AL-CAT-10.6	Alumina	$Au(NH_3)_4(NO_3)_3$	10.6

The IEP of activated carbon is approximately pH = 1. For anionic exchange a pH below 1 would therefore be considered favourable. Given the difficulty in obtaining much variation in the region below pH = 1, it was decided to prepare only one carbon supported catalyst in this region below the IEP (C-AN-0.6) and to prepare the other one outside this favourable region (C-AN-2.3). For cationic exchange, a pH above 1 would be considered favourable, and two carbon supported catalysts were prepared in this region, one just above the IEP (C-CAT-2.4) and one much further away from the IEP (C-CAT-5.0), assuming that these latter conditions would presumably present stronger electrostatic attraction for gold loading.

The IEP of alumina is approximately at pH = 8. For anionic exchange, a pH below 8 would be considered favourable. Two alumina supported catalysts were therefore prepared in this region, one just below the IEP (AL-AN-6.1) and one much further away from the IEP (AL-AN-3.2); these latter conditions would theoretically produce a stronger electrostatic attraction. For cationic exchange, a pH above 8 would be considered favourable. In this early stage of the project there was concern about precipitating gold hydroxide at high pHs and so it was decided at this stage to prepare only one alumina supported catalyst by cationic exchange in the favourable region (AL-CAT-10.6) and to prepare the other catalyst in the unfavourable region (AL-CAT-6.4).

University of Cape Town

Additional catalysts were prepared to allow for further investigation of particular parameters. Firstly, a catalyst represented below in Table 2.2 was prepared with identical conditions to C-AN-0.6 excepting that the ammonia washing stage was omitted.

Table 2.2. Catalysts prepared to investigate the effect of ammonia wash

Catalyst code	Support	Precursor	Initial pH	NH_3 wash
C-AN-0.6	Activated Carbon	$HAuCl_4$	0.6	Yes
C-AN-0.6 no wash	Activated Carbon	$HAuCl_4$	0.6	No

As mentioned above, one batch was divided into four portions to allow for the investigation of the effect of different calcination regimes. These batches are represented below in Table 2.3.

Table 2.3. Catalysts prepared to investigate the effect of calcination conditions

Catalyst code	Support	Precursor	Initial pH	Calcination temperature	Calcination medium
AL-CAT-10.6-300AIR	Alumina	$Au(NH_3)_4(NO_3)_3$	10.6	300℃	Air
AL-CAT-10.6-300H2	Alumina	$Au(NH_3)_4(NO_3)_3$	10.6	300℃	H_2
AL-CAT-10.6-200AIR	Alumina	$Au(NH_3)_4(NO_3)_3$	10.6	200℃	Air
AL-CAT-10.6-200H2	Alumina	$Au(NH_3)_4(NO_3)_3$	10.6	200℃	H_2

Finally, a series of additional catalysts was prepared to explore in more depth the influence of pH of preparation for cationic exchange using alumina as a support, especially given that only one alumina catalyst had been prepared above by cationic exchange in the favourable pH region. These additional alumina catalysts are represented in Table 2.4.

Table 2.4. Catalysts prepared to investigate the effect of preparation pH

Catalyst code	Support	Precursor	Initial pH
AL-CAT-7.6	Alumina	$Au(NH_3)_4(NO_3)_3$	7.6
AL-CAT-8.0	Alumina	$Au(NH_3)_4(NO_3)_3$	8.0
AL-CAT-8.5	Alumina	$Au(NH_3)_4(NO_3)_3$	8.5
AL-CAT-9.0	Alumina	$Au(NH_3)_4(NO_3)_3$	9.0
AL-CAT-9.5	Alumina	$Au(NH_3)_4(NO_3)_3$	9.5
AL-CAT-10.0	Alumina	$Au(NH_3)_4(NO_3)_3$	10.0
AL-CAT-11.0	Alumina	$Au(NH_3)_4(NO_3)_3$	11.0
AL-CAT-12.0	Alumina	$Au(NH_3)_4(NO_3)_3$	12.0

Note that this series of catalysts was prepared by two final year BSc (Chemical Engineering) students for their final year research project which was supervised by J. Case and E. van Steen (Khumalo and Mbolekwa, 2008).

University of Cape Town

2.2 Catalyst characterisation

2.2.1 Gold loading

2.2.1.1 Atomic Absorption Spectroscopy (AAS)

The mass composition of the catalyst was determined using atomic absorption spectroscopy (AAS). The solid catalysts were digested with concentrated acid (details below) and the gold content of this solution was established. The filtrate and wash solutions were also analysed for gold content. Using the information on the gold content of the precursor solutions, a gold balance could be established allowing for some check on the validity of the results.

The acid digestion of the solid catalysts proceeded as follows. 0.1 g of the sample was put into an Erlenmeyer flask which was placed on a heating plate. To this was added 10 ml of a 4:1 HCl/HF mixture, and the contents were heated until boiling. 10 ml of HNO_3 was then added and the mixture was boiled until the volume reduced to approximately 2 ml. Hereafter 5 ml $HClO_4$ was added and the mixture was again boiled until the volume again reduced to approximately 2 ml. At this point a white cloud was observed. The mixture was then made up to 100 ml with deionised water and analysed with AAS.

2.2.1.2 Thermogravimetric Analysis (TGA)

For catalysts with a carbon support, it is possible that the acid digestion does not fully release all gold into solution. Further investigation of the gold loading was then carried out using thermogravimetric analysis (TGA). The ash content of the carbon support was first established as 2.18 %, following which the Au/C catalyst was combusted to yield ash and gold. The sample was loaded in the apparatus with a constant air flow rate and the temperature was increased to 850 °C with a temperature ramp of 15 °C/min, held at 850 °C for 1 hour, and then decreased again to 25 °C using the same ramp. The initial and final mass of the sample was recorded allowing for the determination of the gold loading (wt-%):

$$ash = \frac{2.18\,\% \times (m_i - m_f)}{(1 - 2.18\,\%)}$$

$$Au\ loading = \frac{m_f - ash}{m_i} \times 100$$

University of Cape Town

2.2.2 Gold crystallite size

Three methods were used to determine the size of the gold crystallites on the surface of the support: Transmission Electron Microscopy (TEM), X-Ray Diffraction (XRD) and oxygen chemisorption.

2.2.2.1 Transmission Electron Microscopy (TEM)

A small amount of catalyst was dispersed in methanol and dropped onto a carbon-coated copper grid. The samples were analysed in a JEM 1200EXII (JEOL) TEM apparatus operated at 120 kV. For each sample at least two micrographs were taken (the cost of the analysis did not allow for more images), and sizes of identified gold crystallites were determined by using ImageJ © software on these images. In some cases, more than 100 crystallites were identified for a particular catalyst, but more generally this amount was lower. In the analysis a conservative protocol was adopted where Au crystallites were only identified as such if they displayed both as dark regions and also with roughly spherical or hexagonal shapes. In many cases two crystallites which might look as if they were joined together were assumed rather to be overlapping and therefore measured separately.

2.2.2.2 X-Ray Diffraction (XRD)

X-Ray diffractograms were produced using a Philips PW 1390 diffractometer with Cu-Kα radiation, operated at a wavelength of 1.5418 Å, a voltage of 40kV, a current of 20 mA and using a step size of $2\theta = 0.01$ º.

2.2.2.3 Oxygen chemisorption

It has been noted that chemisorption has not been well established as a characterisation method for gold catalysts compared to its use with other metal catalysts (Berndt et al., 2003). For static oxygen chemisorption on gold catalysts a recent study has shown that reductive pre-treatment with hydrogen is needed to ensure removal of all oxygen on the catalyst surface; it also showed that this treatment does not substantially alter the catalyst crystallite size (Berndt et al., 2003). For static oxygen chemisorption conducted at 200 ºC at low pressures (3-12 mmHg) a good agreement was founded between crystallite sizes calculated

University of Cape Town

from these data (assuming dissociative adsorption) and results from TEM (Berndt et al., 2003).

In the present study static oxygen chemisorption was carried out in an adsorption apparatus ASAP 2020C (Micrometrics) which has a U-shaped quartz tube reactor allowing for pre-treatments under flowing gas followed by measurement of oxygen uptake. Pre-treatment used pure hydrogen at 200 ºC for 16 hours followed by 2 hours of evacuation. Treatment with pure oxygen was conducted at 200 ºC with the majority of measurements in the range 0.1 till 10 mmHg, followed by an increase up to a pressure of approximately 700 mmHg.

The maximum amount of catalyst was loaded for each run; this generally amounted to between 0.3 and 0.6 g. Even with the maximum loading, some samples with poor chemisorption behaviour yielded negative values at low pressures; no further analysis was possible in these cases.

University of Cape Town

2.3 Catalyst testing

The gold catalysed liquid phase oxidation of ethylene glycol was selected as the test reaction in the present study. The desired reaction in which glycolic acid is produced is represented below:

$$\underset{\text{ethylene glycol (EG)}}{HO–CH_2–CH_2–OH} + ½\,O_2 + NaOH \rightarrow \underset{\text{sodium glycolate (GLYA)}}{HO–CH_2–COONa} + 2\,H_2O$$

The experimental set-up for this study, shown in Figure 2.3 below, was based on that described in Berndt et al. (2003), with the exception of using a magnetic instead of a mechanical stirrer.

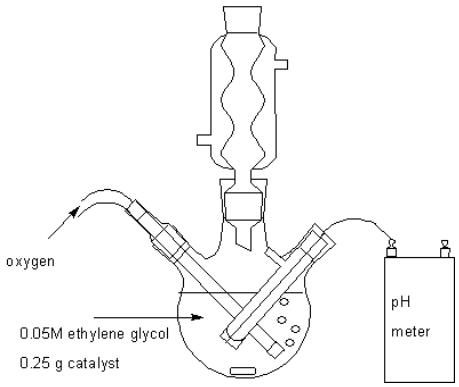

Figure 2.3. Experimental set-up for catalyst testing using ethylene glycol oxidation

The reaction took place in a three-necked round-bottomed flask. A glass-fritted sparger was used for the introduction of oxygen to the reaction mixture, and the pH was measured continuously through the presence of a pH probe. The flask was positioned in a water bath over a magnetic stirrer and heating plate. The stirrer was set at the maximum amount with smooth stirring (before the magnetic bar jumps around); this amounted to 700 rpm in the pilot runs, and 100 rpm in the catalyst testing when a new stirrer plate was used. An overhead condenser was used to ensure that no water vapour left the system.

2.3.1.1 Quantitative measurement of reaction rate using NaOH titration

0.25 g of the catalyst was introduced to the reaction vessel with 200 ml of deionised water. The pH was adjusted using 0.1 M NaOH. Pure oxygen was introduced through the sparger at a rate of approximately 0.5 ml/s, and the solution was stirred for a period of approximately 30 minutes at which point the now stable pH reading was recorded. 0.55 ml (10 mmol) of ethylene glycol was then added and time measurements commenced. In order to measure the rate of acid formation, 0.1 M NaOH was added 1 ml at a time, and the time was recorded when the pH had decreased to its original value, where after a further 1 ml was added. The reaction was allowed to run for 1 hour. These data allowed then for the plotting of conversion versus time and the calculation of initial reaction rates. (Glycolic acid has a pK_a value of 3.83 and thus is fully dissociated in the alkaline reaction medium).

2.3.1.2 High Pressure Liquid Chromatography (HPLC)

The final reaction mixture was made up to 500 ml and a small sample of this was used for analysis on a Merck Hitachi LaChrom HPLC apparatus equipped with UV (210 nm) and RI detectors. The organic products were separated using a BioRad Aminex HPX-87-H column at room temperature and a pressure of 1000 psi. The mobile phase was 0.01M H_2SO_4 with a flow rate of 0.5 ml/min. The reaction products were identified following analysis of standard solutions of potential oxidation products of ethylene glycol.

University of Cape Town

Chapter 3. Results

3.1 Catalyst characterisation

The two key parameters for characterising supported gold catalysts are gold loading and gold crystallite size. Determination of these parameters is presented in the following two sections.

3.1.1 Gold loading

3.1.1.1 Atomic Absorption Spectroscopy (AAS)

Table 3.1 presents the wt-% Au for each prepared catalyst. The theoretical loadings are based on analysis of the precursor solution, assuming 100% loading efficiency, and the actual loadings are based on analysis of the digested solid catalysts. For three of the four activated carbon catalysts practically 100% loading of the gold present can be assumed to have been achieved, taking into account the experimental error associated with the analysis. This indicates a generally strong affinity for gold by the carbon support. The alumina catalysts prepared by anionic exchange had relatively low loadings, while those prepared by cationic exchange in a favourable pH region had a relatively high loading.

The actual loadings range from about 1.5 to 4.5 wt-% Au, with the exception of the catalyst AL-CAT-6.4 which was prepared by cationic exchange at a pH below the IEP of alumina (≈8) and a low loading was thus anticipated. For these catalysts, there are no clear trends regarding the influence of the pH of preparation on Au loading. For the pair C-AN-0.6 and C-AN-2.3 it was expected that the former, prepared by anionic exchange below the IEP of activated carbon (≈1.5), would have a higher loading, and this is noted although the difference is relatively insignificant. This might be due to physical absorption of the complex by the carbon support. For the pair C-CAT-2.4 and C-CAT-5.0, it was expected that the latter would have a higher loading, being further away from the IEP, but this was not found. Likewise for AL-AN-3.2 and AL-AN-6.1, where the former had a lower rather than the expected higher loading. In this case the effect could be due to dissolution of the alumina support at the lower pH.

University of Cape Town

Table 3.1. Au loading of catalysts

Catalyst code	Support	Precursor	Initial pH	Wt-% Au theoretical*	Wt-% Au actual **
C-AN-0.6	Activated Carbon	$HAuCl_4$	0.6	3.64%	4.39%
C-AN-2.3	Activated Carbon	$HAuCl_4$	2.3	4.10%	4.10%
C-CAT-2.4	Activated Carbon	$Au(NH_3)_4(NO_3)_3$	2.4	2.94%	3.12%
C-CAT-5.0	Activated Carbon	$Au(NH_3)_4(NO_3)_3$	5.0	2.94%	2.00%
AL-AN-3.2	Alumina	$HAuCl_4$	3.2	3.59%	1.59%
AL-AN-6.1	Alumina	$HAuCl_4$	6.1	3.81%	2.12%
AL-CAT-6.4	Alumina	$Au(NH_3)_4(NO_3)_3$	6.4	3.43%	0.17%
AL-CAT-10.6	Alumina	$Au(NH_3)_4(NO_3)_3$	10.6	3.43%	2.97%

* Wt- % Au based on analysis of the precursor solution, assuming 100% loading efficiency – these data not available for all the catalysts
** Wt-% Au based on analysis of digested solid catalyst

AAS conducted on samples of the precursor solutions taken at intervals during the aging period, allowed for an analysis of Au uptake over time, presented in Figure 3.1 below. For C-AN-0.6, one of the first catalysts prepared, it can be seen that approximately 99% of the overall Au uptake occurred during the first two hours of aging. It was therefore decided to shorten the aging period to two hours. However, as noted above, the Au uptake over these two hours was relatively low for the alumina catalysts prepared by anionic exchange, and therefore for the remaining catalysts (prepared by cationic exchange) the aging period was reverted to 20 hours. For these catalysts, excluding AL-CAT-6.4 discussed above, approximately 80% of the total Au uptake took place in the first two hours.

University of Cape Town

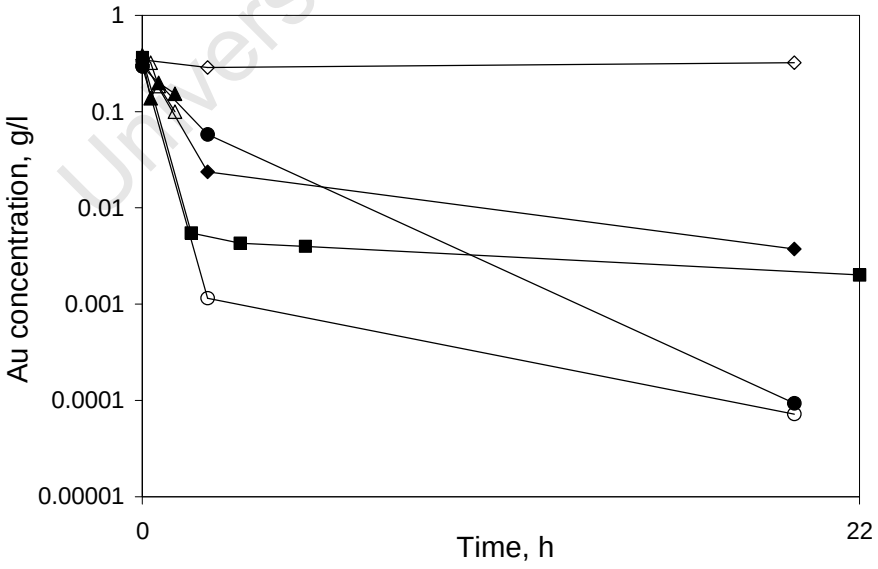

Figure 3.1. Gold concentration of precursor solution over time during catalyst preparation (■ C-AN-0.6; ▲ AL-AN-3.2; Δ AL-AN-6.1; ● C-CAT-2.4; ○ C-CAT-5.0; ♦ AL-CAT-10.6; ◊ AL-CAT-6.4)

A mass balance was conducted to give some indication of the level of error in the AAS results. This compares the combined Au output in the filtrate solutions and the solid catalyst with the Au present in the precursor solution. The difference between the Au input and Au output is represented as 'missing' in Figure 3.2 below. In the three cases mentioned above where a calculated 'loading efficiency' would be greater than 100%, the 'missing' Au is given as a negative amount. What is also clearly represented in this graph are the catalysts with lower uptake, as represented by significant Au in the filtrates, shown in the dotted regions.

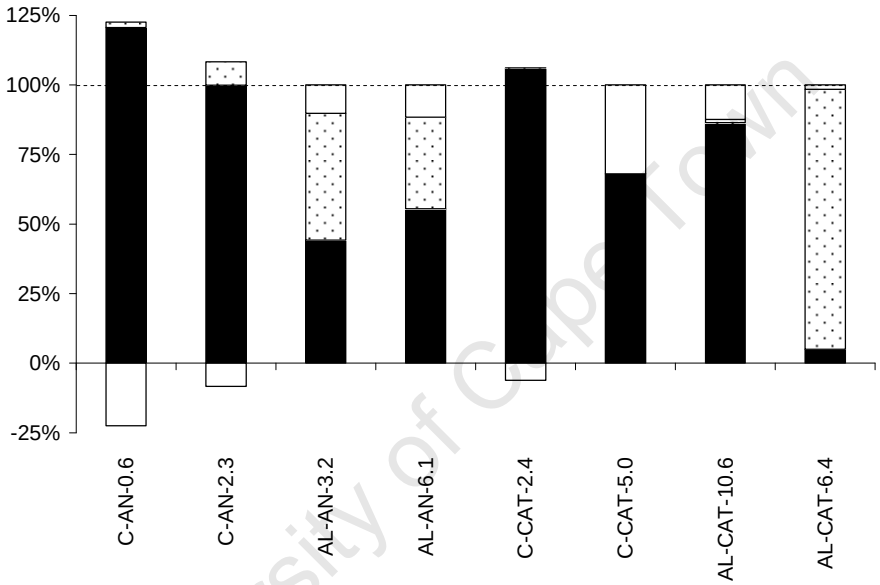

University of Cape Town

Figure 3.2. Gold balance based on AA analysis of precursor solution, filtrates and solid catalyst (black regions: catalyst; dotted regions: combined initial and ammonia wash filtrates; white regions: missing)
(Note that for C-AN-2.3 the analysis of the initial filtrate gave negative results and so only ammonia wash filtrate is represented here)

A range of additional alumina catalysts was prepared by cationic exchange in order to investigate the effect of preparation pH on gold loading. The Au loading of these catalysts is represented in Figure 3.3 below, ordered with increasing pH of preparation. These data show some evidence of stronger electrostatic attraction the further one deviates from the IEP, assuming similar initial precursor solution concentrations[3]. There appears to be a significant increase at pH = 10 followed by a slight decrease at pH = 12.

[3] These measurements were not taken.

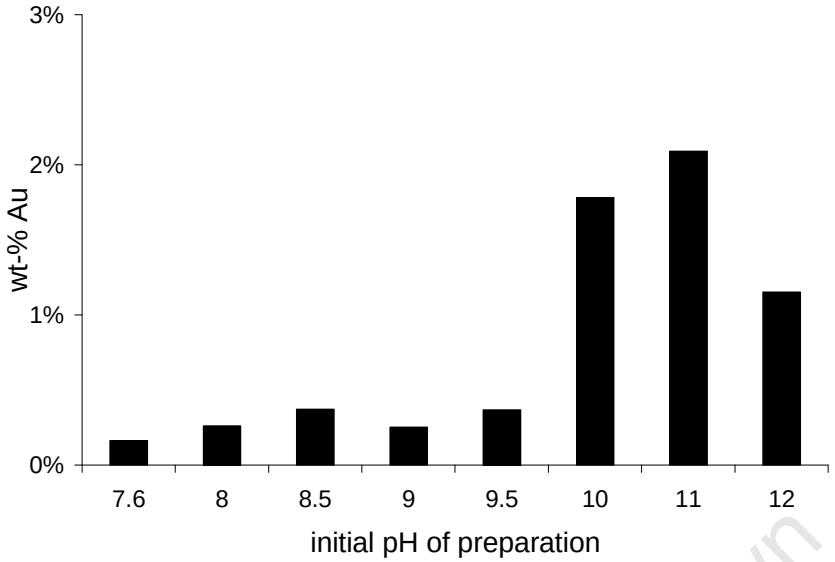

Figure 3.3. Gold loading for Au/Al_2O_3 catalysts prepared at different pHs

For the catalysts prepared by anionic exchange, AAS was conducted both on the initial wash and the subsequent ammonia wash in order to assess the Au lost during this latter additional wash. These results are presented below in Table 3.2. It can be seen that the additional Au lost during the ammonia wash is generally low.

Table 3.2. Au lost during ammonia wash

Catalyst code	% Au lost in NH_3 wash*
C-AN-0.6	1.4%
AL-AN-3.2	2.9%
AL-AN-6.1	6.8%

*calculated as % of total Au in initial precursor solution

3.1.1.2 Thermogravimetric Analysis (TGA)

The AAS on solid carbon supported catalysts relies on an assumption that the acid digestion releases all the Au to solution. In order to allow for some check of this assumption, TGA was conducted on the carbon supported catalysts which had been prepared by anionic exchange, including the additional catalyst which had been prepared without ammonia washing (C-AN-0.6 no wash). For these three catalysts the wt-% Au derived from TGA is compared with that from AAS in Table 3.3 below. There is considerable variance between these two sets of results, and there is no clear trend. If the acid digestion was not completely releasing all Au to solution then one would expect the TGA results to be systematically higher than the

University of Cape Town

AAS results. This is the case in only two out of the three catalysts, and it is therefore not possible to firmly draw that conclusion. More likely these results need to be taken as a further representation of the experimental error in the calculation of Au loading, which is similar in order of magnitude to that derived above from the Au balance.

Table 3.3. Comparison of wt-% Au from TGA and from AAS

Catalyst	Wt-% Au (TGA)	Wt-% Au (AAS)	% error
C-AN-0.6 no wash	3.78%	3.06%	24%
C-AN-0.6	3.48%	4.39%	21%
C-AN-2.3	4.48%	4.10%	9%

3.1.2 Gold crystallite size

3.1.2.1 Transmission Electron Microscopy (TEM)

A sample TEM image for one of the carbon supported catalysts is presented in Figure 3.4 below. The carbon support is evident as a greyish streaked background, and the gold crystals show clearly as round dark crystallites. It should be noted that this was one of the 'better' images for analysis, with a large number of crystals available for measuring.

A sample TEM image of an alumina supported catalyst is given in Figure 3.5 below. The alumina support presents as a speckled background, with the Au crystals again as dark circular regions. Once again, this is one of the 'better' images achieved in the first round of TEM analysis. Subsequently, the catalyst supported in methanol was treated with ultrasound before distribution on the carbon grid, and this led to images such as that represented in Figure 3.6 where the support has broken up into smaller crystallites.

Additional TEM images are given in Appendix A.

University of Cape Town

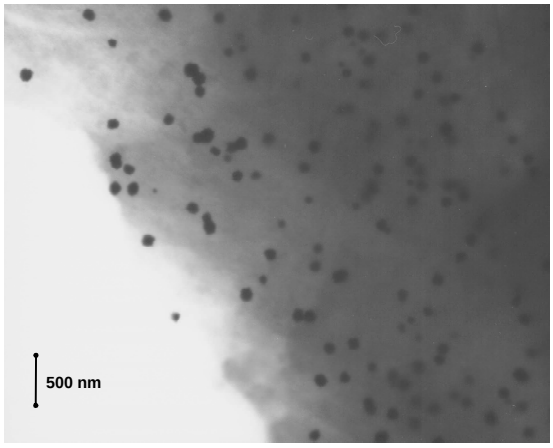

Figure 3.4. TEM image for catalyst C-CAT-5.0

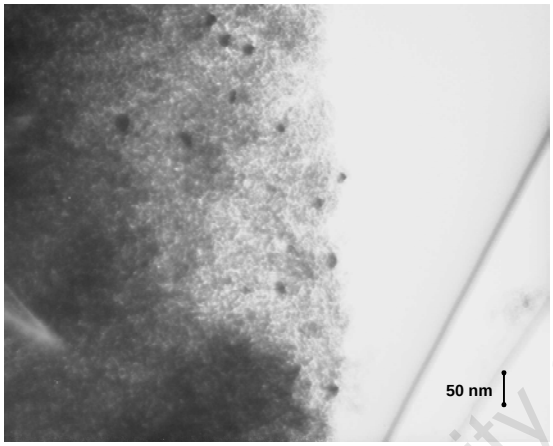

Figure 3.5. TEM image for catalyst AL-CAT-10.6-200AIR

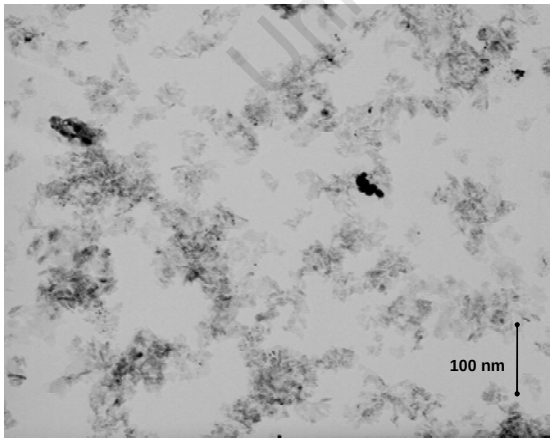

Figure 3.6. TEM image for catalyst AL-CAT-9.5

University of Cape Town

The analysis of TEM images from all carbon supported catalysts is given in Figure 3.7 below. These catalysts generally have fairly large average Au crystallite sizes (calculated by geometric mean to avoid overdue influence of outliers), and mostly display a very large spread in crystallite size. For both anionic and cationic exchange it is the catalysts prepared at the more acidic pHs that have smaller Au crystal sizes and relatively small size distributions. The sample sizes given here illustrate the relatively low numbers of crystallites available for measuring in most of these images, with the exception of C-CAT-5.0.

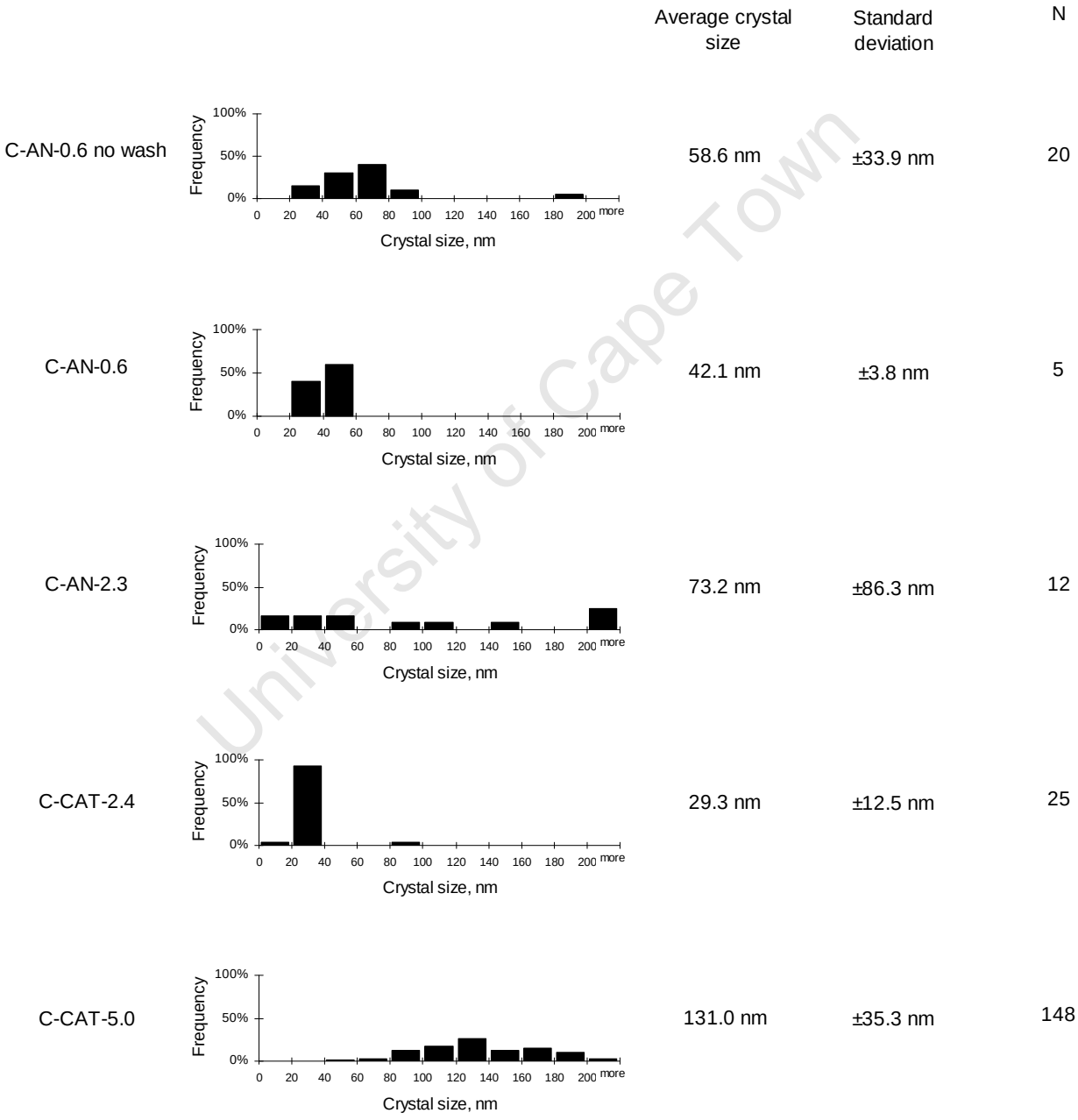

University of Cape Town

Figure 3.7. TEM analysis of all carbon supported catalysts

The analysis of TEM images from all alumina supported catalysts is given in Figure 3.8 and Figure 3.9 below. It will be noted that the alumina catalysts all have smaller Au crystal size than the carbon supported catalysts. They also have narrower size distributions. Out of the initial series of alumina catalysts, it is the catalyst prepared by anionic exchange at the lowest pH which gave the smallest crystallites. Considering the additional catalysts prepared by cationic exchange at a range of pHs, there is no clear influence of pH on crystallite size that can be deduced from these results. Overall it can also be noted that the TEM images of the alumina catalysts yielded more crystallites for measurement; this appears at least partly due to the revised method involving ultrasound treatment which gave better images for analysis.

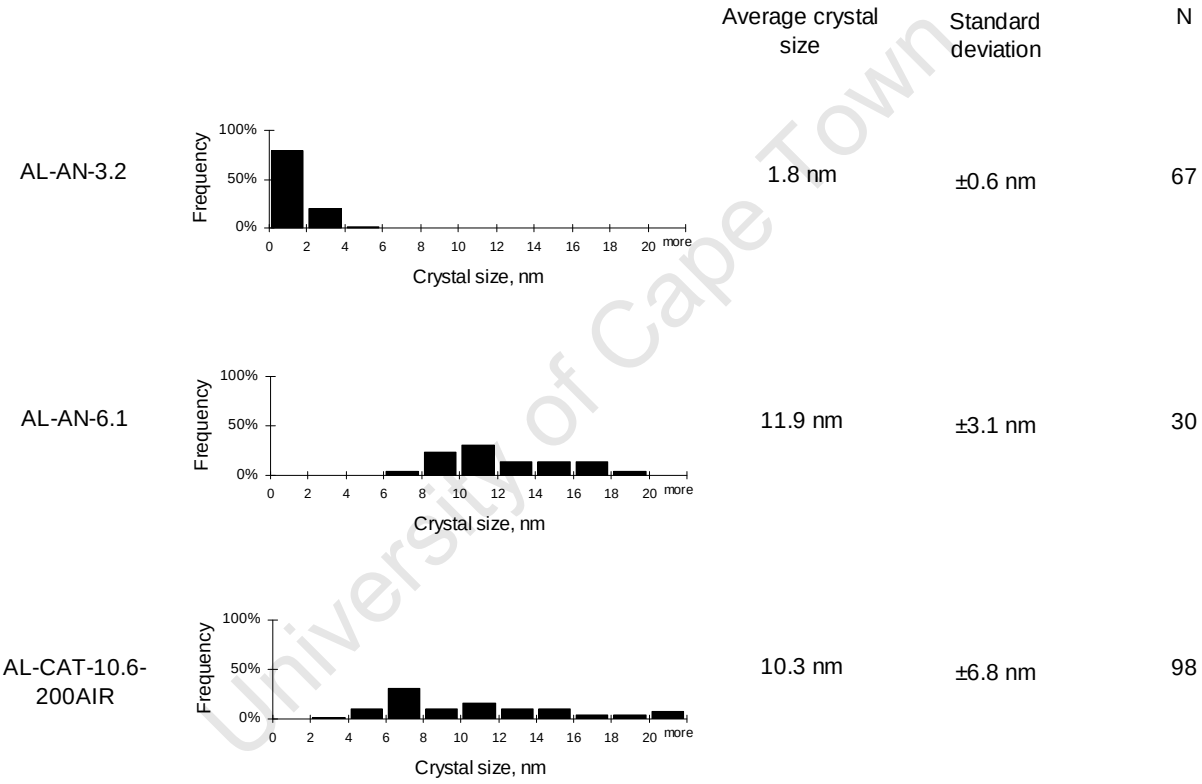

Figure 3.8. TEM analysis of initial series of alumina supported catalysts
(Note that only AL-CAT-10.6-200AIR is represented here: the other AL-CAT-10.6 catalysts did not yield TEM images of an adequate quality for analysis.)

University of Cape Town

		Average crystal size	Standard deviation	N
AL-CAT-7.6	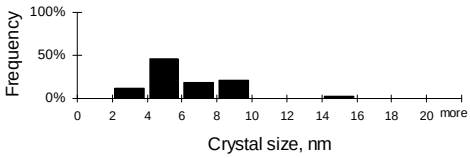	5.8 nm	±2.6 nm	33
AL-CAT-8.0	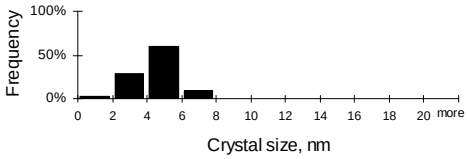	4.1 nm	±1.2 nm	42
AL-CAT-8.5	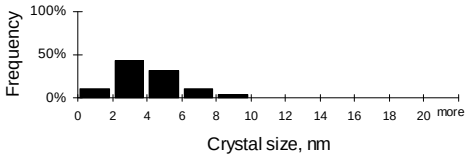	3.5 nm	±1.9 nm	28
AL-CAT-9.0	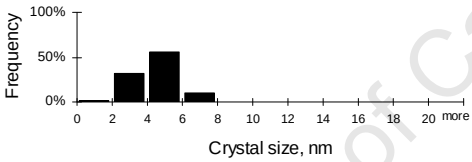	4.1 nm	±1.3 nm	59
AL-CAT-9.5	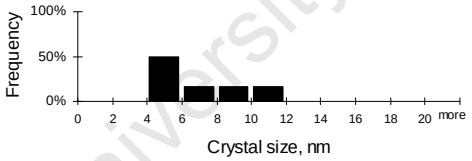	6.3 nm	±2.4 nm	18
AL-CAT-10.0	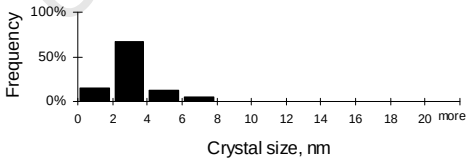	2.8 nm	±1.4 nm	39
AL-CAT-11.0	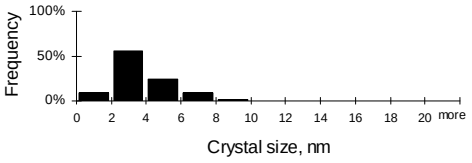	3.4 nm	±1.6 nm	57
AL-CAT-12.0	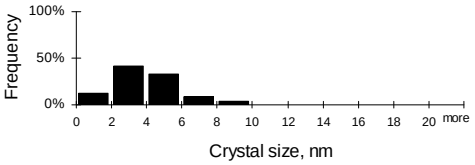	3.7 nm	±1.7 nm	24

Figure 3.9. TEM analysis of additional alumina supported catalysts

University of Cape Town

3.1.2.2 X-Ray Diffraction (XRD)

Figure 3.10 shows a sample diffractogram of one of the carbon supported catalysts with the gold peaks labelled according to the crystalline planes which gave rise to them. Because the carbon is amorphous it does not produce any peaks on the XRD.

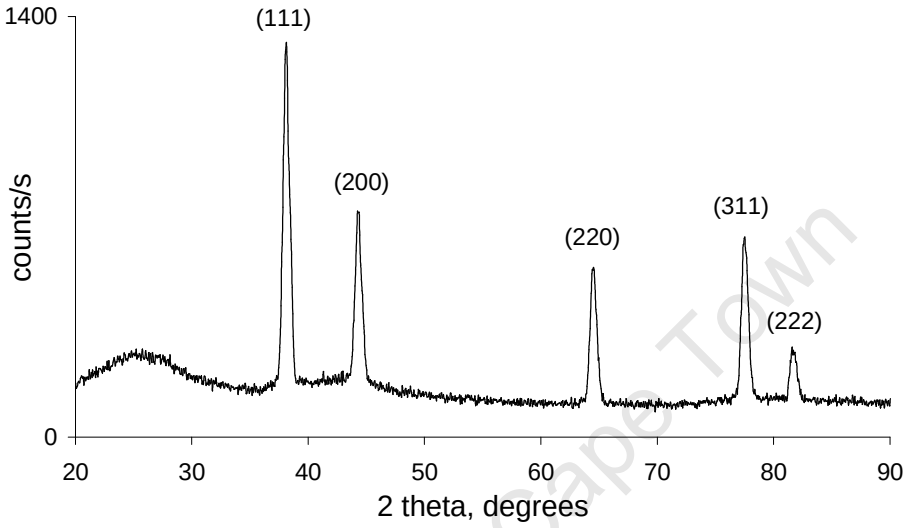

Figure 3.10. Sample diffractogram of carbon supported catalyst

For these diffractograms with clear gold peaks, it was possible to calculate crystallite size from a measurement of peak breadth at half height using the Scherrer equation:

$$d = \frac{K\lambda}{\beta \cos\theta}$$

where β represents this measured breadth, given in radians, corrected for machine broadening (0.002782 rad). θ is the angle at which the peak is measured (also in radians) and the constants are $K = 0.9$ and $\lambda = 1.54 \times 10^{-10}$ m.

The crystallite sizes calculated in this manner are given in Table 3.4 below. From the similarity of results across the different peaks it can be deduced that the Au crystallites are spherical. The only exception here is the (222) peak which as can be seen above has a much lower intensity than the others and therefore would likely have greater error associated with measurement of peak breadth.

University of Cape Town

Table 3.4. Calculation of crystallite size for carbon supported catalysts based on XRD results

Catalyst code	(hkl) plane	Crystallite size, nm
C-AN-0.6 no wash	111	21.8
	200	20.9
	220	21.3
	311	23.7
	222	26.2
C-AN-0.6	111	16.9
	200	16.1
	220	18.9
	311	18.8
	222	21.6
C-AN-2.3	111	32.3
	200	25.2
	220	25.1
	311	23.3
	222	28.4
C-CAT-2.4	111	14.1
	200	15.2
	220	15.4
	311	16.6
	222	23.9
C-CAT-5.0	111	20.9
	200	18.4
	220	17.4
	311	19.9
	222	19.6

University of Cape Town

The diffractograms from the alumina supported catalysts presented significant complications for this analysis given the crystalline nature of the alumina support. Figure 3.11 shows a sample diffractogram for one of these catalysts, with that of blank alumina overlaid.

Simple scaling and subtraction of one diffractogram from another did not give sufficiently clear peaks for a Scherrer equation based analysis. It was not therefore possible to determine the crystallite size for these catalysts, given the scope of this thesis. Further studies could involve a Rietveld refinement of the data.

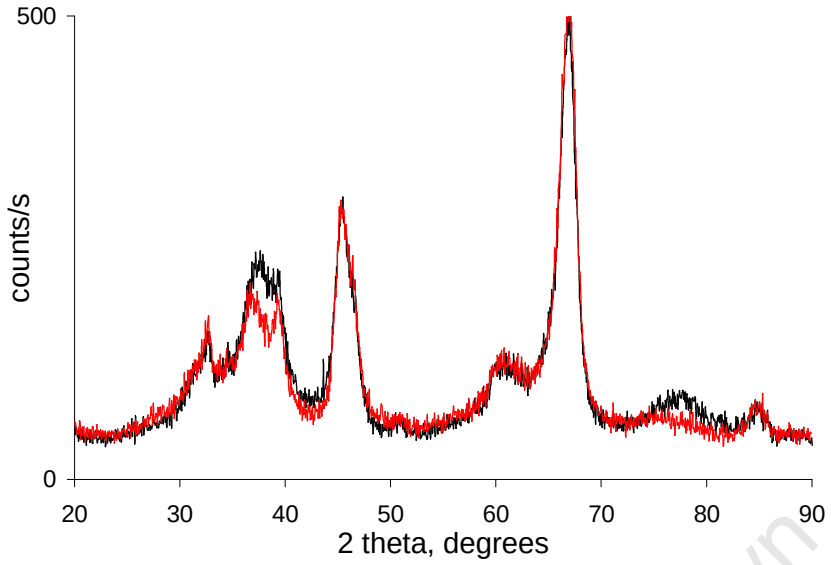

Figure 3.11. Sample diffractogram of alumina supported catalyst with blank alumina overlaid (black: Au/Al_2O_3 catalyst; red: blank Al_2O_3)

3.1.2.3 Oxygen Chemisorption

The adsorption/absorption behaviour for the carbon supported catalysts together with that of blank activated carbon is shown in Figure 3.12 below. It can be seen that blank carbon is a very strong absorber and that in fact the presence of gold crystallites on the surface actually diminishes this chemisorption ability by blocking of the pores. The catalysts appear to cluster into two groups of relatively similar chemisorption behaviour, one notably stronger than the other. It is speculated that this might be due to modifications to the carbon surface during the catalyst preparation phase, since those with the poorer chemisorption behaviour were the two that were prepared under the most highly acidic conditions at pH = 0.6.

University of Cape Town

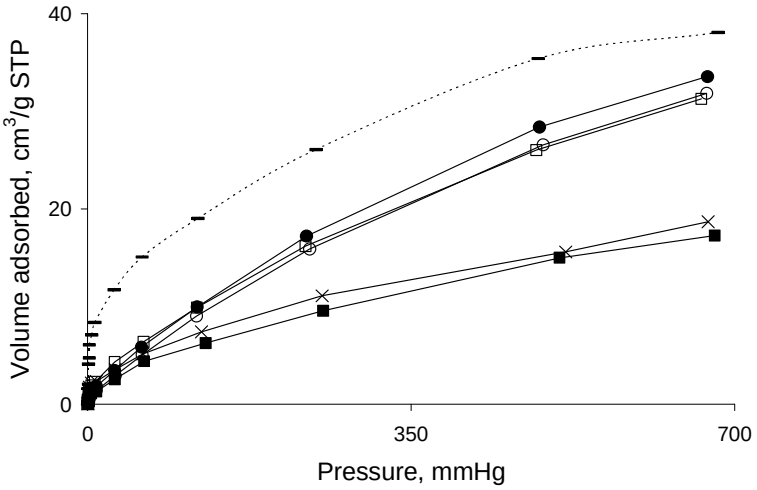

Figure 3.12. Chemisorption behaviour of carbon supported catalysts
(- blank carbon; × C-AN-06 no wash; ■ C-AN-06; □ C-AN-2.3; ● C-CAT-2.4; ○ C-CAT-5.0)

All catalysts were tested for chemisorption before and after calcination. Only those three catalysts with the stronger chemisorption in the above graph gave measurable chemisorption results before calcination. (For the remaining catalysts the adsorption at low pressures was too low and the system yielded negative data points.) These two sets of data are compared below in Figure 3.13. There are no clear trends evident and it can be tentatively concluded that the marginal differences between these sets of data are simply due to experimental error.

University of Cape Town

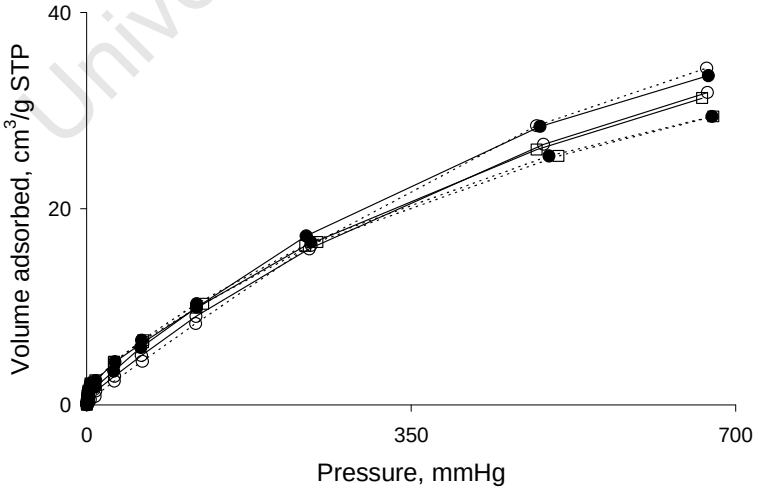

Figure 3.13. Comparison of chemisorption behaviour before and after calcination for three carbon supported catalysts
(dotted line: before calcination; solid line: after calcination)
(□ C-AN-2.3; ● C-CAT-2.4; ○ C-CAT-5.0)

The chemisorption behaviour for the alumina supported catalysts is represented in Figure 3.14 below. These catalysts adsorb much less oxygen than the carbon supported catalysts. Blank alumina did not demonstrate sufficient chemisorption at low pressures for the data to be used. It can therefore be deduced that the chemisorption behaviour of alumina supported gold catalysts is solely due to the Au crystallites present on the alumina support. It needs to be noted that three of the alumina catalysts did not display sufficient adsorption at low pressures for the data to be used (Al-CAT-7.6, AL-CAT-8.5 and AL-CAT-9.0).

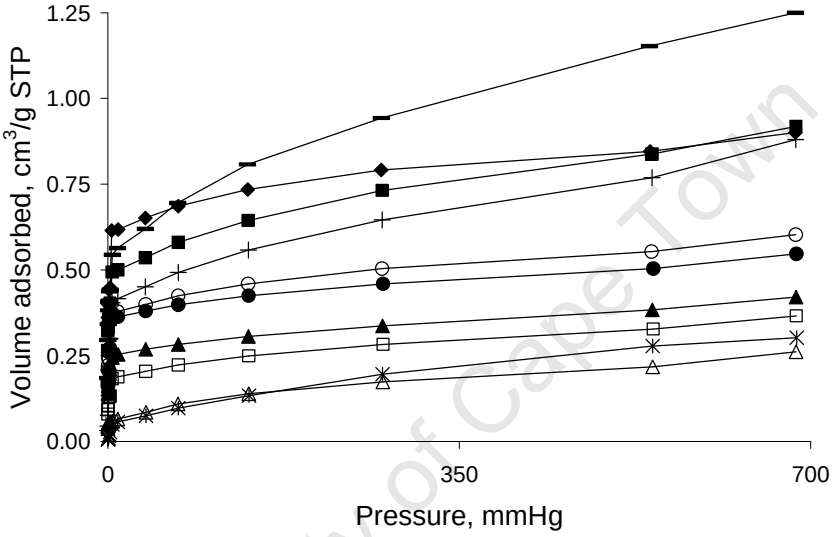

Figure 3.14. Chemisorption behaviour of alumina supported catalysts
(♦ AL-CAT-10.6-300H2; ■ AL-CAT-10.6-200H2; ○ AL-CAT-10.6-200AIR; ▲ AL-AN-3.2; ∆ AL-AN-6.1; ✳ AL-CAT-8.0; + AL-CAT-9.5; □ AL-CAT-10.0; - AL-CAT-11.0; ● AL-CAT-12.0)

There was only one catalyst that demonstrated any measurable chemisorption ability before calcination, and these comparative data are given in Figure 3.15 below. Calcining appears to have a dramatic effect on the chemisorption behaviour of alumina supported catalysts, activating Au crystallites for chemisorption.

University of Cape Town

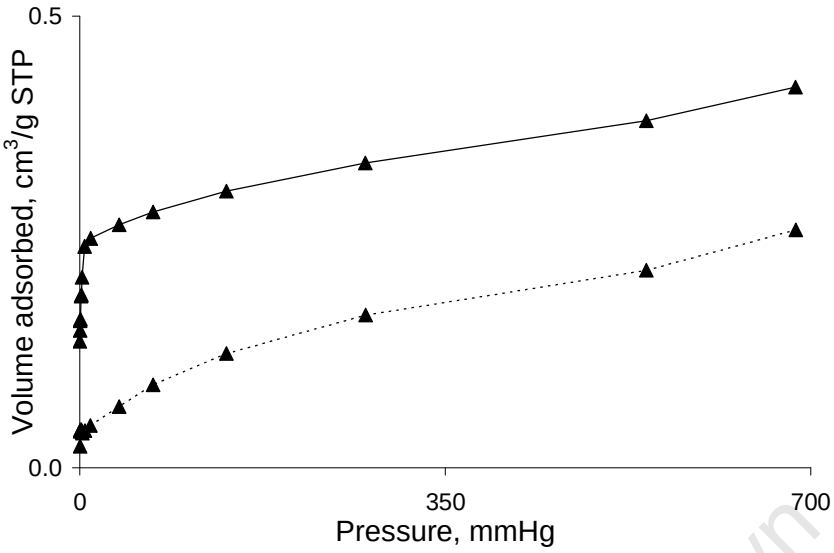

Figure 3.15. Comparison of chemisorption behaviour before and after calcinations for one alumina supported catalyst
(dotted line: before calcination; solid line: after calcination)
(▲ AL-AN-3.2)

Given that the chemisorption behaviour of the alumina supported catalysts was found to be solely due to chemisorption on Au crystallites, it was possible to model these data using the following dual isotherm:

$$V_{O_2-adsorbed} = V_{m,1} \cdot \frac{K_2 \cdot p_{O_2}^{\frac{1}{n}}}{1 + K_2 \cdot p_{O_2}^{\frac{1}{n}}} + V_{m,2} \cdot \frac{K_2 \cdot p_{O_2}^{\frac{1}{m}}}{1 + K_2 \cdot p_{O_2}^{\frac{1}{m}}}$$

The results are graphed below in Figure 3.16, with the isotherm parameters given in Table 3.5.

University of Cape Town

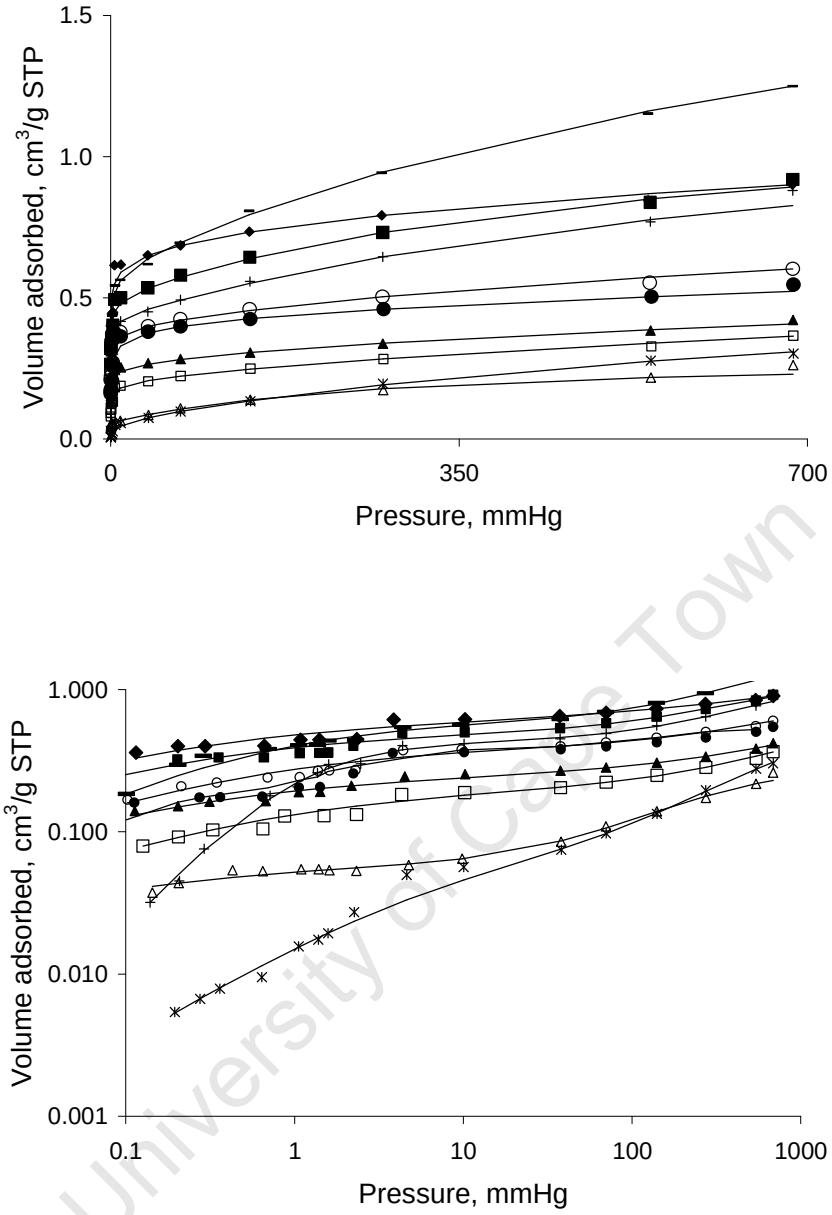

University of Cape Town

Figure 3.16. Modelling of chemisorption behaviour of alumina supported catalysts
(♦ AL-CAT-10.6-300H2; ■ AL-CAT-10.6-200H2; ○ AL-CAT-10.6-200AIR; ▲ AL-AN-3.2; ∆ AL-AN-6.1; ✳ AL-CAT-8.0; + AL-CAT-9.5; □ AL-CAT-10.0; - AL-CAT-11.0; ● AL-CAT-12.0)
(solid line: model)

Table 3.5. Calculated isotherm parameters

	AL-AN-3.2	AL-AN-6.1	AL-CAT-10.6-300H2	AL-CAT-10.6-200AIR	AL-CAT-10.6-200H2	AL-CAT-8.0	AL-CAT-9.5	AL-CAT-10.0	AL-CAT-11.0	AL-CAT-12.0
V_{m1}	0.248	0.060	0.598	0.413	0.518	0.069	0.428	0.205	0.613	0.391
V_{m2}	1.637	0.233	2.739	0.537	0.696	0.585	0.820	1.069	1.501	3.534
n	2.0	2.0	2.0	2.0	2.0	1.4	0.8	2.0	1.6	2.0
m	1.6	1.0	2.0	1.0	1.0	1.0	1.0	1.3	1.0	1.7
K_1	3.317	5.726	3.536	1.966	3.013	0.266	1.026	1.769	1.885	1.323
K_2	0.002	0.003	0.005	0.001	0.002	0.001	0.001	0.001	0.001	0.001
% error*	6.0	3.7	5.3	5.3	5.3	6.3	3.8	3.8	3.8	7.2

*% error defined as average % error over all data points ($|(V_{model} - V_{actual})/ V_{actual}|$)

Using the results for V_{m1} and n as determined above (for the strong adsorption phase) it was possible to calculate crystallite size, d. Firstly the monolayer volume, V_{m1} (cm^3 O_2 / g catalyst), is converted to a measurement of dispersion, D (gmol Au (surface) / gmol Au (total)), using the Au loading determined earlier for each catalyst. Crystallite size, d, can then be calculated using the following equation which is based on an assumption of spherical crystallites:

$$d = \frac{6 \times n \times 197}{D \times N_A \times \rho}$$

with n = 1.15 X 10^{19} atoms/m^2 (Berndt et al., 2003) and the density of Au, ρ = 1.93 X 10^7 g/m^3.

These results are given below in Table 3.6.

Table 3.6. Crystallite size calculated from chemisorption data

Catalyst code	Crystallite size, nm
AL-AN-3.2	4.3
AL-AN-6.1	23.5
AL-CAT-10.6-300H2	3.3
AL-CAT-10.6-200AIR	3.8
AL-CAT-10.6-200H2	4.8
AL-CAT-7.6*	-
AL-CAT-8.0	3.6
AL-CAT-8.5*	-
AL-CAT-9.0*	-
AL-CAT-9.5	1.4
AL-CAT-10.0	5.8
AL-CAT-11.0	2.8
AL-CAT-12.0	2.0

*These catalysts did not display sufficient chemisorption at low pressures for measurable results.

University of Cape Town

3.2 Catalyst testing

3.2.1 Measurement of reaction rate

3.2.1.1 Establishment of reaction conditions for test reaction protocol

The first stage in this section of the study involved establishing a reaction protocol for the testing of the catalysts. The Mintek 'BC1' catalyst (1% Au/TiO_2) was used for this purpose. Early test runs suggested that appropriate levels of reactivity were present at slightly elevated temperatures, and thus all reactions reported here were carried out at 60 °C.

Working with the initial assumption that all reaction products are acidic, and working in the strongly alkaline region, the change in pH due to acid formation can be used to track reaction progress. The first method explored was proposed by Berndt et al.(2003) and involved simply monitoring the decrease in pH and correlating this with the formation of a mono-acid. The results obtained with this 'uncontrolled pH' method are shown in Figure 3.17 below, using a 0.5 M ethylene glycol solution with the initial pH at 13.7.

University of Cape Town

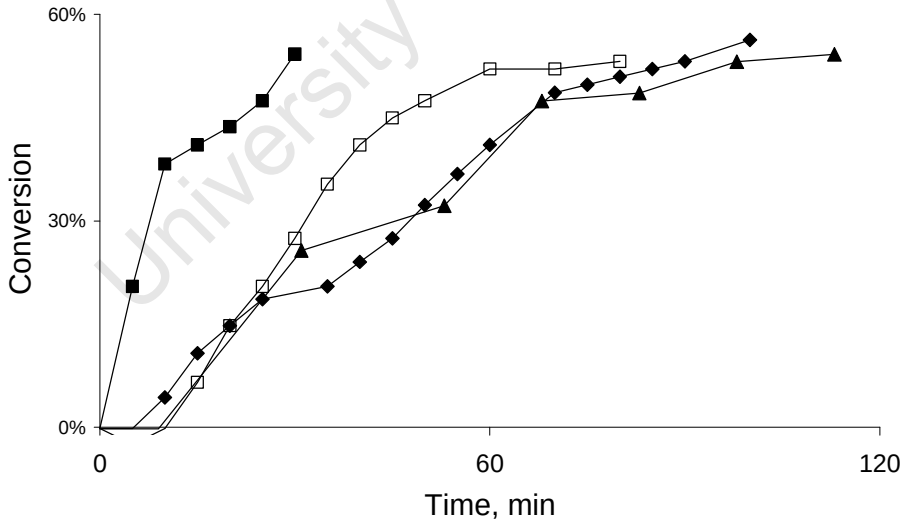

Figure 3.17. Catalyst testing using uncontrolled pH method
(Temperature = 60ºC; Magnetic stirrer 700 rpm; crushed Mintek 'BC1' catalyst; [EG] = 0.5M in 200ml solution; initial pH = 13.7)
(▲ 1 g catalyst; ♦ repeat 1 g catalyst; □ 0.5 g catalyst; ■ 1 g catalyst with sparger)

Two runs with identical conditions were initially conducted to assess reproducibility. These two runs with 1 g catalyst reached a maximum of approximately 50% conversion after an

hour, after which the reaction rate slowed down and appeared to level off. A run with 0.5 g showed rather unexpectedly a higher initial reaction rate, reaching a similar maximum conversion. A final run with this method used a glass sparger instead of a Pasteur pipet to deliver the oxygen to the reaction mixture, and as anticipated this led to a dramatically increased initial reaction rate. However, at about 50% conversion the pH stopped decreasing and actually started to increase (this is not shown on the graph). This was one of a number of perceived problems with the 'uncontrolled pH' method. In addition, it was necessary to work at a very high pH where the formation of up to 0.5 M acid did not cause too dramatic a decrease in pH. Finally, it was noted that the graphical representation of the results was dependent on the initial pH (which represents 0% conversion) and this showed some variation at the start of the reaction.

It was then decided to explore the alternative method given in Berndt et al.(2004) in which dilute NaOH is titrated to maintain a constant pH, with the volume added corresponding to the amount of acid produced. Using this method at a pH of 11 (compared to pH = 9 in Berndt et al. (2004)) with an ethylene glycol concentration of 0.5 M gave the reaction profile shown in Figure 3.18 after 1 hour. Using the pelletized form of the catalyst introduced severe internal mass transfer limitations. The crushed catalyst was therefore used for further experiments.

Comparing the runs with 1 g and 0.5 g catalyst it can be seen that the reaction rate is still determined by external mass transfer limitations under these conditions (halving the catalyst mass does not halve the reaction rate).

It was then decided to reduce the intrinsic reaction rate by decreasing the initial concentration of ethylene glycol to 0.05M (from 0.5M). In order to test for the presence of external mass transfer limitations, runs were conducted with 1 g, 0.5 g and 0.25 g of crushed catalyst. These results are given in Figure 3.19. Inspection of this graph shows an approximate halving of the reaction rate with halving of catalyst mass, which suggests that the reaction is taking place without the significant interference of external mass transfer limitations. Working on the assumption of a linear initial reaction rate, straight lines were fitted to the data. Initial rates per mass of catalyst are given below in Table 3.7; that they have a similar order of magnitude offers some support to the conclusion that the reaction is generally in the kinetic regime.

University of Cape Town

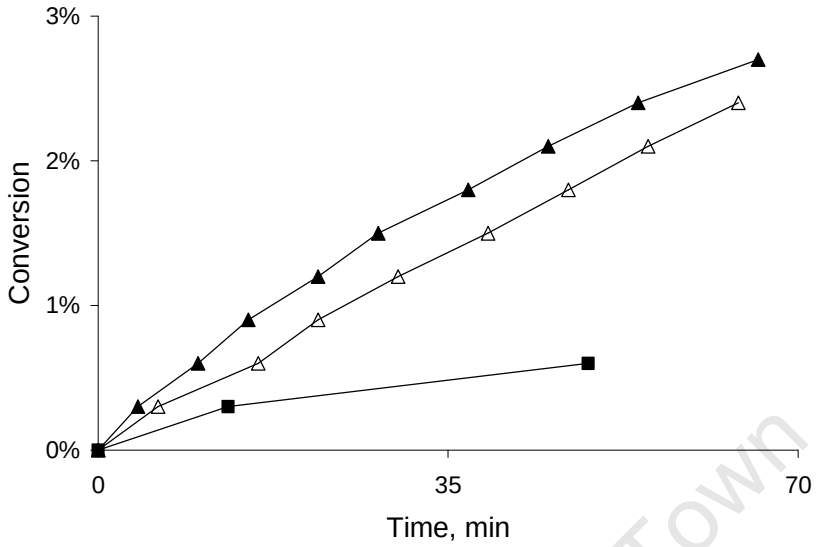

Figure 3.18. Catalyst testing using controlled pH method with 0.5 M EG
(Temperature = 60ºC; Magnetic stirrer 1000 rpm; Mintek 'BC1' catalyst; [EG] = 0.5M in 200ml solution; pH = 11)
(■ 1 g pelletized catalyst; ▲ 1 g crushed catalyst; ∆ 0.5 g crushed catalyst;)

University of Cape Town

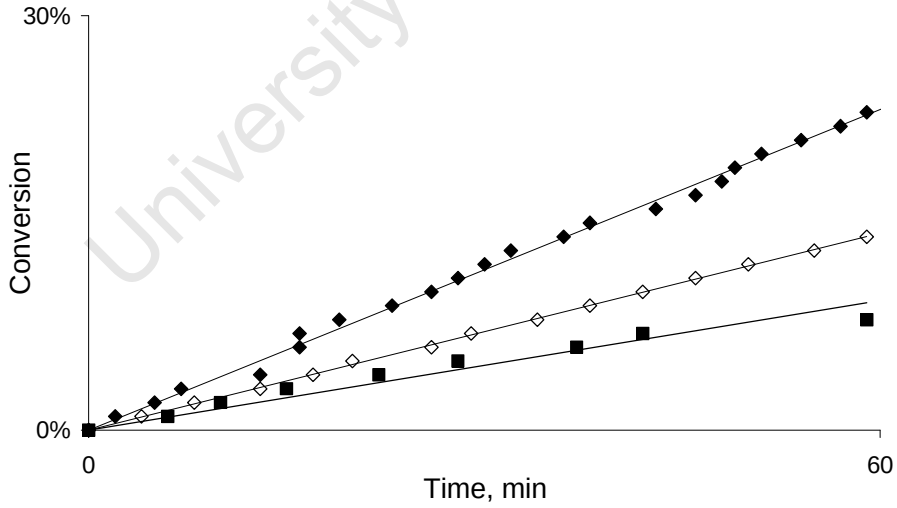

Figure 3.19. Catalyst testing using controlled pH method with 0.05 M EG
(Temperature = 60ºC; Magnetic stirrer 1000 rpm; crushed Mintek 'BC1' catalyst; [EG] = 0.05M in 200ml solution; pH = 11)
(♦ 1 g catalyst; ◊ 0.5 g catalyst; ■ 0.25 g catalyst)

Table 3.7. Calculation of initial reaction rates for runs with different mass of catalyst

Mass of catalyst, g	Initial rate, mmol EG / g cat. min
0.25	0.064
0.5	0.048
1.0	0.039

These results could however still imply the presence of internal mass transfer limitations, and so two runs were carried out with different catalyst particle sizes. The results are shown in Figure 3.20 below.

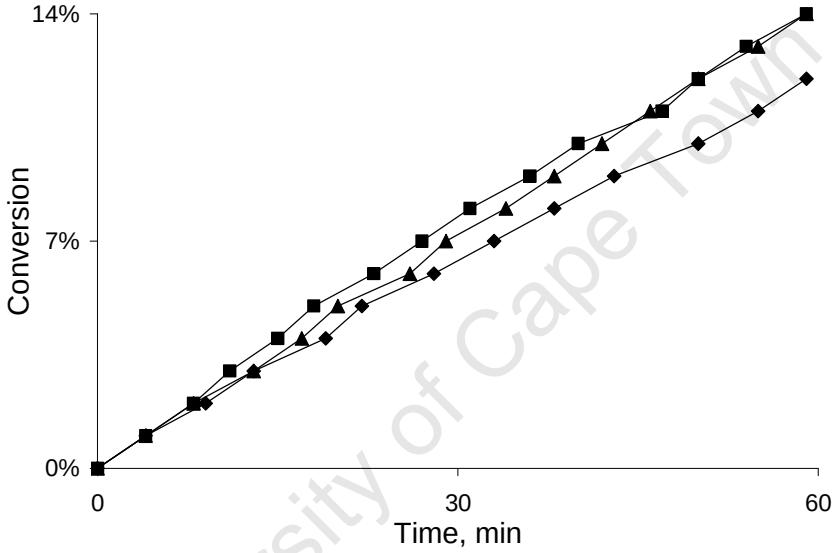

Figure 3.20. Catalyst testing using uncontrolled pH with different catalyst particle sizes (Temperature = 60ºC; Magnetic stirrer 1000 rpm; Mintek 'BC1' catalyst; [EG] = 0.05M in 200ml solution; pH = 11)
(■ d < 250 µm; ♦ d > 250 µm; ▲ 250 µm < d < 500 µm)

University of Cape Town

The line with a slightly lower overall reaction rate is that where particle size was greater than 250 µm with no upper bounds on particle size. The other two lines show very similar reaction rates: the one has particle size less than 250 µm and the other has particles greater than 250 µm but also less than 500 µm. On this basis the reaction was determined to be fully controlled by kinetic considerations if particle size was maintained below 500 µm.

The test reaction protocol for this study was therefore settled at the following conditions: 60 ºC, 1 atm, 0.05 M ethylene glycol, pH=11, 0.25 g of catalyst with crystallite size below 500 µm. The oxygen flow rate would be maintained at 0.5 ml/s and the stirrer at 1000 rpm.

The reaction progress would be monitored by titration with 0.1 M NaOH, with each ml added representing a 1 % increase in conversion.

The final set of experiments with the Mintek BC1 catalyst was conducted to explore the impact of pH on reaction rate and selectivity. These results are shown in Figure 3.21 below.

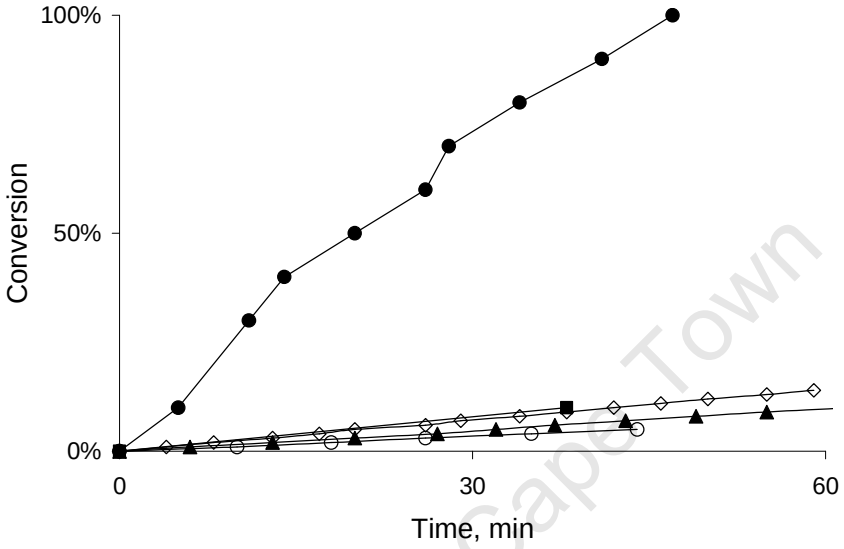

Figure 3.21. Catalyst testing with controlled pH method at different pHs
(Temperature = 60ºC; Magnetic stirrer 1000 rpm; crushed Mintek 'BC1' catalyst d< 500 µm; [EG] = 0.05M in 200ml solution)
(○ pH = 8; ▲pH = 10; ◊ pH = 11; ■ pH = 12; ● pH = 13)

University of Cape Town

It can be seen that the reaction rate increases marginally with pH until pH = 12, whereafter there is a dramatic increase when the pH is increased to 13. This could be speculated to be related to the dehydrogenation mechanism for alcohol oxidation referred to earlier. The last run provided an important verification of this method of determining the reaction rate, in that the pH increased until 100% conversion, then remained constant thereafter.

3.2.1.2 Activity of prepared catalysts

All catalysts were tested before calcination and showed no activity. The calcined catalysts were then tested, and the calcined carbon supported catalysts showed no activity. To further explore this finding, a run was conducted with the World Gold Council X40S Au/C catalyst, and this also showed no activity. All the calcined alumina supported catalysts showed activity for ethylene glycol oxidation under the test conditions.

To investigate the effect of calcination medium and temperature, the alumina supported catalyst prepared by cationic exchange at pH = 10.6 was split into four batches and each subjected to a different calcining regime. The activity of these catalysts is represented in Figure 3.22 below.

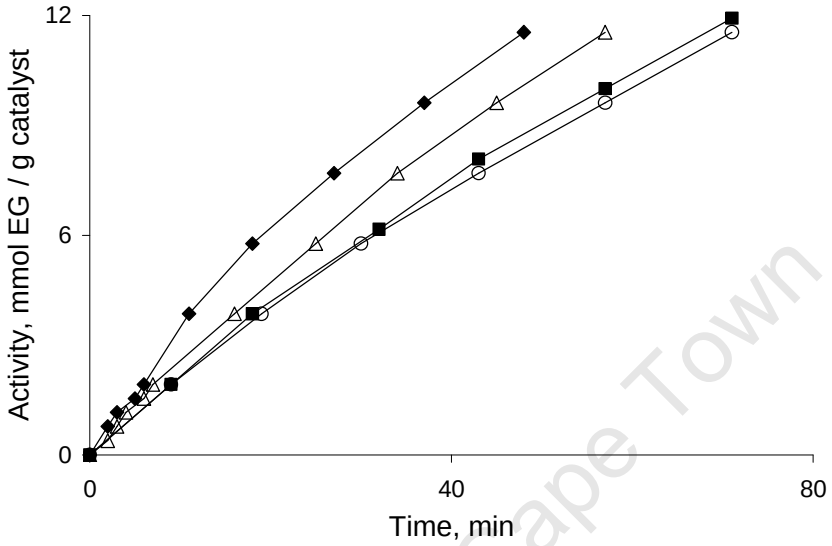

Figure 3.22. Activity of Al-CAT-10.6 catalysts calcined under different regimes
(Δ AL-CAT-10.6-300AIR; ♦ AL-CAT-10.6-300H2; ■ AL-CAT-10.6-200H2; ○ AL-CAT-10.6-200AIR)

University of Cape Town

It can be seen that the catalysts calcined at 300 ºC are slightly more active than those calcined at 200 ºC, with the 300 ºC catalyst calcined in hydrogen slightly more active than that calcined in air. It was therefore decided to calcine all remaining catalysts in hydrogen at 300 ºC.

The activity for all active catalysts calcined at 300 ºC in hydrogen is represented in Figure 3.23. It can be seen that the catalyst prepared by cationic exchange at pH=10.6 discussed above remains the most active catalyst, followed by that prepared anionically at pH=3.2. Assuming a linear initial reaction rate, these rates were determined from the initial slopes of the curves in Figure 3.23. These results are given in Table 3.8.

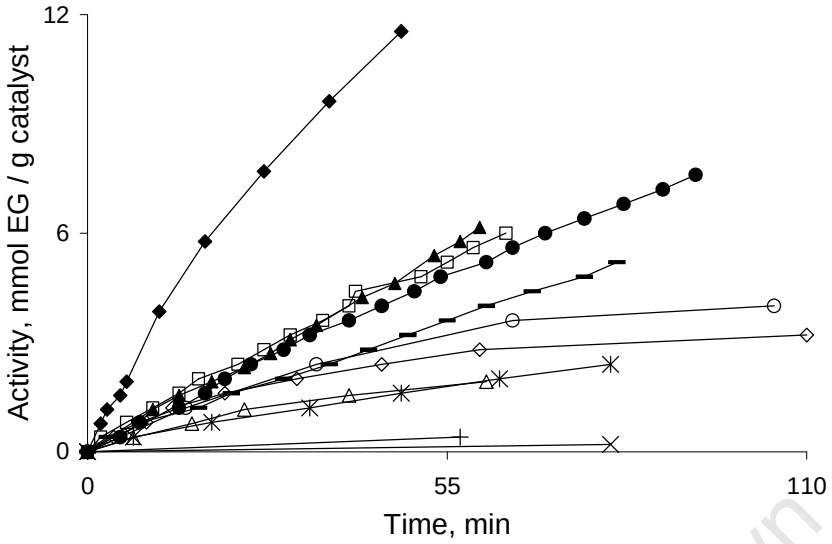

Figure 3.23. Activity of all active prepared catalysts
(Temperature = 60ºC; Magnetic stirrer 1000 rpm; d< 500 µm; [EG] = 0.05M in 200ml solution)
(▲ AL-AN-3.2; ∆ AL-AN-6.1; ♦ AL-CAT-10.6-300H2; × AL-CAT-7.6; ✳ AL-CAT-8.0; ◊ AL-CAT-8.5; ○ AL-CAT-9.0; + AL-CAT-9.5; □ AL-CAT-10.0; - AL-CAT-11.0; ● AL-CAT-12.0)

Table 3.8. Initial reaction rates for active catalysts

Catalyst code	Initial reaction rate, mmol EG/g cat. min
AL-AN-3.2	0.106
AL-AN-6.1	0.048
AL-CAT-10.6-300AIR	0.267
AL-CAT-10.6-300H2	0.327
AL-CAT-10.6-200AIR	0.214
AL-CAT-10.6-200H2	0.204
AL-CAT-7.6	0.003
AL-CAT-8.0	0.038
AL-CAT-8.5	0.082
AL-CAT-9.0	0.070
AL-CAT-9.5	0.007
AL-CAT-10.0	0.105
AL-CAT-11.0	0.068
AL-CAT-12.0	0.093

3.2.2 Atomic Absorption Spectroscopy (AAS) analysis of reaction solution

For the series of alumina catalysts prepared by cationic exchange at a range of pHs, AAS was conducted on final filtered reaction mixtures to assess whether any gold had leached into solution from the catalyst. In contrast to the observations of Berndt et al. (2004), gold was detected in the reaction solution, represented below in Table 3.9 as a percentage of the gold present on the solid catalyst used in the test run. Future research will need to involve a

University of Cape Town

testing of this solution for catalytic activity to ensure that it is only supported gold that is acting as a catalyst in this process.

Table 3.9. Analysis of Au present in final reaction solution

Catalyst code	% Au leached*
AL-CAT-7.6	26%
AL-CAT-8.0	15%
AL-CAT-8.5	8%
AL-CAT-9.0	12%
AL-CAT-10.0	3%
AL-CAT-11.0	3%
AL-CAT-12.0	4%

* calculated as a % of Au present on the solid catalyst
** this analysis was not conducted for catalyst AL-CAT-9.5

3.2.3 High Pressure Liquid Chromatography (HPLC)

3.2.3.1 Qualitative HPLC analysis

Possible products resulting from the oxidation of ethylene glycol were identified and purchased, and standard solutions of these were analysed by HPLC. Table 3.10 gives the retention times initially obtained. Marginal shifts were noted in retention times of these standard substances over successive runs, due most probably to changes in room temperature (the column was not heated), small changes in mobile phase composition, and changes in system pressure.

Table 3.10. HPLC retention times for possible product range

	UV	RI
Ethylene glycol	-	19.5 min
Oxalic acid	8.4 min	8.9 min
Glyoxylic acid	11.5 min	11.9 min
Glycolaldehyde	14.5 min	15.0 min
Glycolic acid	15.2 min	15.6 min
Diethylene glycol	-	20.9 min
Tetraethylene glycol	-	22.0 min

Additional studies were conducted with the Mintek ‘BC1’ catalyst to explore the effect of pH on selectivity; these results are given in Appendix B.

Figure 3.24 shows the HPLC-UV chromatograms for all reaction mixtures from the active prepared catalysts (i.e. all alumina catalysts), as well as a chromatogram from one of the inactive carbon catalysts. The injection peak is noted between 7 and 8 minutes. Glycolic

University of Cape Town

acid appears as a peak between 15.5 and 15.8 minutes, and is noted on all chromatograms with the exception of AL-CAT-7.6 (AL-CAT-8.0, AL-CAT-8.5 and AL-CAT 9.0 all show very small glycolic acid peaks with magnification). The AL-CAT-10.6 catalysts all show a peak at 9.3 min which also appears in some of the other AL-CAT catalysts, namely those prepared at pHs 8.0, 10.0 and 12.0. AL-CAT-8.0 shows an unidentified peak at 17.5 min. These latter peaks have not been identified amongst the range of products sampled in Table 3.10 above, and is not clear whether they represent reaction by-products or simply contaminants in the system.

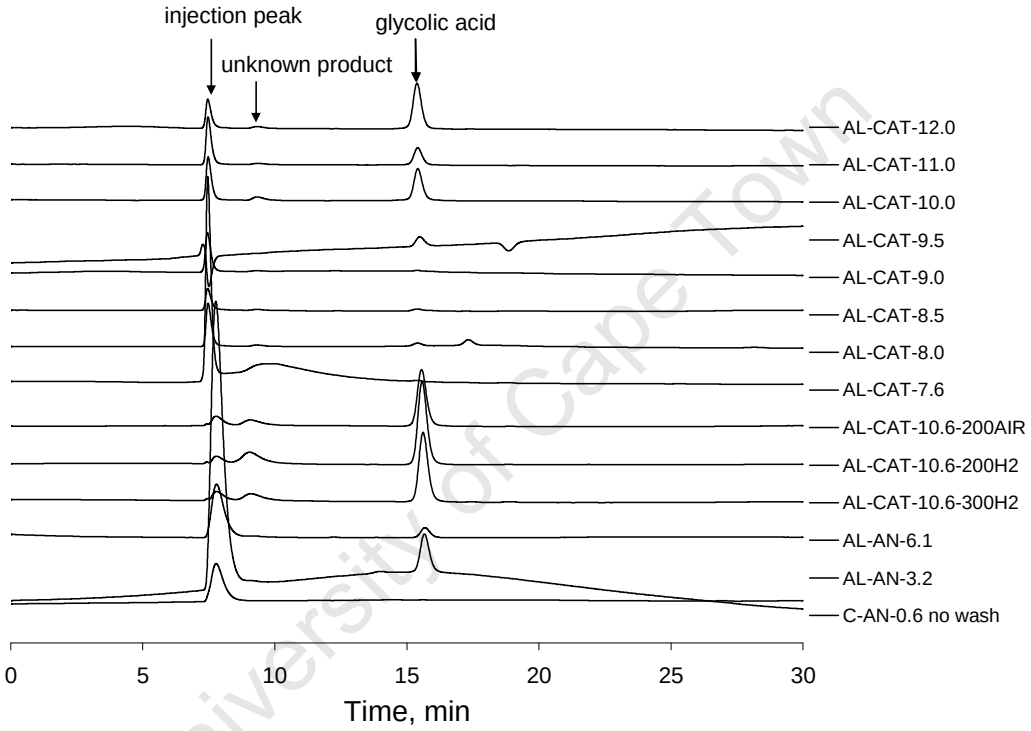

University of Cape Town

Figure 3.24. HPLC-UV chromatograms for all reaction mixtures

Figure 3.25 shows the HPLC-RI chromatograms for all reaction mixtures, as well as that for the same sample carbon catalyst represented above. Glycolic acid appears between 16.0 and 16.3 min. Even with magnification there is no such peak evident for additional catalysts AL-CAT-7.6 through to AL-CAT-9.0. Unreacted ethylene glycol is noted as a peak between 19.7 and 19.8 min. The carbon catalyst shows a small peak at 10.7 min, suggesting that although no drop in pH had been noted there might have been some other reaction that was taking place. However, this peak does not link to any of the potential products identified above and so this supposition cannot be confirmed. In two of the reaction mixtures there was a peak at

28 min. However, this peak had appeared in other data quite unrelated to this project and so it was assumed that this was a contaminant in the injection system.

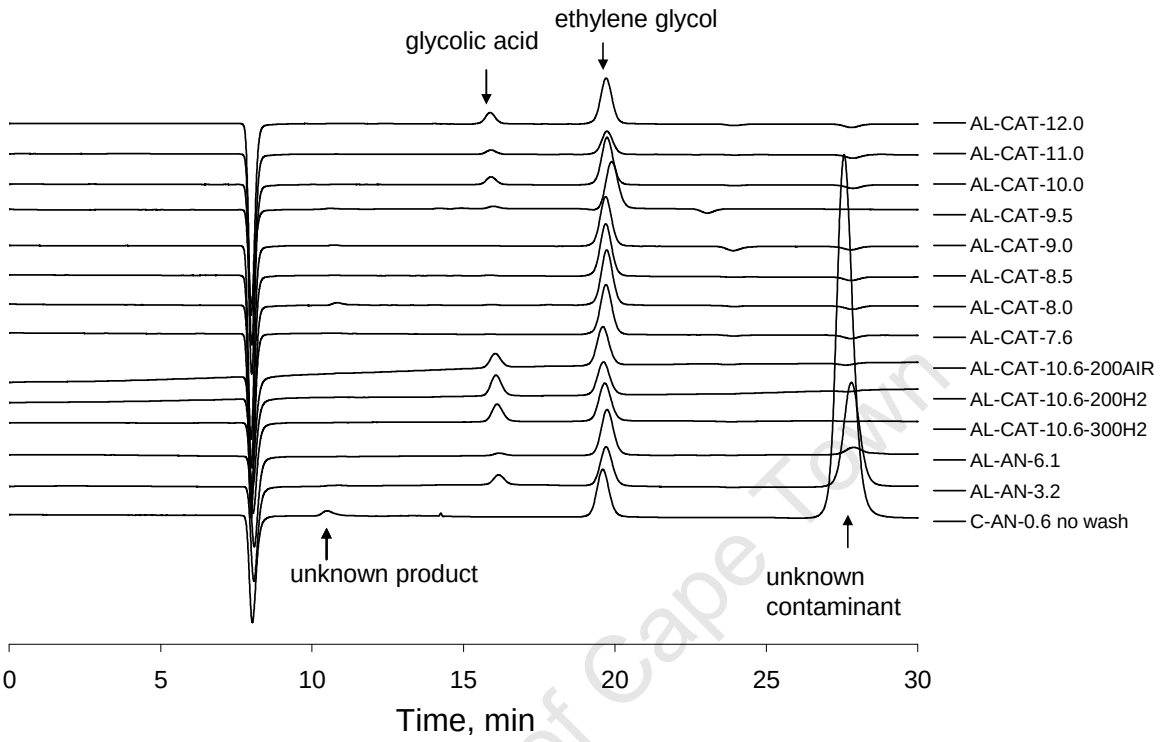

Figure 3.25. HPLC-RI chromatograms for all reaction mixtures

3.2.3.2 Quantitative HPLC analysis

An initial method of calibration using an internal standard was explored; these results are given in Appendix C. However, given the possibility that the internal standard could mask a reaction by-product, it was decided rather to calibrate HPLC peak areas by using standard solutions of glycolic acid and ethylene glycol of a range of concentrations matching the reaction mixtures. These results allowed for the construction of calibration curves to determine concentrations from peak areas (glycolic acid in both UV and RI chromatograms; ethylene glycol in the RI chromatograms). These curves are given in Appendix D. Using these data and measuring peak areas in the chromatograms produced from the various reaction mixtures, it was possible to calculate the yield of glycolic acid in mmol, as well as consumption of ethylene glycol. The ratio of these two amounts can be considered an indication of selectivity to glycolic acid. These results are given below in Table 3.11, with

University of Cape Town

reaction progress expressed as mmol EG / g catalyst over the reaction period to allow comparison with titration data.

Table 3.11. Conversions based on HPLC peak areas

Catalyst code	Total yield of glycolic acid, mmol / g cat	Total consumption of ethylene glycol, mmol / g cat	Selectivity to glycolic acid
AL-AN-3.2	5.71	12.24	47%
AL-AN-6.1	1.25	6.20	20%
AL-CAT-10.6-300AIR	-	-	-
AL-CAT-10.6-300H2	9.97	13.90	72%
AL-CAT-10.6-200AIR	12.10	18.04	67%
AL-CAT-10.6-200H2	7.83	13.97	56%
AL-CAT-7.6	0.00	7.91	0%
AL-CAT-8.0	0.20	4.60	4%
AL-CAT-8.5	0.19	6.42	3%
AL-CAT-9.0	0.06	8.25	1%
AL-CAT-9.5	1.45	4.48	32%
AL-CAT-10.0	4.73	10.28	46%
AL-CAT-11.0	2.49	26.18	10%
AL-CAT-12.0	5.99	11.09	54%

University of Cape Town

Chapter 4. Discussion

4.1 Methodological issues

4.1.1 Methods for determining Au loading

The primary method used for determining Au loading on the prepared catalysts was Atomic Absorption Spectroscopy (AAS). For the initial series of catalysts, measurements were taken of the Au concentration of the precursor solutions and the filtrates. Solid catalysts were subjected to an acid digestion in order to provide a gold solution which could be analysed. It was expected that this latter process could contribute to a significant source of experimental error.

Using the above measurements, a gold balance was conducted to assess the overall level of error in this process and to give some indication of the validity of the gold loadings that had been determined. The overall gold balance was presented in Figure 3.2 on page 30. Extracted from that figure and presented here in Table 4.1 are the values for the 'missing gold' which can be considered a measure of percentage error in these data.

Table 4.1. 'Missing gold' in gold balance

Catalyst code	Missing Au
C-AN-0.6	-23%
C-AN-2.3	-8%
AL-AN-3.2	10%
AL-AN-6.1	12%
C-CAT-2.4	-6%
C-CAT-5.0	32%
AL-CAT-10.6	12%
AL-CAT-6.4	2%

It can be noted that in some instances the error is significant, ranging up to 32% in the case of C-CAT-5.0, where the Au concentration in the filtrate was exceptionally low (see Figure 3.1 on page 29) but where the Au wt-% on the solid catalyst only accounted for about 70% of the initial Au in the precursor solution. In this case a likely explanation would be that the acid digestion has not fully released all the gold into solution and that the Au wt-% on the solid catalyst is an underestimation. The other catalyst associated here with a large degree of error

University of Cape Town

is notably also a carbon supported catalyst, C-AN-0.6, where it would appear that the Au wt-% on the solid catalyst is overestimated.

Thermogravimetric Analysis (TGA) was therefore conducted to obtain a second measure on the gold loading of the carbon supported catalysts. These results, presented in Table 3.3 on page 32, did not suggest a systematic underestimation of Au loading (as would be expected if the acid digestion did not fully release all Au) or, indeed, a systematic overestimation. For C-AN-0.6, the Au wt-% derived from TGA would allow for a better gold balance, but for C-AN-2.3 the TGA result presents an even worse fit. Further research is needed to explore this situation; for the moment it should therefore be noted that the Au wt-% for the carbon supported catalysts in this study is associated with a relatively large error.

For the alumina catalysts, the error is in the region of 10%, which is considered quite normal in the field (McPherson, 2008). Fortunately for the present study it is the alumina catalysts that were active for the test reaction, and that therefore form a particular focus of interest. For the series of alumina catalysts prepared by cationic exchange at a range of pHs there was no AAS on the Au precursor solutions, and therefore no Au balance was possible. However, we can assume a relatively high degree of accuracy on the Au wt-% of these catalysts as determined by AAS, given the gold balance on the initial alumina catalysts.

4.1.2 Methods for determining crystallite size

In this study three methods were employed for determining crystallite size: Transmission Electron Microscopy (TEM), X-Ray Diffraction (XRD) and oxygen chemisorption. TEM gave images with measurable Au crystallites for both carbon and alumina supported catalysts. XRD only gave measurable Au peaks for carbon supported catalysts given the interference of the crystalline support for alumina catalysts. Oxygen chemisorption was only useful for determining crystallite size with alumina supported catalysts as for the carbon catalysts the carbon support showed a large oxygen uptake. Therefore for each type of catalyst we have a maximum of two values for crystallite size, summarized in Table 4.2 below.

University of Cape Town

Table 4.2. Au crystallite size determined by different methods

Catalyst code	Size, nm (TEM)	Size, nm (XRD) (111)	Size, nm (chemisorption)
C-AN-0.6 no wash	58.6	21.8	-
C-AN-0.6	42.1	16.9	-
C-AN-2.3	73.2	32.3	-
C-CAT-2.4	29.3	14.1	-
C-CAT-5.0	131.0	20.9	-
AL-AN-3.2	1.8	-	4.3
AL-AN-6.1	11.9	-	23.5
AL-CAT-10.6-300H2	-*	-	3.3
AL-CAT-10.6-200AIR	10.3	-	3.8
AL-CAT-10.6-200H2	-*	-	4.8
AL-CAT-7.6	5.8	-	-**
AL-CAT-8.0	4.1	-	3.6
AL-CAT-8.5	3.5	-	-**
AL-CAT-9.0	4.1	-	-**
AL-CAT-9.5	6.3	-	1.4
AL-CAT-10.0	2.8	-	5.8
AL-CAT-11.0	3.4	-	2.8
AL-CAT-12.0	3.7	-	2.0

* poor TEM images
** insufficient chemisorption at low pressures

University of Cape Town

For carbon catalysts it can be seen that the TEM results are generally about double of those arrived at via XRD, with the exception of C-CAT-5.0 where the TEM images yielded an average of 131.0 nm while XRD gave only 20.9 nm. Porta et al. (2000) however find very similar values for crystallite size from TEM and XRD in their study on Au/C catalysts. From our experience with TEM it is clear that an overestimation of crystallite size is possible with this method, given that images are taken where Au crystallites are most easily identifiable, and these will tend to be areas where the crystallites are large. Although the aim is to identify single crystallites it is possible that in many cases what is measured are aggregations. The XRD results gave results with a high degree of internal consistency (see Table 3.4 on page 38) and so it is suggested that these might be considered a less biased set of results for further use in the present study.

For alumina catalysts it can be noted that the crystallite size derived from chemisorption data (mostly using dissociative adsorption, n=2) offer a similar order of magnitude to those from TEM, with all crystallites equal to or under 10 nm with the exception of AL-AN-6.1. There is however no definite quantitative correlation between the two sets of results. This ties up with the work of Berndt et al.(2003) who found a similar level of agreement between the results from these two methods for Au/Al_2O_3 catalysts. For calculating crystallite size from chemisorption data they found the best agreement with an assumption of dissociative

adsorption, also supported in earlier work by Fukushima et al. (1979). It is worth noting that Berndt et al. (2003) do not offer a single average crystallite size from TEM but rather a range of crystallites 'predominantly observed'. Shastri et al. (1984) also note the problems with trying to link up a single average crystallite size from chemisorption with what is observed on TEM, especially given the possibility of a bimodal distribution of crystallite sizes. In the present study it can be noted that the chemisorption results modeled very well onto a dual isotherm, and the results presented here are at least closely matched to that theoretical position. It does however also need to be borne in mind that the uncertainty associated with the gold loading measurement has a direct effect on the size as calculated from chemisorption results. Nonetheless, the concerns regarding the TEM methodology are no less relevant here, especially noting the difficulty of identifying gold crystallites against the alumina background. For the present study it was decided therefore to work primarily with the chemisorption results for any further quantitative trend analysis with other variables for the alumina supported catalysts.

4.1.3 Test reaction protocol for determining reaction rate and selectivity

Following Berndt et al. (2004), titration with NaOH maintaining constant pH was the chief method employed in this study to determine the rate of production of glycolic acid in the test reaction of ethylene glycol oxidation. The calibration of HPLC peak areas gave a useful set of data with which to assess the validity of the titration method. These results are compared in Figure 4.1 below, with maximum conversion expressed in terms of mmol EG consumed / g cat in order for correspondence with the maximum values plotted in Figure 3.23 on page 51. Each data point represents a catalyst tested, the solid line represents equal values on both axes, while the dotted line represents HPLC conversions one quarter of those measured by titration. Given that total oxidation of ethylene glycol to carbonate would result in four additional H^+ ions compared to the single H^+ associated with glycolic acid, it should be expected that all data points should fall in between these two lines. This is generally the case, except for a few outliers. There is no overall correlation, but a broad trend where the more active catalysts as measured by titration are also the more active as determined by HPLC. Nonetheless, this should suggest a significant error on the reaction rate as measured by titration.

University of Cape Town

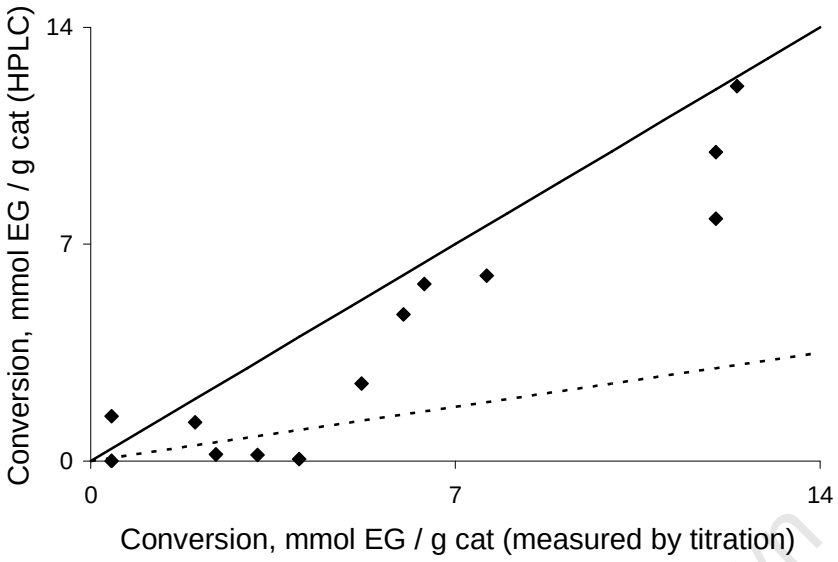

Figure 4.1. Comparison of conversion as determined by titration and by HPLC

From the HPLC chromatograms of the reaction mixture where there are unidentifiable peaks these cannot be assigned to any of the obvious oxidation byproducts of ethylene glycol. Using HPLC calibration however, a comparison of calibrated peak areas for ethylene glycol to glycolic acid yields a selectivity value. These are considerably less than 100% in all cases. There has to be some query on the validity of these as selectivity values, given the absence of identifiable byproduct peaks in most chromatograms. Furthermore, all existing studies on gold catalysed ethylene glycol oxidation (Prati and Martra, 1999, Bianchi et al., 2000, Biella et al., 2002a, Berndt et al., 2003, Berndt et al., 2004) report very high selectivities to glycolic acid. The results from the present study do not allow a comparison of selectivities for the different prepared catalysts. At most it can be stated that for most catalysts we do not see any peaks other than those of the reactant and the desired products, and that the quantification of selectivity is for the moment yet unresolved.

University of Cape Town

4.2 Research questions

4.2.1 Ion exchange as a gold catalyst preparation method

4.2.1.1 Loading efficiency

In the present study, the gold precursor concentrations were set so as to allow a maximum theoretical gold loading of approximately 4 % for anionic exchange, and about 3 % for cationic exchange (this lower value due to gold loss during the synthesis of the cationic precursor, tetraammine gold nitrate). Exact values for this gold precursor concentration were used to determine overall loading efficiency, based on the Au wt-% of the solid catalysts analysed by AAS with acid digestion pretreatment. This parameter was only available for the initial series of catalysts; unfortunately for the further series of alumina catalysts prepared by cationic exchange at a range of pHs there was no initial measurement of gold concentration for the precursor solutions.

Significantly, this study has shown that 100 % loading efficiency is possible for gold catalysts prepared by ion exchange. This was obtained in three cases; notably all were carbon supported catalysts, and this includes both carbon catalysts prepared by anionic exchange, roundly refuting the statement of Ivanova et al.(2004) that anionic exchange would not be possible with supports like carbon which have an IEP below 2, based on the electrostatic adsorption theory. It is clear that a carbon support offers ample possibilities for ionic gold uptake. Interestingly, the only carbon supported catalyst that did not yield 100 % loading efficiency was that prepared by cationic exchange at a pH that one would have anticipated as favourable, being above and far away from the IEP. Further studies would clearly be profitable in this area to illuminate the mechanisms of adsorption better.

An ammonia wash was incorporated into the procedure for preparing carbon supported catalysts by anionic exchange, in order to exclude the presence of chloride, based on the work of Ivanova et al. (2006c). They note a loss of about 30 % of Au in all cases during this washing stage. Notably, in the present study a loss of Au of 7 % or less is noted in the three cases where this sampling took place. Comparing the two catalysts prepared under identical conditions except for the ammonia wash, both TEM and XRD results show that including this wash resulted in smaller crystallites, as would be expected theoretically with chloride being associated with increased sintering.

University of Cape Town

For the alumina supported catalysts there is only one data point to suggest that high loadings are feasible with ion exchange: this is for the catalyst prepared cationically in the favourable pH region. Given that the catalyst prepared in the unfavourable pH region for cationic exchange gave a loading of only 5% it is clear that pH has a determining effect. Further research is needed to fully determine the impact of pH. Although a full measure of loading efficiency was not obtainable for the additional series of alumina catalysts prepared to investigate the influence of pH, the graph of Au wt-% versus pH of preparation as shown in Figure 3.3 on page 31 does give some pointers. If it is assumed that all of these catalysts had relatively similar starting Au concentrations, then it can be concluded that there is a strong increase in loading as one moves away from the IEP (in the favourable region). The decrease in Au wt-% at pH = 12 can potentially be attributed to dissolution of the alumina support at this high pH.

For alumina catalysts prepared by anionic exchange the loading efficiencies are much lower, even when in pH regions which theoretically should be favourable.

Overall the loading efficiencies achieved in the present study would suggest that ion exchange compares very favourably with deposition precipitation, the traditional method of gold catalyst preparation, where a systematic study has shown loading efficiencies to vary from 20% to 60% (Wolf and Schüth, 2002).

University of Cape Town

4.2.1.2 Crystallite size

It was noted above that the carbon catalysts generally displayed very high loading efficiencies with ion exchange. This could be related to the parallel observation that they also showed large crystallite sizes as measured by TEM and XRD. However, here it is also worth noting that the carbon supported catalyst with the smallest crystallite size, C-CAT-2.4, also showed 100% loading efficiency. This suggests there is no direct relation between Au loading and crystallite size, but there might be an overall trend for carbon catalysts compared to other supports. The TEM histograms also suggest that many of these carbon supported catalysts had very large crystallite size distributions. Given that many of the key gold catalysis studies demonstrate the need for gold crystallite sizes less than 10 nm, on this basis it might be suggested that ion exchange is not an optimum method for preparation of carbon supported catalysts. Nonetheless, it is worth noting that deposition precipitation and impregnation also yield Au/C crystallite sizes in this region; it is only by immobilization of

gold sols on supports that one can obtain Au crystallites smaller than 10 nm (Prati and Porta, 2005, Demirel et al., 2007b).

The alumina supported catalysts prepared by ion exchange yielded much smaller crystallites, smaller than 10 nm in nearly all cases. The exception is AN-AL-6.1 which was prepared by anionic exchange below but close to the IEP of alumina. At this stage there are no clear trends suggesting the influence of pH of preparation on crystallite size, but it can be generally concluded that ion exchange can deliver favourable crystallite sizes for alumina supported gold catalysts. This confirms the earlier findings of Ivanova et al. (2006c) with respect to anionic exchange and is a novel finding for cationic exchange with tetraammine gold which, as noted earlier, has not previously been reported for alumina supported gold catalysts.

In Figure 4.2, monolayer oxygen uptake during chemisorption is plotted against Au loading following an analysis suggested by Berndt et al. (2003). If all catalysts had identical crystallite size distributions then a linear plot would be expected. In their case they note a leveling off in the curve suggesting increasing crystallite sizes with an increase in Au loading, as might be expected given the theoretically enhanced possibility for sintering. In the data presented below there is no evident relationship between Au wt-% and oxygen uptake, confirming the earlier supposition that this study has not been able to identify any clear determinants of crystallite size for alumina catalysts prepared by ion exchange.

University of Cape Town

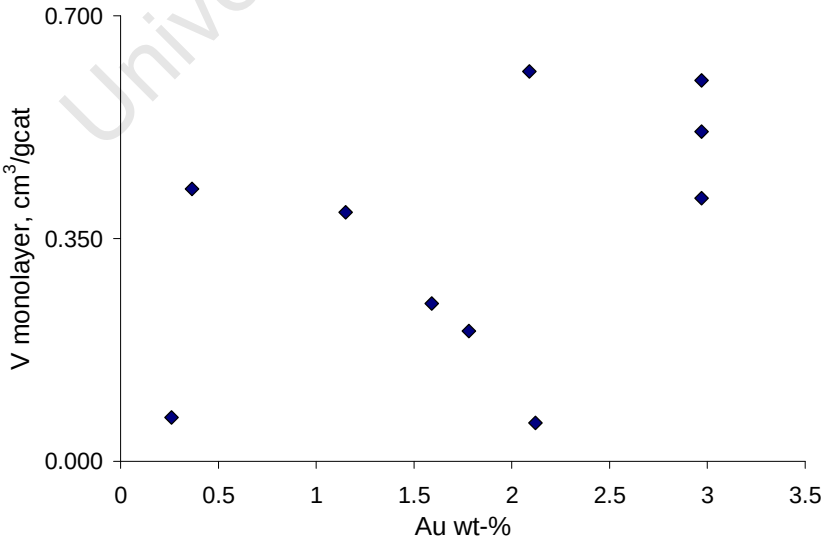

Figure 4.2. Chemisorption monolayer oxygen uptake vs. Au loading

One batch of alumina supported catalysts, AL-CAT-10.4, was divided into smaller batches in order to explore the impact of calcination regime; crystallite size characterisations were carried out for three of these batches. The results at hand do not allow for any strong conclusions in this regard: the TEM images were only usable for one of these batches; chemisorption results suggest, if anything, a larger crystallite size for the lower calcination temperature which seems unlikely.

4.2.2 Determinants of reaction rate and selectivity for ethylene glycol oxidation

A surprising finding of this study was that carbon supported gold catalysts are completely inactive for ethylene glycol oxidation under the reaction conditions tested here (60 ºC, 1 atm). It might have been assumed that this could be due to the larger crystallite sizes prevalent in these prepared catalysts; yet the World Gold Council X40S 0.8% Au/C catalyst was also inactive under these conditions and it has average crystallite sizes of 10.5 nm (TEM) and 6.7 nm (XRD) (World Gold Council, n.d.). This catalyst was prepared and tested by Rossi and co-workers and is stated as being active for ethylene glycol oxidation at 3 atm; all the work that this group has conducted on this reaction has been at elevated pressures but it is not stated whether this pressure was found to be necessary for any reaction to take place. As it stands there do not appear to be any reports in the literature which investigate the activity of Au/C catalysts for ethylene glycol oxidation at atmospheric pressure.

The following discussion will therefore concern itself with the alumina catalysts which displayed activity for ethylene glycol oxidation under the test conditions. The initial reaction rates determined earlier and given in Table 3.8 on page 51 will be used as primary indicators of activity. Expressed per mass of Au, these initial rates range from 2 to 15 mmol EG / g Au . min. These rates are approximately an order of magnitude lower than those reported in a previous study with gold on alumina catalysts (prepared by deposition precipitation with crystallite sizes approximately 1 – 2 nm) where 10 - 50 mmol ethylene glycol / g Au . min was obtained from working at an ethylene glycol concentration of 0.5 M (compared to 0.05 M in the present study), a temperature of 76 ºC (compared to 60 ºC) and pH=9 (compared to pH=11) (Berndt et al., 2004).

The present study did not set out to investigate the lifetime or stability of the gold catalysts; however an AAS of the reaction solution did show the presence of a considerable proportion

University of Cape Town

of gold leached from the catalyst. It is worth noting that Berndt et al.(2004) do not find any gold in the reaction solution from any of their catalyst batches, yet they do notice an increase in Au crystallite size between runs which they ascribe to the leaching and subsequent deposition of gold on the alumina support.

As noted earlier, this study has not been able to deliver quantitative measures of catalyst selectivity, and so this parameter will be omitted from the following discussion.

4.2.2.1 Au loading

Figure 4.3 overleaf shows a plot of initial reaction rates against Au loading. If no other effects were operating and all catalysts had the same sized crystallites a linear dependence of reaction rate (measured per g catalyst) on Au loading could be expected. For a preliminary analysis one could consider most of the prepared alumina catalysts having crystallite sizes of a similar order of magnitude (except for AL-AN-6.1), and it is therefore useful to begin with a consideration of reaction rates versus Au loading as in this figure. Here we do not find a direct correlation although those catalysts with lowest loading have lowest rates and the four AL-CAT-10.6 batches all have considerable higher activity than all other prepared alumina catalysts (this was also noted earlier in Figure 3.23 on page 51), as well as the highest gold loading in this series. In between there are a series of catalysts with widely ranging Au loadings but similar initial reaction rates. Clearly there are other determinants of catalyst activity in operation. We turn therefore to a closer examination of the influence of crystallite size.

University of Cape Town

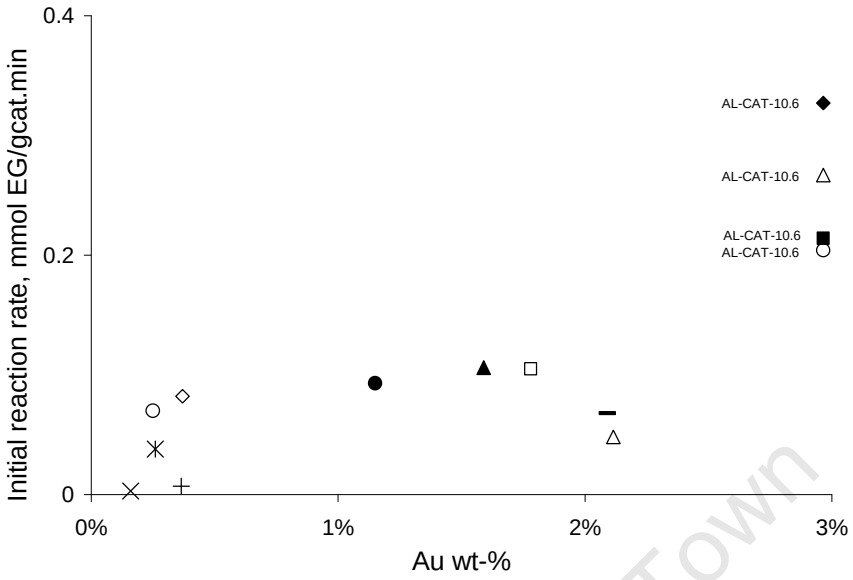

Figure 4.3. Initial reaction rate versus Au loading
(Prefix AL-CAT-10.6: ∆ 300AIR; ♦ 300H2; ■ 200H2; ○ 200AIR)
(▲ AL-AN-3.2; ∆ AL-AN-6.1; × AL-CAT-7.6; ✳ AL-CAT-8.0; ◊ AL-CAT-8.5;
○ AL-CAT-9.0; + AL-CAT-9.5; □ AL-CAT-10.0; - AL-CAT-11.0; ● AL-CAT-12.0)

4.2.2.2 Au crystallite size

In order to determine whether any crystallite size effects are present, reaction rates (measured per g catalyst) can be plotted against oxygen uptake in chemisorption (also measured per g catalyst) (Berndt et al., 2003). This keeps the data free from error associated with measures of Au loading. One expects a general increase in reaction rate with increased chemisorption; if the relationship is directly proportional then there is no crystallite size effect at play. If any maxima are noted then these could be considered indicators of preferred crystallite sizes for this reaction. Figure 4.4 overleaf gives this analysis for the present data.

University of Cape Town

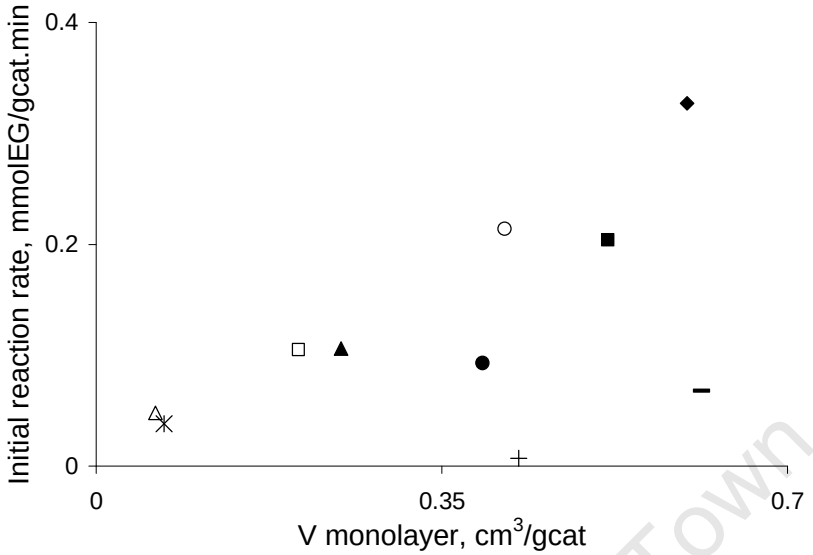

Figure 4.4. Correlation between initial reaction rate and monolayer oxygen uptake during chemisorption
(Δ AL-AN-6.1; ✳ AL-CAT-8.0□ AL-CAT-10.0; ▲ AL-AN-3.2; ● AL-CAT-12.0; + AL-CAT-9.5; ○ AL-CAT-10.6-200AIR; ■ AL-CAT-10.6-200H2; ♦ AL-CAT-10.6-300H2; - AL-CAT-11.0)

Figure 4.4 shows a general trend of increasing reaction rate with chemisorption, with three notable outliers. It is possible that these outliers are due to inaccuracies in the measurement of reaction rate by titration for these particular catalysts. The absence of any distinct maxima in this plot suggests there is no significant effect of crystallite size on reaction rate. Most of the catalysts represented here have fairly similar crystallites sizes (less than 5 nm) and so the range in which this has been tested is relatively limited. Nonetheless, the catalyst Al-AN-6.1 with significantly larger crystallites features in this graph with a low oxygen uptake (as would be expected) as well as a matching low reaction rate. At this point it can therefore be concluded that the present study does not yield any evidence of a crystallite size effect for gold catalysed ethylene glycol oxidation with alumina supported catalysts.

A similar analysis to Figure 4.4 is presented in Figure 4.5 where the yield of glycolic acid is plotted against the oxygen uptake in chemisorption. Similar trends are noted.

University of Cape Town

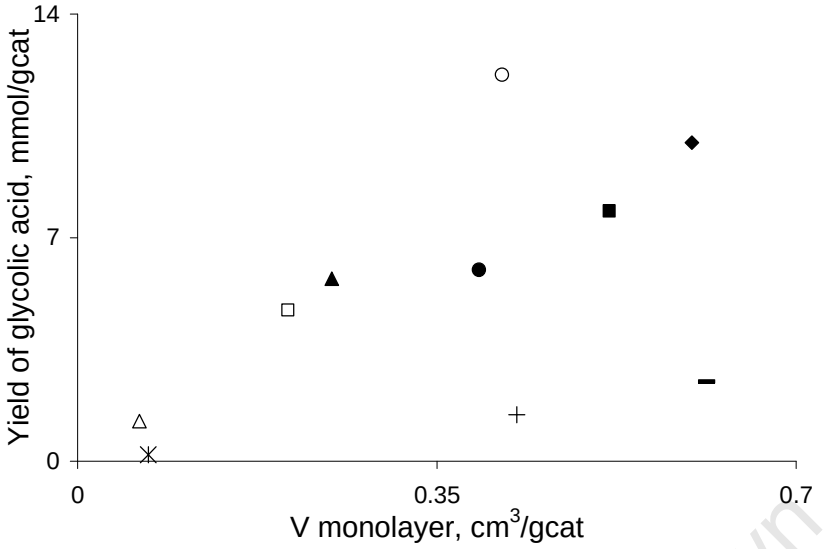

Figure 4.5. Correlation between yield of glycolic acid and monolayer oxygen uptake
(Δ AL-AN-6.1; ✳ AL-CAT-8.0□ AL-CAT-10.0; ▲ AL-AN-3.2; ● AL-CAT-12.0; + AL-CAT-9.5;
○ AL-CAT-10.6-200AIR; ■ AL-CAT-10.6-200H2; ♦ AL-CAT-10.6-300H2; - AL-CAT-11.0)

Further evidence comes from the plot of initial reaction rates (per g Au) against crystallite size (measured by chemisorption) in Figure 4.6 below. Once again it is clear that crystallite size cannot at this stage be considered a determinant of catalyst activity for this reaction.

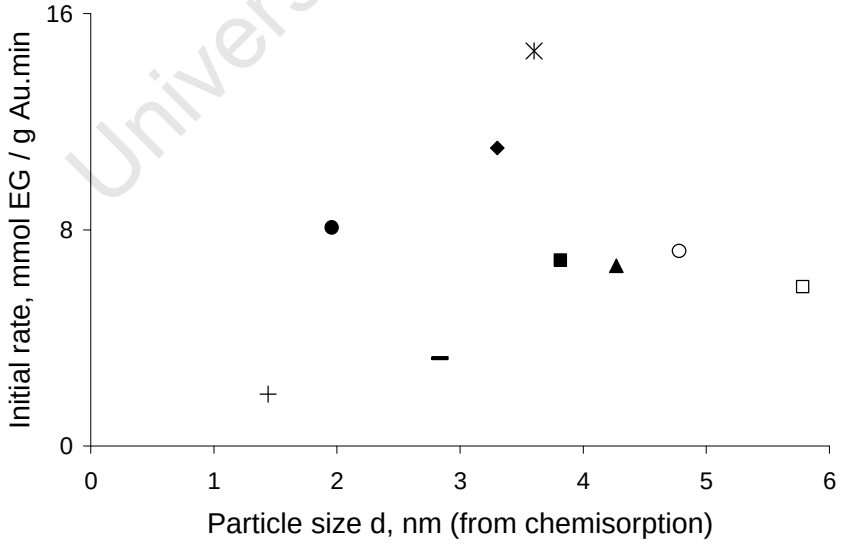

Figure 4.6. Initial reaction rates versus crystallite size
(▲ AL-AN-3.2; ♦ AL-CAT-10.6-300H2; ■ AL-CAT-10.6-200H2; ○ AL-CAT-10.6-200AIR; ✳ AL-CAT-8.0; + AL-CAT-9.5; □ AL-CAT-10.0; - AL-CAT-11.0; ● AL-CAT-12.0)
(Omitted for purposes of scaling is AL-CAT-6.1 with size of 23.5 nm and rate of 2.3 mmol / g Au.min)

University of Cape Town

Chapter 5. Conclusions

This study focused on ion exchange as a method of gold catalyst preparation, with an investigation of the activity of catalysts prepared by this method in the oxidation of ethylene glycol at atmospheric pressure.

Regarding the utility of ion exchange as a method of gold catalyst preparation, the study has demonstrated that impressive loading efficiencies can be achieved: full loading can take place with carbon as support, but high loading efficiencies are also obtainable with alumina under certain conditions. The carbon supported catalysts do not generally produce favourable crystallite size distributions, whereas alumina generally delivers small nanocrystallites in narrow size distributions. The pH of the preparation medium appears to exert an influence largely in support of Brunelle's (1978) electrostatic theory, with maximum uptake at pHs further away from the IEP in the favourable region for electrostatic attraction, but this would require further corroboration.

Ethylene glycol oxidation at atmospheric pressure was selected as the test reaction for this study. It is noted that there appears to be only one set of reports in the literature to date using alumina supported gold catalysis for this reaction under these conditions (Berndt et al., 2003, Berndt et al., 2004). Gold catalysed ethylene glycol oxidation with both carbon and other metal oxide supports has also been reported on, but tests were conducted at elevated pressure (Bianchi et al., 2000, Porta et al., 2000, Biella et al., 2002a). The present study found that carbon supported gold catalysts are inactive for ethylene glycol oxidation at atmospheric pressure at a temperature of 60ºC and using 0.05 M ethylene glycol. The alumina supported gold catalysts all displayed activity under these conditions. Differences in activity could not be ascribed to crystallite size.

An underlying contribution of this study centred on a range of methodological issues. Regarding methods for determining gold loading, considerable error was found to be associated with results from AAS. It would be advisable in the future to couple these results with those from another analytical method such as Inductively Coupled Plasma Mass Spectrometry (ICP-MS).

University of Cape Town

With regard to the determination of crystallite size, for each of the carbon and alumina supported catalysts, two methods were found to be applicable: TEM, for both types of catalyst, XRD for carbon catalysts only and chemisorption for alumina catalysts alone. This latter method is not well established in the literature on gold catalysis and so the findings in this study can be considered a contribution. The results were found to fit a dual isotherm model, and, using an assumption of dissociative adsorption, to deliver crystallite sizes in general agreement with those arrived at by TEM.

As a test reaction, ethylene glycol oxidation at atmospheric pressure was found to be convenient. With 0.05 M ethylene glycol and at a temperature of 60 ºC, measurements could be taken in the kinetic regime without interference from external or internal mass transfer. Titration using NaOH was found to be a relatively accurate method for following reaction progress. For the present study this titration was conducted manually, in order to avoid any potential electronic interference, but further work is needed to correlate these results with those which can be obtained with an autotitrator, so as to be able to automate such measurements in future. HPLC was used to identify reaction products and unreacted reactants. At this stage it has not been possible to quantify selectivity, although in most cases there are no obvious peaks arising from reaction by-products.

This is clearly a fruitful area for future work, both in further exploring ion exchange as a preparation method, as well as developing catalysts for ethylene glycol oxidation.

University of Cape Town

References

AKITA, T., LU, P., ICHIKAWA, S., TANAKA, K. & HARUTA, M. (2001) Analytical TEM study on the dispersion of Au nanoparticles in Au/TiO2 catalyst prepared under various temperatures. *Surface and Interface Analysis,* 31**,** 73-78.

ANDREEVA, D. (2002) Low temperature water gas shift over gold catalysts. *Gold Bulletin,* 35**,** 82-88.

BEEMING, B. (2009) *Synthesis and characterisation of carbon supported gold catalysts prepared by ion-exchange*. MSc thesis, University of Cape Town, Cape Town.

BELTRAME, P., COMOTTI, M., PINA, C. D. & ROSSI, M. (2006) Aerobic oxidation of glucose II. Catalysis by colloidal gold. *Applied Catalysis A: General,* 297**,** 1-7.

BERNDT, H., MARTIN, A., PITSCH, I., PRÜSSE, U. & VORLOP, K. D. (2004) Partial oxidation of polyvalent oxygen substituted compounds on nano-scale gold catalysts. *Catalysis Today,* 91-92**,** 191-194.

BERNDT, H., PITSCH, I., EVERT, S., STRUVE, K., POHL, M.-M., RADNIK, J. & MARTIN, A. (2003) Oxygen adsorption on Au/Al_2O_3 catalysts and relation to the catalytic oxidation of ethylene glycol to glycolic acid. *Applied Catalysis A: General,* 244**,** 169-179.

BIANCHI, C., PORTA, F., PRATI, L. & ROSSI, M. (2000) Selective liquid phase oxidation using gold catalysts. *Topics in Catalysis,* 13**,** 231-236.

BIELLA, S., CASTIGLIONI, G. L., FUMAGALLI, C., PRATI, L. & ROSSI, M. (2002a) Application of gold catalysts to selective liquid phase oxidation. *Catalysis Today,* 72**,** 43-49.

BIELLA, S., PRATI, L. & ROSSI, M. (2002b) Selective oxidation of D-glucose on gold catalyst. *Journal of Catalysis,* 206**,** 242-247.

BOND, G. C. & THOMPSON, D. T. (1999) Catalysis by gold. *Catalysis Review - Science Engineering,* 41**,** 319-388.

BOND, G. C. & THOMPSON, D. T. (2000) Gold-catalysed oxidation of carbon monoxide. *Gold Bulletin,* 33**,** 41-51.

BRUNELLE, J. P. (1978) Preparation of catalysts by metallic complex adsorption on mineral oxides. *Pure and Applied Chemistry,* 50**,** 1211-1229.

BULUSHEV, D. A., YURANOV, I., SUVOROVA, E. I., BUFFAT, P. A. & KIWI-MINSKER, L. (2004) Highly dispersed gold on activated carbon fibers for low-temperature CO oxidation. *Journal of Catalysis,* 224**,** 8-17.

CARRETTIN, S., MCMORN, P., JOHNSTON, P., GRIFFIN, K. & HUTCHINGS, G. J. (2002) Selective oxidation of glycerol to glyceric acid using a gold catalyst in aqueous sodium hydroxide. *Chemical Communications,* 2002**,** 696-697.

CARRETTIN, S., MCMORN, P., JOHNSTON, P., GRIFFIN, K., KIELY, C. J., ATTARD, G. A. & HUTCHINGS, G. J. (2004) Oxidation of glycerol using supported gold catalysts. *Topics in Catalysis,* 27**,** 131-136.

CARRETTIN, S., MCMORN, P., JOHNSTON, P., GRIFFIN, K., KIELY, C. J. & HUTCHINGS, G. J. (2003) Oxidation of glycerol using supported Pt, Pd and Au catalysts. *Physical Chemistry Chemical Physics,* 5**,** 1329-1336.

CENTENO, M. A., CARRIZOSA, I. & ODRIOZOLA, J. A. (2003) Deposition-precipitation method to obtain supported gold catalysts: dependence of the acid-base properties of the support exemplified in the system TiO_2-TiO_xN_y-TiN. *Applied Catalysis A: General,* 246**,** 365-372.

University of Cape Town

CHOUDARY, T. V. & GOODMAN, D. W. (2002) Oxidation catalysis by supported gold nano-clusters. *Topics in Catalysis,* 21**,** 25-34.

COMOTTI, M., PINA, C. D., FALLETTA, E. & ROSSI, M. (2006a) Aerobic oxidation of glucose with gold catalyst: Hydrogen peroxide as intermediate and reagent. *Advanced Synthesis & Catalysis,* 348**,** 313-316.

COMOTTI, M., PINA, C. D., FALLETTA, E. & ROSSI, M. (2006b) Is the biochemical route always advantageous? The case of glucose oxidation. *Journal of Catalysis,* 244**,** 122-125.

DEMIREL-GÜLEN, S., LUCAS, M. & CLAUS, P. (2005) Liquid phase oxidation of glycerol over carbon supported gold catalysts. *Catalysis Today,* 102**,** 166-172.

DEMIREL, S., KERN, P., LUCAS, M. & CLAUS, P. (2007a) Oxidation of mono- and polyalcohols with gold: Comparison of carbon and ceria supported catalysts. *Catalysis Today,* 122**,** 292-300.

DEMIREL, S., LEHNERT, K., LUCAS, M. & CLAUS, P. (2007b) Use of renewables for the production of chemicals: Glycerol oxidation over carbon supported gold catalysts. *Applied Catalysis B: Environmental,* 70**,** 637-643.

DEMIREL, S., LUCAS, M., WÄRNÅ, J., SALMI, T., MURZIN, D. & CLAUS, P. (2007c) Reaction kinetics and modelling of the gold catalysed glycerol oxidation. *Topics in Catalysis,* 44**,** 299-305.

ENACHE, D. I., KNIGHT, D. W. & HUTCHINGS, G. J. (2005) Solvent-free oxidation of primary alcohols to aldehydes using supported gold catalysts. *Catalysis Letters,* 103**,** 43-52.

FU, L., WU, N. Q., YANG, J. H., QU, F., JOHNSON, D. L., KUNG, M. C., KUNG, H. H. & DRAVID, V. P. (2005) Direct evidence of oxidized gold on supported gold catalysts. *Journal of Physical Chemistry B,* 109**,** 3704-3706.

FUKUSHIMA, T., GALVAGNO, S. & PARRAVANO, G. (1979) Oxygen chemisorption on supported gold. *Journal of Catalysis,* 57**,** 177-182.

GUERREIRO, E. D., GORRIZ, O. F., RIVAROLA, J. B. & ARRÚA, L. A. (1997) Characterization of Cu/SiO_2 catalysts prepared by ion exchange for methanol dehydrogenation. *Applied Catalysis A, General,* 165**,** 259-271.

HARUTA, M. (1997) Size- and support-dependency in the catalysis of gold. *Catalysis Today,* 36**,** 153-166.

HARUTA, M. (2004) Gold as a novel catalyst in the 21st century: Preparation, working mechanism and applications. *Gold Bulletin,* 37**,** 27-36.

HARUTA, M. & DATÉ, M. (2001) Advances in the catalysis of Au nanoparticles. *Applied Catalysis A: General,* 222**,** 427-437.

HARUTA, M., TSUBOTA, S., KOBAYASHI, T., KAGEYAMA, H., GENET, M. J. & DELMON, B. (1993) Low-temperature oxidation of CO over gold supported on TiO_2, α-Fe_2O_3, and Co_3O_4. *Journal of Catalysis,* 144**,** 175-192.

HASHMI, A. S. K. (2007) Gold-catalyzed organic reactions. *Chemical Reviews,* 107**,** 3180-3211.

HAYASHI, T., INAGAKI, T., ITAYAMA, N. & BABA, H. (2006) Selective oxidation of alcohol over supported gold catalysts: methyl glycolate formation from ethylene glycol and methanol. *Catalysis Today,* 117**,** 210-213.

HUTCHINGS, G., CARRETTIN, S., LANDON, P., EDWARDS, J., ENACHE, D., KNIGHT, D., XU, Y.-J. & CARLEY, A. (2006) New approaches to designing selective oxidation catalysts: Au/C a versatile catalyst. *Topics in Catalysis,* 38**,** 223-230.

HUTCHINGS, G. & HARUTA, M. (2005) A golden age of catalysis: A perspective. *Applied Catalysis A: General,* 291**,** 2-5.

University of Cape Town

IVANOVA, S., PETIT, C. & PITCHON, V. (2004) A new preparation method for the formation of gold nanoparticles on an oxide support. *Applied Catalysis A, General,* 267**,** 191-201.

IVANOVA, S., PITCHON, V. & PETIT, C. (2006a) Application of the direct exchange method in the preparation of gold catalysts supported on different oxide materials. *Journal of Molecular Catalysis A: Chemical,* 256**,** 278-283.

IVANOVA, S., PITCHON, V., PETIT, C., HERSCHBACH, H., DORSSELAER, A. V. & LEIZE, E. (2006b) Preparation of alumina supported gold catalysts: Gold complexes genesis, identification and speciation by mass spectrometry. *Applied Catalysis A, General,* 298**,** 203-210.

IVANOVA, S., PITCHON, V., ZIMMERMANN, Y. & PETIT, C. (2006c) Preparation of alumina supported gold catalysts: Influence of washing procedures, mechanism of particles size growth. *Applied Catalysis A, General,* 298**,** 57-64.

JANSSENS, T. V. W., CARLSSON, A., PUIG-MOLINA, A. & CLAUSEN, B. S. (2006) Relation between nanoscale Au particle structure and activity for CO oxidation on supported gold catalysts. *Journal of Catalysis,* 240**,** 108-113.

JØRGENSEN, B., EGHOLM CHRISTIANSEN, S., DAHL THOMSEN, M. L. & CHRISTENSEN, C. H. (2007) Aerobic oxidation of aqueous ethanol using heterogeneous gold catalysts: Efficient routes to acetic acid and ethyl acetate. *Journal of Catalysis,* 251**,** 332-337.

KETCHIE, W. C., MURAYAMA, M. & DAVIS, R. J. (2007) Selective oxidation of glycerol over carbon-supported AuPd catalysts. *Journal of Catalysis,* 250**,** 264-273.

KHUMALO, P. & MBOLEKWA, E. (2008) *Testing and characterization of gold catalysts prepared via cationic exchange*. Final year Chemical Engineering project thesis, University of Cape Town.

KIM, C. H. & THOMPSON, L. T. (2006) On the importance of nanocrystalline gold for Au/CeO_2 water-gas shift catalysts. *Journal of Catalysis,* 244**,** 248-250.

KLUYTMANS, J. H. J., MARKUSSE, A. P., KUSTER, B. F. M., MARIN, G. B. & SCHOUTEN, J. C. (2000) Engineering aspects of the aqueous noble metal catalysed alcohol oxidation. *Catalysis Today,* 57**,** 143-155.

MALLAT, T. & BAIKER, A. (2004) Oxidation of alcohols with molecular oxygen on solid catalysts. *Chemical Reviews,* 104**,** 3037-58.

MCPHERSON, J. (2008) Personal communication. Johannesburg, Mintek.

MILLER, J. T., KROPF, A. J., ZHA, Y., REGALBUTO, J. R., DELANNOY, L., LOUIS, C., BUS, E. & VAN BOKHOVEN, J. A. (2006) The effect of gold particle size on Au-Au bond length and reactivity toward oxygen in supported catalysts. *Journal of Catalysis,* 240**,** 222-234.

MIRESCU, A., BERNDT, H., MARTIN, A. & PRÜßE, U. (2007) Long-term stability of a 0.45% Au/TiO_2 catalyst in the selective oxidation of glucose at optimised reaction conditions. *Applied Catalysis A, General,* 317**,** 204-209.

MIRESCU, A. & PRÜßE, U. (2007) A new environmental friendly method for the preparation of sugar acids via catalytic oxidation on gold catalysts. *Applied Catalysis B, Environmental,* 70**,** 644-652.

NIELSEN, I. S., TAARNING, E., EGEBLAD, K., MADSEN, R. & CHRISTENSEN, C. H. (2007) Direct aerobic oxidation of primary alcohols to methyl esters catalyzed by a heterogeneous gold catalyst. *Catalysis Letters,* 116**,** 35-40.

OKUMURA, M. & HARUTA, M. (2000) Preparation of supported gold catalysts by liquid-phase grafting of gold acethylacetonate for low-temperature oxidation of CO and of H_2. *Chemistry Letters,* 29**,** 396-397.

University of Cape Town

ÖNAL, Y., SCHIMPF, S. & CLAUS, P. (2004) Structure sensitivity and kinetics of D-glucose oxidation to D-gluconic acid over carbon-supported gold catalysts. *Journal of Catalysis,* 223**,** 122-133.

PHALA, N. S. & VAN STEEN, E. (2007) Intrinsic reactivity of gold nanoparticles: Classical, semi-empirical and DFT studies. *Gold Bulletin,* 40**,** 150-153.

PORTA, F. & PRATI, L. (2004) Selective oxidation of glycerol to sodium glycerate with gold-on-carbon catalyst: an insight into reaction selectivity. *Journal of Catalysis,* 224**,** 397-403.

PORTA, F., PRATI, L., ROSSI, M., COLUCCIA, S. & MARTRA, G. (2000) Metal sols as a useful tool for heterogeneous gold catalyst preparation: reinvestigation of a liquid phase oxidation. *Catalysis Today,* 61**,** 165-172.

PRATI, L. & MARTRA, G. (1999) New gold catalysts for liquid phase oxidation. *Gold Bulletin(Switzerland),* 32**,** 96-101.

PRATI, L. & PORTA, F. (2005) Oxidation of alcohols and sugars using Au/C catalysts: Part 1. Alcohols. *Applied Catalysis A: General,* 291**,** 199-203.

PRATI, L. & ROSSI, M. (1998) Gold on carbon as a new catalyst for selective liquid phase oxidation of diols. *Journal of Catalysis,* 176**,** 552-560.

RIAHI, G., GUILLEMOT, D., POLISSET-THFOIN, M., KHODADADI, A. A. & FRAISSARD, J. (2002) Preparation, characterization and catalytic activity of gold-based nanoparticles on HY zeolites. *Catalysis Today,* 72**,** 115-121.

SCHREIER, M. & REGALBUTO, J. R. (2004) A fundamental study of Pt tetraammine impregnation of silica 1. The electrostatic nature of platinum adsorption. *Journal of Catalysis,* 225**,** 190-202.

SHASTRI, A. G., DATYE, A. K. & SCHWANK, J. (1984) Gold-titania interactions: temperature dependence of surface area and crystallinity of TiO_2 and gold dispersion. *Journal of Catalysis,* 87**,** 265-277.

SKIBSTED, L. H. & BJERRUM, J. (1974) Studies on gold complexes. I. Robustness, stability and acid dissociation of the tetrammine gold(III) ion. *Acta Chemica Scandinavica A,* 28**,** 740-746.

STEINHAUSER, G., EVERS, J., JAKOB, S., KLAPÖTKE, T. M. & OEHLINGER, G. (2008) A review on fulminating gold (Knallgold). *Gold Bulletin,* 41**,** 305.

TUZOVSKAYA, I., BOGDANCHIKOVA, N., GURIN, V., DATYE, A., PESTRYAKOV, A. & SIMAKOV, A. (2003) Novel method of preparation of gold nanoparticles by ion exchange. *North American Catalysis Society Meeting.* Cancun, Mexico.

VALDEN, M., LAI, X. & GOODMAN, D. W. (1998) Onset of catalytic activity of gold clusters on titania with the appearance of nonmetallic properties. *Science,* 281**,** 1647-1650.

WIELAND, B., LANCASTER, J. P., HOAGLUND, C. S., HOLOTA, P. & TORNQUIST, W. J. (1996) Electrochemical and infrared spectroscopic quantitative determination of the Platinum-catalyzed ethylene glycol oxidation mechanism at CO adsorption potentials. *Langmuir,* 12**,** 2594-2601.

WOLF, A. & SCHÜTH, F. (2002) A systematic study of the synthesis conditions for the preparation of highly active gold catalysts. *Applied Catalysis A: General,* 226**,** 1-13.

WORLD GOLD COUNCIL (n.d.) Gold Reference Catalyst Data Sheet Type D.

ZANELLA, R., DELANNOY, L. & LOUIS, C. (2005) Mechanism of deposition of gold precursors onto TiO_2 during the preparation by cation adsorption and deposition-precipitation with NaOH and urea. *Applied Catalysis A: General,* 291**,** 62-72.

ZWANE, S. (2004) *Vanadia-promoted Co-Al_2O_3 Fischer-Tropsch catalysts*. MSc thesis, University of Cape Town.

University of Cape Town

Appendix A. Sample TEM images

C-AN-0.9 no wash

200 nm

C-AN-0.9

100 nm

C-AN-2.3

University of Cape Town

}200 nm

C-CAT-2.4

}50 nm

C-CAT-5.0

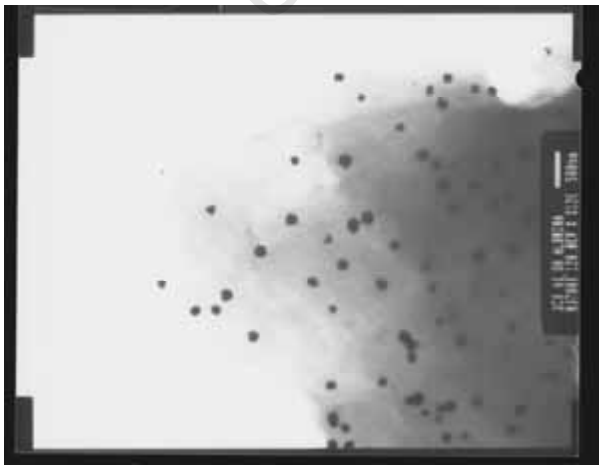

}500 nm

University of Cape Town

AL-AN-3.2

AL-AN-6.1

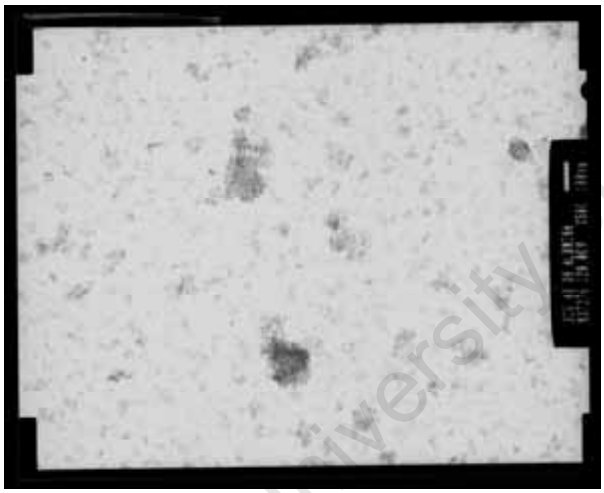

University of Cape Town

AL-CAT-10.6

}50 nm

University of Cape Town

AL-CAT-7.6

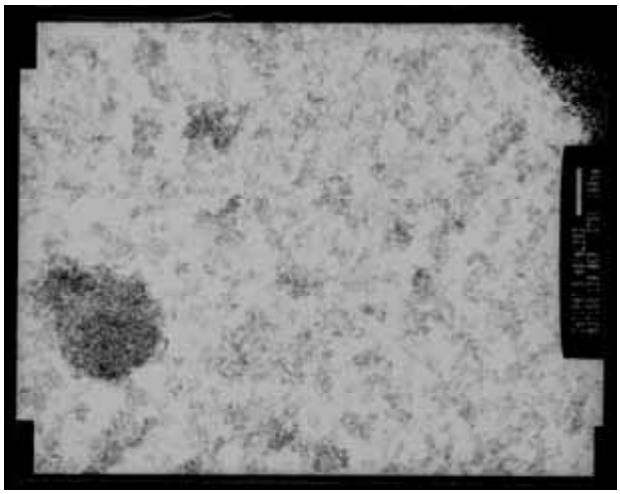

AL-CAT-8.0

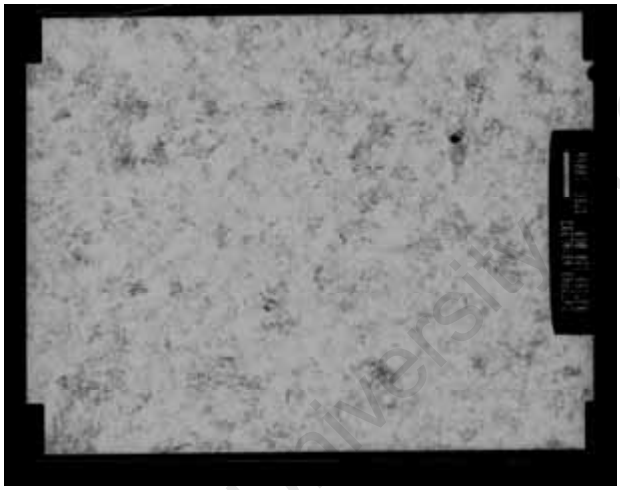

University of Cape Town

AL-CAT-8.5

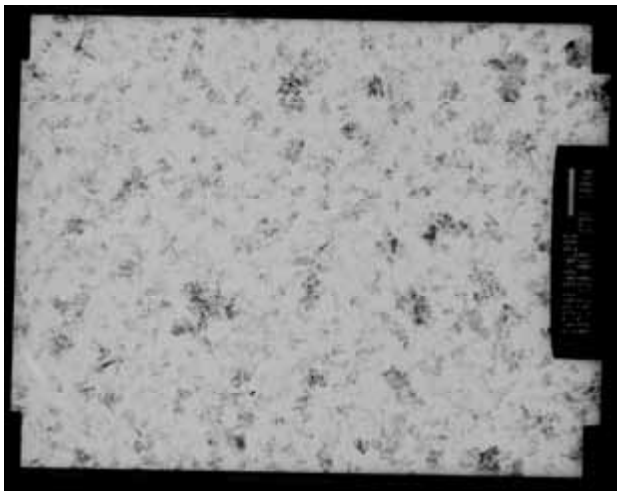

University of Cape Town

AL-CAT-9.0

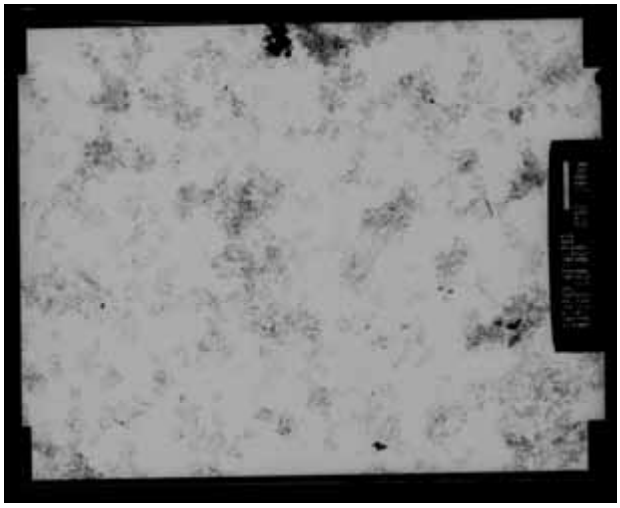

100 nm

AL-CAT-9.5

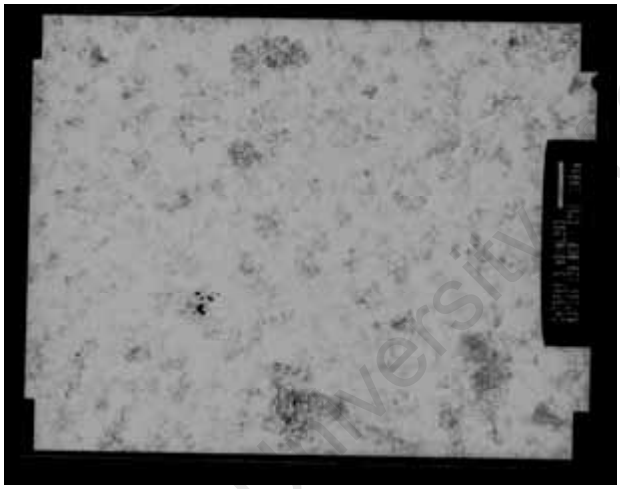

100 nm

AL-CAT-10.0

University of Cape Town

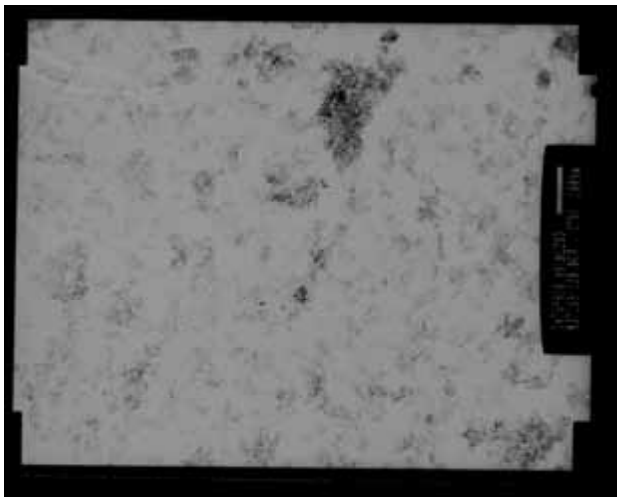

}100 nm

University of Cape Town

AL-CAT-11.0

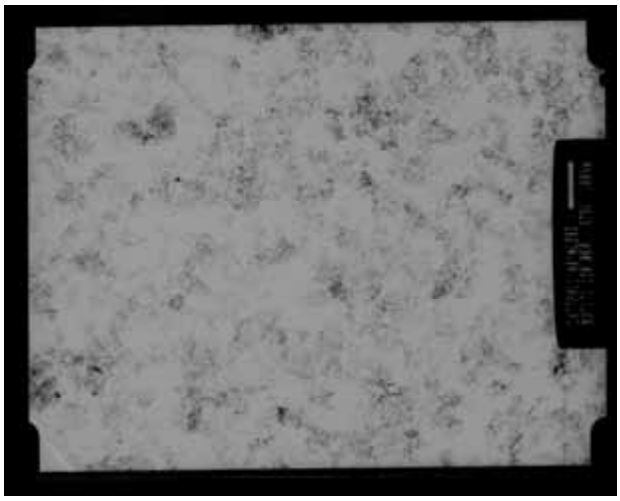

}100 nm

AL-CAT-12.0

}100 nm

University of Cape Town

Appendix B. Influence of pH of reaction on selectivity

Selecting chromatograms which did not have the 'temporary' peaks evident yielded the following analysis of the influence of pH on products:

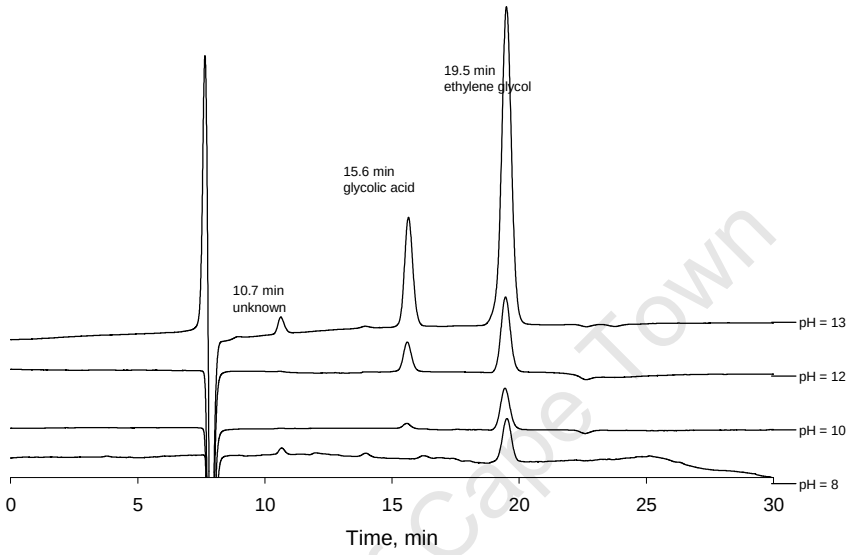

Figure: Influence of pH on products

At both low pH (8) and high pH (13) a product is formed with a retention time of 10.7 min. This is yet to be identified. At intermediate pH there appears to be approximately 100% selectivity to glycolic acid.

University of Cape Town

Appendix C. Calibration of peak area with internal standard

In order to provide some verification of the reaction rate as measured by NaOH titration, a calibration was performed on the HPLC peak areas, using oxalic acid as an internal standard added to the final reaction mixture. Firstly, a standard mixture of oxalic acid and glycolic acid, and ethylene glycol with known concentrations was analysed, given that glycolic acid gives a response in both the RI and UV chromatograms. Using the assumptions that

$$\frac{n_{oxalic,std}}{n_{glycolic,std}} = f \frac{Area_{oxalic,std}}{Area_{glycolic,std}}$$

the parameter, *f*, was calculated for each of the detectors:

UV: $f = 0.043187$

RI: $f = 0.723409$

This then allowed for calculation of conversion for two of the pilot runs using the Mintek 'BC1' catalyst. The results are given in the table below.

Table: Comparison of conversion calculated with HPLC calibration and with NaOH titration

Data for calculating conversion	Run 1 (pH = 12)	Run 2 (pH = 13)
UV glycolic acid peak area	51%	84%
RI glycolic acid peak area	46%	86%
Titration with NaOH	15%	100%

University of Cape Town

The internal consistency between the conversions calculated with UV data and those with the RI data is pleasing. The comparison with the titration data yields mixed results. For Run 1 there is no easy explanation for the dramatically lower conversion as suggested by the data. For Run 2, given that there had been an unknown peak at 10.7 min it is possible that this might account for the missing 15%. As noted earlier the 100% conversion arising from the titration data is strongly supported by the observation that the pH was constant thereafter.

A calibration of the ethylene glycol peak was attempted for the RI chromatogram, using f parameters calculated as above comparing the oxalic acid to ethylene glycol peak. This yielded quite nonsensical results, suggesting 28 mmol of ethylene glycol present in Run 1, and 42 mmol in Run 2, when only 10 mmol had been initially present as reactant. An

unidentified 19.0 min peak had been present in some of the pilot run reaction mixtures and ascribed to the presence of gas bubbles; it is therefore possible that this unidentified peak might have been interfering here with the ethylene glycol peak.

University of Cape Town

Appendix D. Calibration curves for HPLC

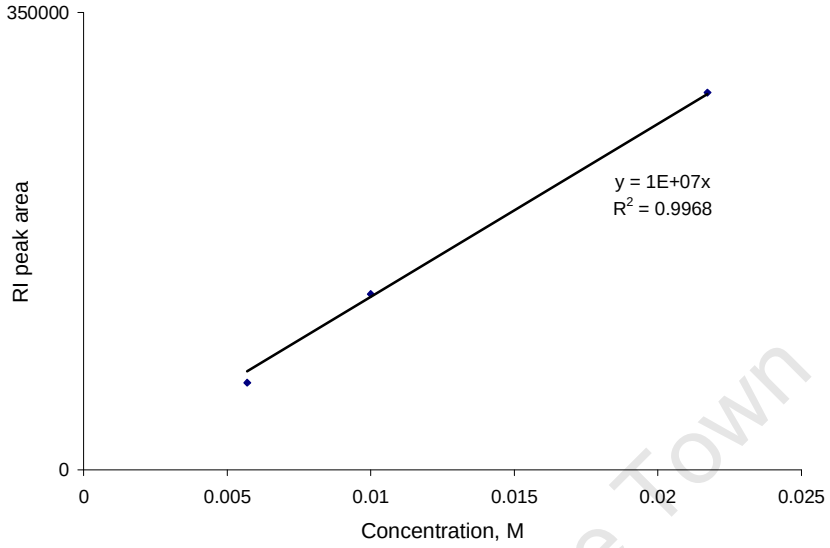

Figure: Calibration curve for ethylene glycol (RI)

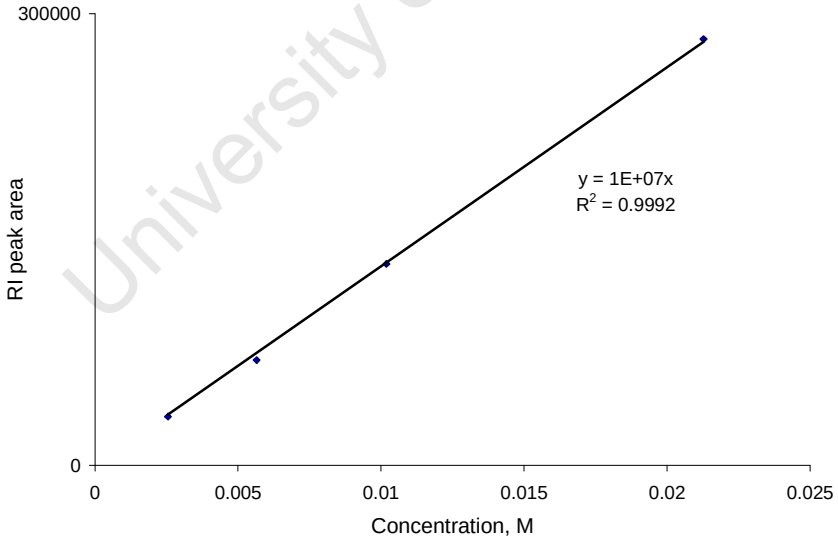

Figure: Calibration curve for glycolic acid (RI)

University of Cape Town

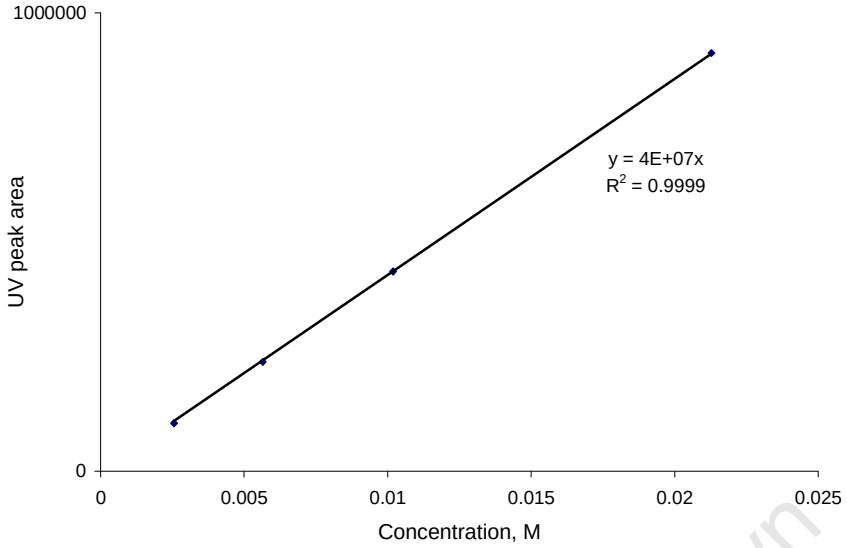

Figure: Calibration curve for glycolic acid (UV)

University of Cape Town